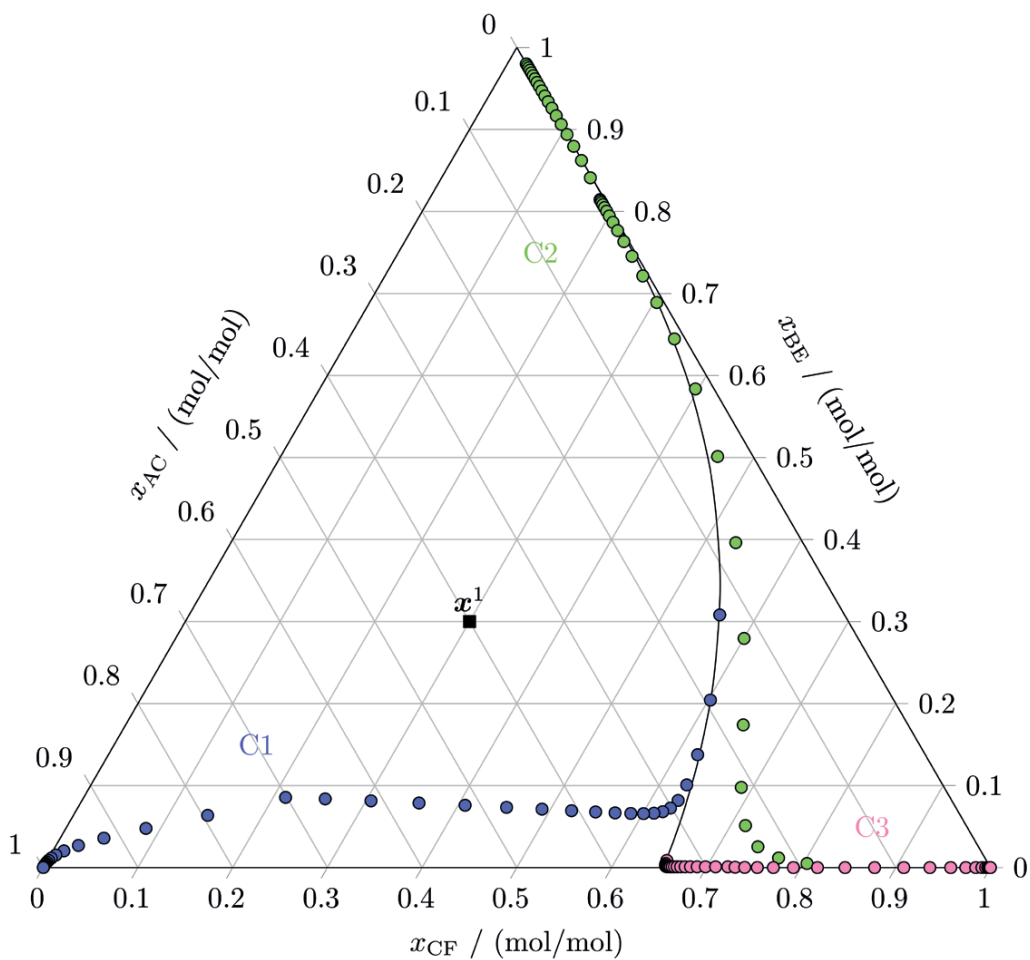


Anna Hoffmann

Integrated simulation and optimization of distillation-based flowsheets



Fraunhofer-Institut für
Techno- und Wirtschaftsmathematik ITWM

Integrated simulation and optimization of distillation-based flowsheets

Anna Hoffmann

FRAUNHOFER VERLAG

Kontakt:

Fraunhofer-Institut für Techno- und Wirtschaftsmathematik ITWM
Fraunhofer-Platz 1
67663 Kaiserslautern
Telefon +49 631/31600-0
Fax +49 631/31600-1099
E-Mail info@itwm.fraunhofer.de
URL www.itwm.fraunhofer.de

Bibliografische Information der Deutschen Nationalbibliothek

Die Deutsche Nationalbibliothek verzeichnet diese Publikation in der Deutschen Nationalbibliografie; detaillierte bibliografische Daten sind im Internet über <http://dnb.d-nb.de> abrufbar.
ISBN (Print): 978-3-8396-1179-1

D 386

Zugl.: Kaiserslautern, TU, Diss., 2016

Druck: Mediendienstleistungen des
Fraunhofer-Informationszentrum Raum und Bau IRB, Stuttgart

Für den Druck des Buches wurde chlor- und säurefreies Papier verwendet.

© by **FRAUNHOFER VERLAG**, 2017

Fraunhofer-Informationszentrum Raum und Bau IRB
Postfach 80 04 69, 70504 Stuttgart
Nobelstraße 12, 70569 Stuttgart
Telefon 07 11 9 70-25 00
Telefax 07 11 9 70-25 08
E-Mail verlag@fraunhofer.de
URL <http://verlag.fraunhofer.de>

Alle Rechte vorbehalten

Dieses Werk ist einschließlich aller seiner Teile urheberrechtlich geschützt. Jede Verwertung, die über die engen Grenzen des Urheberrechtsgesetzes hinausgeht, ist ohne schriftliche Zustimmung des Verlages unzulässig und strafbar. Dies gilt insbesondere für Vervielfältigungen, Übersetzungen, Mikroverfilmungen sowie die Speicherung in elektronischen Systemen.

Die Wiedergabe von Warenbezeichnungen und Handelsnamen in diesem Buch berechtigt nicht zu der Annahme, dass solche Bezeichnungen im Sinne der Warenzeichen- und Markenschutz-Gesetzgebung als frei zu betrachten wären und deshalb von jedermann benutzt werden dürften. Soweit in diesem Werk direkt oder indirekt auf Gesetze, Vorschriften oder Richtlinien (z.B. DIN, VDI) Bezug genommen oder aus ihnen zitiert worden ist, kann der Verlag keine Gewähr für Richtigkeit, Vollständigkeit oder Aktualität übernehmen.

Integrated simulation and optimization of distillation-based flowsheets

**Vom Fachbereich Mathematik der
Technischen Universität Kaiserslautern
zur Verleihung des akademischen Grades
Doktor der Naturwissenschaften
(Doctor rerum naturalium, Dr. rer. nat.)
genehmigte**

Dissertation

von

Anna Hoffmann

1. Gutachter: Prof. Dr. Karl-Heinz Küfer,
Technische Universität Kaiserslautern
2. Gutachter: Prof. Dr. Lorenz T. Biegler,
Carnegie Mellon University, Pittsburgh

Datum der Disputation: 21. Dezember 2016

D 386

Danksagung

Die vorliegende Arbeit ist in enger Kooperation und mit finanzieller Unterstützung der Abteilung Optimierung des Fraunhofer-Institut für Techno- und Wirtschaftsmathematik (ITWM) in Kaiserslautern und des Lehrstuhls für Thermodynamik der Technischen Universität Kaiserslautern entstanden.

Mein besonderer Dank gilt meinem Doktorvater Prof. Dr. Karl-Heinz Küfer für seine Unterstützung während der Anfertigung meiner Dissertation, sowie für die Möglichkeit, ein sehr spannendes und herausforderndes Thema bearbeiten zu können. Für viele hilfreiche fachliche Diskussionen und Inspiration bedanke ich mich ganz herzlich bei Dr. Michael Bortz und Dr. Jan Schwientek. Ein großer Dank gebührt auch meinen Kolleginnen und Kollegen der Abteilung Optimierung im Fraunhofer ITWM, insbesondere Dr. Volker Maag, Andreas Dinges, Dr. Gregor Foltin und Dr. Richard Welke für geduldige Hilfe bei Programmierfragen und IT-Problemen und Jasmin Kirchner für ihre unermüdliche Unterstützung bei organisatorischen Dingen. Für die Implementierungen im Rahmen ihrer Hiwi-Tätigkeit danke ich Juliane Ritter.

Ich hatte während der vergangenen drei Jahre das große Glück, nicht nur im Fraunhofer ITWM, sondern auch am Lehrstuhl für Thermodynamik der Technischen Universität Kaiserslautern hervorragend betreut zu werden. Mein herzlicher Dank gilt Prof. Dr.-Ing. Hans Hasse für viele interessante Diskussionen und wertvolle Anregungen. Sein Rückhalt und Vertrauen in meine Arbeit haben mich stets motiviert und wesentlich zum Gelingen dieser Arbeit beigetragen. Zudem möchte ich Jun. Prof. Dr.-Ing. Jakob Burger einen großen Dank für die ausgezeichnete Betreuung aussprechen. Viele Ergebnisse der

vorliegenden Arbeit konnten nur durch seine kritischen Rückfragen und Neugier entstehen. Bei meinen Kolleginnen und Kollegen am Lehrstuhl für Thermodynamik bedanke ich mich ebenfalls für die wunderbare Arbeitsatmosphäre und auch dort wurde ich von Daniel Stihler, Jennifer Bergmann und Monika Reim in technischen und organisatorischen Belangen stets tatkräftig unterstützt.

Prof. Dr. Lorenz T. Biegler danke ich herzlich für die Begutachtung meiner Arbeit und viele wertvolle Kommentare und Anregungen.

Für das Korrekturlesen meiner Arbeit ein herzliches Dankeschön meinen Kolleginnen und Kollegen Esther Bonacker, Helene Krieg, Rasmus Schroeder, Anne Friebel, Fabian Jirasek, Elmar Kessler und Niklas Schmitz. Ein ganz besonderer Dank gilt Dr.-Ing. Katrin Stöbener – die ich im letzten Jahr meiner Promotion sehr vermisst habe – für unzählige Kaffeerunden mit fachlicher und weniger fachlicher Diskussion.

Zuletzt danke ich von Herzen meiner Familie, meinen Freunden und Max für viel Unterstützung, Zuspruch und Geduld während meiner Promotion.

Contents

| | |
|---|-----------|
| List of Symbols | ix |
| I. Modeling and problem definition | 1 |
| 1. Introduction and overview | 3 |
| 1.1. Asymptotic limiting cases for distillation columns | 5 |
| 1.2. Modeling principles for distillation processes | 7 |
| 1.3. Process simulation and optimization | 8 |
| 1.4. Shortcut techniques for distillation processes | 10 |
| 1.5. Contributions | 12 |
| 1.6. Outline | 15 |
| 2. Mathematical principles | 17 |
| 2.1. Nonlinear optimization | 17 |
| 2.2. Multi-criteria optimization | 19 |
| 2.3. Ordinary differential equations and the shooting method | 21 |
| 3. Embedding process simulation in an optimization problem | 25 |
| 3.1. General idea | 26 |
| 3.2. Flash units | 29 |
| 3.3. Distillation columns in combination with the shooting method | 32 |

| | |
|---|------------|
| 3.4. Simultaneous process simulation and optimization | 38 |
| 3.5. Starting values | 38 |
| 3.6. Extensions of the presented approach | 40 |
| II. Solution approaches | 43 |
| 4. Stage-to-stage calculations of simple distillation columns | 45 |
| 4.1. System of equations | 45 |
| 4.2. Derivation of an equivalent fixed-point problem | 48 |
| 4.3. Application of the Banach fixed-point theorem | 51 |
| 4.3.1. Existence of a fixed point | 51 |
| 4.3.2. Uniqueness of the fixed point and convergence of the fixed-point iteration | 63 |
| 4.3.3. Rate of convergence | 72 |
| 4.4. A numerical example | 72 |
| 4.4.1. Example separation problem | 73 |
| 4.4.2. Energy bounds derived with the Banach fixed-point theorem | 74 |
| 4.4.3. Number of stages needed for the desired separation | 81 |
| 4.4.4. Speed of convergence of the fixed-point iteration | 81 |
| 4.4.5. Minimum energy needed for the desired separation | 87 |
| 5. Stage-to-stage calculations of general distillation columns | 91 |
| 5.1. System of equations | 91 |
| 5.2. Derivation of an equivalent fixed-point problem | 92 |
| 5.3. Application of the Banach fixed-point theorem | 93 |
| 5.3.1. Existence of a fixed point | 93 |
| 5.3.2. Uniqueness of the fixed point and convergence of the fixed-point iteration | 101 |
| 6. Distillation-based flowsheets comprising several unit operations | 109 |
| 6.1. The modular and the simultaneous approach | 109 |
| 6.2. The simultaneous approach: Calculation order within one iteration | 110 |

| | |
|---|------------|
| III. Numerical analysis | 117 |
| 7. Numerical results | 119 |
| 7.1. Implementation details | 119 |
| 7.2. Comparison of optimization algorithms | 120 |
| 7.3. Separation of acetone and chloroform | 125 |
| 7.3.1. Single distillation column | 125 |
| 7.3.2. Pressure-swing distillation | 130 |
| 7.3.3. Benzene as entrainer | 133 |
| 7.4. Separation of water and ethanol using tetrahydrofuran as entrainer | 140 |
| 7.4.1. Single distillation column | 140 |
| 7.4.2. A distillation-based flowsheet | 143 |
| 8. Conclusions and perspectives | 147 |
| A. Chemical modeling | 151 |
| A.1. Terminology | 151 |
| A.2. Physical property models of the example systems | 154 |
| A.2.1. Pure component properties | 154 |
| A.2.2. Vapor-liquid equilibrium | 155 |
| A.2.3. Caloric data for the example systems | 156 |
| B. Comments on Assumption 4.3 | 159 |
| List of publications | 161 |
| Bibliography | 163 |
| Index | 175 |
| Scientific Career | 177 |
| Wissenschaftlicher Werdegang | 179 |

List of Symbols

Abbreviations

| | |
|-----|----------------------------------|
| AC | acetone |
| BE | benzene |
| BVM | boundary value method |
| BVP | boundary value problem |
| CF | chloroform |
| CMO | constant molar overflow |
| CRV | constant relative volatility |
| ET | ethanol |
| IVP | initial value problem |
| LLE | liquid-liquid equilibrium |
| LP | linear program |
| MCO | multi-criteria optimization |
| MED | minimum energy demand |
| MIP | mixed-integer program |
| NLP | nonlinear program |
| ODE | ordinary differential equation |
| RBM | rectification body method |
| SQP | sequential quadratic programming |
| THF | tetrahydrofuran |
| VLE | vapor-liquid equilibrium |
| W | water |

Functions

| | |
|------------------|--|
| $\Delta h_{v,i}$ | enthalpy of vaporization of pure component i |
| γ_i | activity coefficient of pure component i |
| l | enthalpy of a liquid boiling mixture at given pressure |
| v | enthalpy of a vapor dewing mixture at given pressure |
| \mathcal{L} | Lagrangian function |
| $c_{p,i}^l$ | heat capacity at constant pressure of the liquid phase of pure component i |
| $c_{p,i}^v$ | heat capacity at constant pressure of the vapor phase of pure component i |
| h^l | molar liquid enthalpy |
| h^v | molar vapor enthalpy |
| h_i^l | enthalpy of the liquid phase of pure component i |
| h_i^v | enthalpy of the vapor phase of pure component i |
| p_i^S | vapor pressure of pure component i |

Sets

| | |
|-------------------------------|--|
| \mathbb{N} | set of non-negative integers $\{0, 1, 2, \dots\}$ |
| \mathbb{N}^* | set of positive integers $\{1, 2, 3, \dots\}$ |
| \mathbb{R} | set of real numbers |
| \mathcal{F}_{N_C} | set of all physically meaningful compositions of a mixture |
| $\mathcal{I}_{\text{constr}}$ | set of indices for the constraints |
| \mathcal{I}_{eq} | set of indices for the model equations |
| \mathcal{I}_{opt} | set of indices for the optimization variables |
| \mathcal{I}_{var} | set of indices for the process variables |
| \mathcal{S}_{eq} | set of indices for the equality specifications |
| $\mathcal{S}_{\text{ineq}}$ | set of indices for the inequality specifications |

Symbols

| | |
|-------------|----------------------------------|
| \dot{n}_i | molar flow rate of component i |
| \dot{Q} | heat duty |
| \dot{Q}_C | condenser duty |
| \dot{Q}_R | reboiler duty |
| B | bottom stream molar flow rate |
| D | distillate molar flow rate |

| | |
|---------------------|--|
| F | molar feed flow rate |
| F_k | molar flow rate of feed stream k |
| fs | number of feed streams |
| i | counter for components |
| L | molar liquid flow rate |
| L^n | molar liquid flow rate flowing from stage n to stage $n - 1$ |
| L^R | reflux molar flow rate |
| n | counter for stages |
| N_C | number of components |
| N_F | feed stage |
| N_S | number of stages |
| N_{constr} | number of constraints |
| N_{dof} | number of degrees of freedom |
| N_{eq} | number of model equations |
| N_{opt} | number of optimization variables |
| N_{var} | number of process variables |
| p | pressure |
| p^F | pressure of the feed stream |
| R | reflux ratio |
| S_l | molar flow rate of side-draw stream l |
| sd | number of side-draws |
| T | temperature |
| T^F | temperature of the feed stream |
| T^{VLE} | temperature at equilibrium |
| V | molar vapor flow rate |
| V^n | molar vapor flow rate flowing from stage n to stage $n + 1$ |
| V^R | reboil molar flow rate |
| x_i | mole fraction of component i in the liquid phase |
| y_i | mole fraction of component i in the vapor phase |

Vectors

| | |
|--------------------------|------------------------|
| λ, μ | Lagrangian multipliers |
| \mathbf{g}_{eq} | model equations |
| \mathbf{s}_{eq} | equality constraints |

List of Symbols

| | |
|----------------------------|--|
| \mathbf{s}_{ineq} | inequality constraints |
| \mathbf{x} | composition vector of mole fractions in the liquid phase |
| \mathbf{x}_{dep} | dependent process variables |
| \mathbf{x}_{opt} | optimization variables |
| \mathbf{x}_{var} | process variables |
| \mathbf{y} | composition vector of mole fractions in the vapor phase |



Part I.

Modeling and problem definition

CHAPTER 1

Introduction and overview

The present thesis is motivated by chemical engineering: process simulation and optimization with a focus on distillation-based flowsheets. In this context, a process consists of a number of unit operations connected by streams. Such a structure can be represented by a so-called flowsheet. In general, the process should be designed in a way that certain engineering demands are fulfilled, e.g. product purities, product yield, or maximum costs. The design of a process includes the choice of units in combination with their respective connections (layout of the flowsheet) and also the choice of values for the specific design variables for each unit (operating point). Within the scope of this work, we assume that the layout of the flowsheet is given and we focus on choosing the design variables for each unit, such as operating pressure, temperature, energy demand, or product streams, just to name a few. In reality, such a process will be dynamic, which mathematically means that all process variables like product streams, pressures, and temperatures are varying in time. For the planning of a process, however, it is significantly easier to neglect the variation in time and to find a suitable steady state. In practice, the process will be steered towards this steady state over time via a suitable control loop. In this thesis, we will restrict ourselves to the design of this utopian steady state. For this purpose, we will employ a well-established mathematical model that describes distillation-based processes in steady state as a basis for process simulation. A suitable simulation will map the design variables, which serve as input variables for the simulation, to values for the unknown

process variables that are output of the simulation. The entire set of process variables can then be used to determine whether the process meets the engineering demands and to evaluate objective functions that measure product quality. If such a simulation routine is at hand, it can be integrated with an optimization algorithm that will find optimal choices of process variables taking engineering demands and physical laws into account as constraints. Mathematically, we face a nonlinear, in general non-convex, and multi-criteria optimization problem.

The steady state behavior of a distillation-based flowsheet is modeled by default via a system of linear and nonlinear equations that reflect conservation and thermodynamic laws. More complex units such as distillation columns, consisting of a number of equilibrium stages, are described by a large number of model equations and process variables, whereas the number of degrees of freedom is typically small. These large nonlinear systems of equations cannot be solved analytically. Therefore, they are solved numerically, most often by use of Newton-type or quasi-Newton-type methods.

Commercial process simulation environments typically address square systems of nonlinear systems in which the number of unknown process variables and the number of equations have to be identical. In order to accomplish this in practice, the degrees of freedom have to be fixed, i.e. values for process variables have to be guessed and assigned by the experienced user. In a next step, the simulation software attempts to solve the resulting square system of equations using a Newton-type method. In this procedure, convergence failures occur quite often, which can have different reasons: On the one hand, the internal starting values for the Newton-type method could lie outside the locally guaranteed region of convergence. Unfortunately, there is no global theory of convergence for iterative solution methods of general systems of nonlinear equations. On the other hand, the guessed values for the fixed process variables could be infeasible. Observing a failure of the algorithm, it is typically not obvious for the user which reason applies. Hence, process simulation conducted in the described way does not always guarantee an output for a given input, as in order to obtain the output a nonlinear system of equations has to be solved. These drawbacks severely compromise an integration of simulation and optimization in the described way. In case of a convergence failure, the user has to come up with new guesses for the fixed process variables until convergence is reached and all unknown process variables are determined. As an alternative to this unsatisfying trial-and-error approach, in practice, a stepwise

assembly of the overall system of equations is often used where one starts from a smaller subsystem and carefully builds up the overall process. However, both concepts potentially turn the simulation and optimization of a flowsheet into a very time-consuming procedure.

In this thesis, our aim is to develop an approach for process simulation that guarantees the mapping between the input and output variables and substitutes the frequently used trial-and-error approach described above that is based on the empirical knowledge of the specific user. The central ideas for such an approach are presented in the following section.

1.1. Asymptotic limiting cases for distillation columns

One of the most complex units in distillation-based flowsheets is a distillation column. In this section, we describe simplified models for distillation columns using asymptotic limiting cases whose mathematical simulation is much simpler and will help us to tackle the aforementioned convergence problems.

A linear model for infinite reflux ratio and infinite number of stages

We want to consider the asymptotic limiting case of distillation columns with an infinite number of stages and infinite reflux ratio, which is defined as the ratio of the reflux to the overhead product. An infinite reflux ratio implies infinitely large internal streams and thus requires infinite heat duty. In this limiting case, the underlying model equations that describe the distillation processes significantly simplify to a linear model, which is in general relatively easy to solve. Furthermore, the distillation columns have ideal separation properties with respect to the thermodynamical properties of the considered multi-component system. Energy balances are not taken into account in the simplified model.

Solving the linear model yields the product streams of the distillation columns and convergence failures are prevented. This approach is also known as ∞/∞ -analysis in the literature. With a finite number of stages and finite reflux ratio the ideal separation assumed here can never be achieved and can thus only be regarded as a benchmark for rigorous process simulation. However, the calculated product streams typically describe the process quite well and serve as an excellent initial guess for the product streams that are calculated for distillation columns with finite reflux ratio and a finite number of stages.

But not only the double asymptotic limiting case is of interest. It is also worthwhile analyzing the limiting cases of distillation columns with an infinite reflux ratio but finite number of stages and vice versa. From these limiting cases we can borrow additional ideas in order to tackle the problems that we currently face in process simulation and optimization.

Distillation columns with infinite reflux ratio and finite number of stages

Within the scope of the novel approach presented in this thesis, we use upward or downward stage-to-stage calculations starting with the product stream at one end of the distillation column in combination with the reboiler or condenser duty, respectively, given as input variables for stage-to-stage calculations. The transition from one stage to the next is formulated as a fixed-point problem. For an infinitely large reflux ratio we show that convergence of the stage-to-stage calculations, and thus of the mapping between input and output variables, is immediately guaranteed. Furthermore, we assume continuity for the transition from an infinite reflux ratio to a finite reflux ratio. This raises the question how small the reflux ratio, and thus the reboiler or condenser duty, respectively, can be chosen in order to still have a guaranteed mapping between input and output variables. The rigorous analysis conducted in this work answers this question: We apply the Banach fixed-point theorem to the derived fixed-point problems and state conditions under which the considered mapping is contractive and maps from a certain set to itself. This means that a unique fixed point exists and convergence towards it is guaranteed. Hence, stage-to-stage calculations meet our demands for a simulation in the sense that we have a deterministic and also guaranteed mapping from the input variables to the remaining process variables for input variables arbitrarily chosen from a region of convergence that we can quantify.

Distillation columns with finite reflux ratio and infinite number of stages

If we increase the number of stages for fixed column height, the difference equation that is solved by stage-to-stage calculations turns in the limiting case of infinitely many stages into an ordinary differential equation. Moreover, the approach proposed in this thesis uses a larger number of process variables as input for stage-to-stage calculations than there are degrees of freedom in the distillation model and thus we have to solve a boundary value problem for the ordinary differential equation. This means that the input variables for stage-to-stage calculations, which correspond to the initial values of the ordinary differential equation, need to be adapted in a suitable way in order to obtain a feasible

solution. A method from the theory of ordinary differential equations that solves boundary value problems is the so-called (single) shooting method. In this work, the task will be embedded in an optimization problem, which finds feasible (or optimal) input variables in a targeted way by using suitable optimization algorithms.

In this thesis, the ideas arising in the above limiting cases will be transferred to distillation columns with finite reflux ratio and a finite number of stages. As a result, a novel approach for process simulation and optimization of distillation-based flowsheets is presented. Using ∞/∞ -analysis we can generate excellent initial guesses for the input variables of stage-to-stage calculations. By application of the Banach fixed-point theorem we can guarantee convergence of stage-to-stage calculations for suitable input variables. And finally, the input variables for stage-to-stage calculations can be adapted in an outer optimization loop such that a feasible or even optimal solution is finally found, which is similar to applying the shooting method to ordinary differential equations.

In the following, the modeling principles for steady state simulation of the considered processes are introduced. Furthermore, we discuss different existing methods for process simulation and optimization of distillation-based flowsheets and present a short review on existing techniques for conceptual process design with a focus on distillation, which is the most widely used technique for separating fluid mixtures.

1.2. Modeling principles for distillation processes

Distillation processes in steady state are usually described by the equilibrium stage model (Thiele & Geddes, 1933) based on the so-called MESH equations (material balances, equilibrium conditions, summation equations for the concentrations, heat (or better: energy) balances, see also Wang & Henke (1966), and Appendix A).

Despite the important simplifications in this type of model, it is known to describe distillation processes reasonably well, so that it has been used for distillation design very successfully for many decades, and there is no good reason to believe that this will change in the near future.

Describing distillation processes based on MESH equations leads to a large system of nonlinear equations with many unknowns and only few degrees of freedom, which has to be solved for process simulation. As a result, the internal and external streams of the column are obtained (flow rate, composition, and temperature) for the steady state operation of

the column. Furthermore, the heat flows in the reboiler and condenser are determined. The model of the physical properties of the fluid mixtures is in general nonlinear. For further reading, see e.g. Biegler et al. (1997) or Holland (1981).

1.3. Process simulation and optimization

Commercial simulation environments

As already mentioned, in order to perform process simulation with commercial process simulators, the user has to specify a precise value for each degree of freedom. The number of degrees of freedom is given by the problem and cannot be changed. After fixing the degrees of freedom, the simulation software tries to solve the resulting nonlinear system of equations where the number of variables equals the number of equations, usually using Newton-type methods (Naphtali & Sandholm, 1971; Ishii & Otto, 1973; Vickery & Taylor, 1986) including the inside-out method by Boston & Sullivan (1974). See also Kelley (1995) and Dennis & Schnabel (1996) for a more mathematical view on Newton-type methods. Convergence failures may turn process simulation into a very time-consuming task. This is especially cumbersome in process optimization in which the underlying system of nonlinear equations has to be solved many times.

In general, the approach described above does not reflect the demands in process engineering. Product purities, for example, require rather inequality constraints than equality constraints. The fact that certain values have to be fixed impedes a full exploration of process limitations and restricts the user to a small subset of the solution space. Freeing optimization variables and changing equality to inequality constraints to extend the feasible solution space is typically done only in a subsequent optimization step, which requires repeated calls of the simulation with different parameters and increases the risk of encountering numerical failures.

Flowsheet simulators can be classified as modular or equation-oriented. In the (sequential) modular mode the different units of a flowsheet are simulated individually as subprograms and in case recycle streams are present the entire flowsheet is iteratively converged at a higher level introducing tear streams. In the equation-oriented mode all process equations are assembled and solved simultaneously. An advantage of the equation-oriented mode is the fact that the user is slightly more flexible in terms of design specifications. However, this mode requires a large-scale nonlinear equation solver and is much harder to initialize

than the modular mode. We also refer to Biegler et al. (1997, Chap. 8) for further discussion on modular and equation-oriented flowsheeting methods and recent work of Dowling & Biegler (2015).

State of the art process simulation software usually covers the simulation and optimization of standard unit models such as distillation columns, heat exchangers, reactors, and many more as well as the treatment of an entire flowsheet. Widely used process simulators are ASPEN PLUS[®], HYSYS[®], and PROII[®], just to name a few. For more information on process simulation environments the reader is referred to Biegler et al. (1997, Appendix C) and Biegler (2014).

Simultaneous simulation and optimization

Instead of solving large systems of nonlinear equations during simulation, as done in most process simulation environments, one could also embed process simulation in an optimization problem by incorporating all model equations as constraints whereas the process variables serve as optimization variables (Biegler et al., 1997; Dowling & Biegler, 2015). An important advantage of this equation-based optimization approach is the possibility to include an arbitrary number of additional equalities and inequalities that represent the desired process design. The large nonlinear system of equations is no longer solved via Newton-type methods. Instead a solution is found by solving the optimization problem using nonlinear optimization solvers that have full access to all model equations and process variables. This approach enables simultaneously converging and optimizing a flowsheet by adding suitable objective functions. One challenge of this approach is the fact that the resulting optimization problems are large and may be difficult to solve. Large-scale sequential quadratic programming (SQP) strategies have been developed and analyzed by Murray & Wright (1978), Nocedal & Overton (1985), Schmid & Biegler (1994), and Biegler et al. (1995).

Process simulation and process optimization can also be performed simultaneously by applying infeasible path optimization (see Biegler & Hughes, 1982; Biegler & Cuthrell, 1985; Biegler, 1985; Biegler et al., 1997). Thereby, the different units of a flowsheet are simulated individually and in sequence as building blocks by solving the corresponding square systems of equations. Optimization is incorporated at a higher level in order to iteratively converge the tear streams that have been introduced to break recycle streams. Hence, only those process variables and equations that correspond to the tear streams need to be considered in the optimization problem. This approach is easy to construct

and to initialize due to the fact that it relies on building blocks that have been studied extensively. However, the systems of equations for the different unit models have to be solved many times during the execution and intermediate convergence failures due to inappropriate starting points or unreachable specifications have to be prevented.

Alternative approaches

Furthermore, we also want to mention that there exist completely different approaches for the calculation of distillation columns. One possibility are collocation methods that yield a reduced order model (Cho & Joseph, 1983a,b, 1984; Srivastava & Joseph, 1985, 1987a,b; Stewart et al., 1985; Huss & Westerberg, 1996a,b) whereas the idea of collocation is originally applied in the context of numerically solving differential equations. Recent work (Kim et al., 2010; Kim & Linninger, 2010; Ruiz et al., 2011) combines the minimum bubble-point distance algorithm embedded in the temperature collocation method with column profile maps aiming for rigorous separation design.

1.4. Shortcut techniques for distillation processes

The question whether given specifications are feasible has been widely addressed in conceptual process design, which is in general based on simplified models or so-called shortcut techniques. In contrast to the described approach using the full set of MESH equations, shortcut techniques facilitate a fast evaluation of alternatives. One area of research discusses the question of minimum flow and minimum energy demand (MED) in distillation, especially in awareness of rising energy costs. One of the earliest papers in this field and the basis for subsequent research is the work of Lewis & Matheson (1932) and Underwood (1948) for ideal mixtures under the simplifying assumption of constant relative volatility (CRV) and constant molar overflow (CMO). Doherty and co-workers (Levy et al., 1985; Van Dongen & Doherty, 1985; Levy & Doherty, 1986) introduced the boundary value method (BVM), which is based on stage-to-stage calculations of column profiles at CMO. In this method, the rectifying profile is integrated from top to the feed stage while the stripping profile is integrated from bottom to the feed stage and a feasible column configuration requires the rectifying and stripping profiles to intersect. The BVM can only be applied to mixtures with up to four components. Julka & Doherty (1990) extended this method to multi-component systems using the zero-volume criterion.

A significant advantage of shortcut methods using stage-to-stage calculations is the fact that, under the assumption of CMO and based on the knowledge of the top and bottom product compositions, it is possible to derive explicit expressions for all unknown compositions. Hence, this method usually results in stable and efficient distillation calculations as it does not require sophisticated solution strategies for nonlinear equation systems.

There exist several other methods, which we do not want to discuss in detail, such as the method by Köhler et al. (1991), which is based on reversible distillation and the eigenvalue method by Pöllmann et al. (1994). The rectification body method (RBM) proposed by Bausa et al. (1998) introduces triangular rectification bodies for the stripping and rectifying section of a column and requires these rectification bodies to intersect for a feasible column design. Urdaneta et al. (2004) extended the RBM to reactive distillation whereas Zhang & Linninger (2004) introduced a BVM based on minimum bubble-point distance. Halvorsen & Skogestad (2003) proposed the concept of V_{\min} diagram in order to visualize the relation between minimum energy consumption and feed distribution. A new concept, the so-called column profile maps, was proposed by Tapp et al. (2004) and Holland et al. (2004). This method based on difference point equations assuming CRV and CMO allows for the graphical representation of all possible profiles achievable by the difference point X_{Δ} and reflux ratio R_{Δ} enabling the user to get an insight into the system behavior and to choose the optimal profile for the desired separation. The work of Lucia et al. (2006) and Lucia et al. (2008) uses the shortest stripping line approach in order to find minimum energy requirements.

Köhler et al. (1995) and Bausa et al. (1998) give a comprehensive survey of methods for calculating the MED. In summary, we can conclude that many of the proposed methods in the field of minimum energy consumption are based on stage-to-stage calculations of distillation columns mostly under the simplifying assumption of CRV and CMO.

Shortcuts techniques can also be applied in order to identify feasible separations. One example is the ∞/∞ -analysis developed by Petlyuk & Avet'yan (1971) and Serafimov et al. (1973) as the limiting case of the equilibrium stage model for columns with an infinite number of stages and infinite reflux. In this limiting case, a simplified model with optimal separation properties is obtained. This analysis was used to predict multiple steady states in azeotropic distillation (Bekiaris et al., 1993, 1996; Bekiaris & Morari, 1996; Güttinger

& Morari, 1997) and recently also for conceptual process design (Ryll et al., 2012, 2013). Recent work of Petlyuk et al. (2015) enables the search and identification of feasible splits of extractive distillations.

However, even if we can assure that the chosen specifications are feasible using sophisticated techniques as described above, convergence failures can still occur due to inappropriate starting values when applying Newton's method.

1.5. Contributions

In this thesis, we want to address the problems in process simulation of distillation-based flowsheets introduced above and present an approach that facilitates robust, flexible, and simultaneous steady state process simulation and optimization of distillation-based flowsheets using ideas from ∞/∞ -analysis based on a simplified model for an asymptotic limiting case.

A new approach for simultaneous process simulation and optimization

We have seen that process simulation in commercial systems is in general conducted via first fixing all degrees of freedom and then solving the large nonlinear systems of equations. In this thesis, we break this paradigm and propose an approach that embeds process simulation in an optimization problem that only includes a small subset of the process variables and the model equations explicitly as optimization variables and constraints, respectively. As the resulting optimization problems consist only of a few optimization variables and constraints they do not require large-scale optimization solvers. However, the question arises which process variables and model equations should be included explicitly in the optimization problem and whether all process variables can be determined in a guaranteed way when knowing the optimization variables and using the remaining model equations. This question has to be answered individually for each unit model. This need should not be considered as a drawback of the approach but rather as a positive feature which adds flexibility. Tailored strategies are presented for flash units and distillation columns, and it is shown how these ideas can be extended to distillation-based flowsheets with recycle streams. In order to compute all process variables of a distillation column, an algorithm based on the stage-to-stage solution of fixed-point problems is used in the present work, which is shown to have guaranteed convergence for a suitable choice of input

variables. A good guess for almost all input variables of the stage-to-stage calculations can be generated by ∞/∞ -analysis, and we derive guidelines for the choice of the missing input variables.

The Banach fixed-point theorem applied to stage-to-stage calculations of distillation columns

Due to the inherent structure of the equilibrium stage distillation column model it is quite natural to decompose the system of equations and to consider stage-to-stage calculations of distillation columns instead of solving the underlying equations for all stages simultaneously. Early work in this field stems from Lewis & Matheson (1932) and Thiele & Geddes (1933) and is based on equation tearing. Holland (1963), Billingsley (1970), and Haas et al. (2007) enhanced the method of Thiele and Geddes. In the work of Friday & Smith (1964) different tearing techniques for solving the MESH equations were analyzed. Depending on the type of problem, the bubble-point method, a modification of the approach by Amundson & Pontinen (1958), or the sum-rates method, developed by Sujata (1961) in conjunction with the tridiagonal matrix formulation as described in Burningham & Otto (1967), was suggested. In more recent work, the sum-rates method was modified by Lucia and co-workers who developed a method that is good for both wide boiling and narrow boiling mixtures (Sridhar & Lucia, 1990a,b; Lucia & Li, 1992). Rose et al. (1958) developed the relaxation method, which uses stage-to-stage calculations and computes the gradual changes in the stage and product compositions until a steady state is reached. This method was extended for example by Ketchum (1979) and Mori and co-workers (Mori et al., 1987b,a, 1990).

In this thesis, a new numerically stable and efficient approach for stage-to-stage calculations of distillation columns is presented that does not use the assumption of CMO but the full set of MESH equations. A feature of this approach is that the nonlinear system of equations for the transition from one stage to the next is reformulated as a fixed-point problem. This fixed-point problem can be solved by fixed-point iteration without computing derivatives based on only a small number of given input variables. In contrast to several other approaches for stage-to-stage calculations with energy balances, the number of fixed variables does not depend on the number of stages of the column. Only a small set of particular variables has to be given at either bottom or top of the column in order to determine the column profile via stage-to-stage calculations. The fixed-point iteration converges in general very fast. To get a better insight into this

phenomenon, a detailed analysis is conducted in this work. Here, the asymptotic limiting case of a distillation column with an infinite reflux ratio is of special interest. In this special case, the underlying model equations significantly simplify and convergence of the fixed-point iteration is guaranteed. We apply the Banach fixed-point theorem to the derived fixed-point problems and prove that a unique fixed point exists and that the convergence to that point is guaranteed, if certain minimum requirements on the energy, which we derive, are fulfilled.

Stage-to-stage calculations as a boundary value problem

In order to calculate a distillation column by a stage-to-stage approach, the pressure, the flow rate and composition of a product stream, and the duty of the reboiler, or condenser respectively, are specified at one end of the column and serve as input for the simulation. Depending on the choice of these values several scenarios are possible. If the duty does not fulfill certain minimum requirements that are derived here using the Banach fixed-point theorem, there exists no solution to the MESH equations and it is not possible to conduct stage-to-stage calculations of the column. Even if the energy requirements are fulfilled, it is still not guaranteed that the fixed variables at one end of the column yield a feasible solution. This is due to the fact that we fixed more variables than there are degrees of freedom for the column, i.e. the column is over-specified. By embedding stage-to-stage calculations in an optimization problem, the given values serve as optimization variables and can be adapted in a way that a feasible distillation column is obtained. This idea is closely related to the solution of boundary value problems (BVP) (Stoer & Bulirsch, 2005, Chap. 7.3) for ordinary differential equations (ODE) using the shooting method. The stage-to-stage calculations can be regarded as the solution of an ODE with fixed step size and the fixed process variables at one end of the column are related to the given initial value for an ODE. The "boundary value" that should be achieved is the composition of the second product stream of the column, which is already fixed using the overall material balance of the column but also computed as simulation output of the stage-to-stage calculations.

An algorithm for the calculation order of the unit operations in a distillation-based flowsheets

The new approach for integrated process simulation and optimization is not only applicable to single units but, in this thesis, we also present the extension of the approach to distillation-based flowsheets, which typically consist of several units of the same or different types that are connected via streams. Analogously to the modular and the equation-oriented approach in classical process simulation, this novel approach can also be realized in a modular or a simultaneous way. Whereas the modular approach can be realized relatively straightforward, the simultaneous way requires determination of a feasible calculation order of the units in a flowsheet within one iteration. We present an algorithm that translates a distillation-based flowsheet into a graph representation and computes a feasible calculation order of the units.

1.6. Outline

The remainder of the thesis is organized as follows:

Chapter 2 briefly reviews the mathematical principles that are applied in this thesis. We mainly focus on the theory of nonlinear optimization, multi-criteria optimization and shooting methods for ordinary differential equations.

In Chapter 3 we present a novel approach that embeds process simulation in an optimization problem with a small number of optimization variables and constraints focusing on single units. We present tailored strategies of setting up the optimization problem for a flash unit and a distillation column using the shooting method and discuss the advantages and possible extensions of the approach.

Chapter 4 is devoted to the development and detailed analysis of a numerically robust algorithm for stage-to-stage calculations of distillation columns that facilitates the computation of all unknown process variables for the column based on given input variables. In this chapter, we restrict ourselves to simple columns with only one feed and no side-draws. The transition from one stage to the next one is formulated as a fixed-point problem and by applying the Banach fixed-point theorem it is possible to derive energy bounds that guarantee the existence and convergence of a fixed point. We illustrate the theoretical results from Chapter 4 with a numerical example in Section 4.4. For our numerical studies a binary system containing acetone and chloroform is considered.

In Chapter 5 we extend the algorithm for stage-to-stage calculations of distillation columns to general columns with an arbitrary number of feed streams and side-draws. For the general case, we conduct a similar analysis as in Chapter 4 and due to these similarities we omit most proofs in this chapter.

The presented approach for integrated process simulation and optimization is extended to distillation-based flowsheets consisting of several units and recycle streams in Chapter 6. We present two different approaches: the modular and the simultaneous approach and state an algorithm that determines the calculation order of the different units within one iteration for the simultaneous approach.

In Chapter 7 we present typical examples for process simulation and optimization of single units and distillation-based flowsheets comprising several columns and also recycle streams. By means of suitable examples we illustrate the robustness of the presented approach with respect to poor initial values and the gain in flexibility with regard to the problem formulation. Furthermore, we have guidelines at hand for the choice of input variables for the distillation and do not have to fix all degrees of freedom as a prerequisite for process simulation which makes it in general easier to find a feasible solution. Besides typical nonlinear optimization problems, we also present examples that are concerned with mixed-integer and multi-criteria optimization problems.

We conclude in Chapter 8 with a summary and a short outlook on future research directions.

CHAPTER 2

Mathematical principles

In this chapter, the mathematical principles that are needed for the approach developed in this thesis are presented. In Section 2.1, the theory and a solution strategy for nonlinear optimization problems are briefly reviewed. Section 2.2 presents well-known concepts for multi-criteria optimization. Section 2.3 is devoted to the theory of shooting methods which are originally designated for the solution of boundary value problems in the context of ordinary differential equations.

2.1. Nonlinear optimization

In this section, we review the theory of nonlinear optimization that is needed in this work. An elaborate description of the relevant concepts can be found in Bazaraa et al. (1993), Bertsekas (1999), Geiger & Kanzow (1999), and Geiger & Kanzow (2002).

An *optimization problem* in general form can be written in the following way: Let $n \in \mathbb{N}^*$, $m, p \in \mathbb{N}$, and f, g_i , and h_j functions mapping from \mathbb{R}^n to \mathbb{R} for all $i = 1, \dots, m$, and $j = 1, \dots, p$. We want to find a solution of

$$\begin{aligned}
 \min_{\mathbf{x} \in \mathbb{R}^n} \quad & f(\mathbf{x}) \\
 \text{s.t.} \quad & g_i(\mathbf{x}) \leq 0, \quad i = 1, \dots, m \\
 & h_j(\mathbf{x}) = 0, \quad j = 1, \dots, p.
 \end{aligned} \tag{2.1}$$

The function f is called *objective function* of (2.1). Each of the constraints $g_i(\mathbf{x}) \leq 0$, $i = 1, \dots, m$, is called an *inequality constraint* and each of the constraints $h_j(\mathbf{x}) = 0$, $j = 1, \dots, p$, is called an *equality constraint*. The constraint functions g_i can also be summarized as a vector valued function $\mathbf{g} : \mathbb{R}^n \rightarrow \mathbb{R}^m$ and the constraint functions h_j can be summarized in the same way as $\mathbf{h} : \mathbb{R}^n \rightarrow \mathbb{R}^p$. In case we have $m = p = 0$, we call (2.1) an *unconstrained optimization problem*, otherwise we are talking about a *constrained optimization problem*.

If the objective f and the constraints \mathbf{g} and \mathbf{h} are linear functions of \mathbf{x} , the problem is called a *linear optimization problem* (LP). If the objective f or the constraints \mathbf{g} , and \mathbf{h} depend not only on real variables $\mathbf{x} \in \mathbb{R}^n$ but also on integer variables $\mathbf{y} \in \mathbb{R}^k$ we call (2.1) a *mixed-integer optimization problem* (MIP). In this work, we concentrate on *nonlinear optimization problems* (NLPs), in which at least some of the constraints or the objective are nonlinear.

Any $\mathbf{x} \in \mathbb{R}^n$ that satisfies all constraints is called a *feasible solution*. A feasible solution \mathbf{x}^* such that $f(\mathbf{x}) \geq f(\mathbf{x}^*)$ for any feasible $\mathbf{x} \in \mathbb{R}^n$ is called an *optimal solution* to (2.1).

W.l.o.g. we can restrict ourselves to the consideration of minimization problems as a maximization problem can be transformed into a minimization problem by writing

$$\max_{\mathbf{x} \in \mathbb{R}^n} f(\mathbf{x}) = - \min_{\mathbf{x} \in \mathbb{R}^n} -f(\mathbf{x}). \tag{2.2}$$

Many efforts have been made in order to develop solution strategies for constrained nonlinear optimization problems. One widely-used approach is the *sequential quadratic programming* (SQP). SQP methods are iterative methods. In each iteration step $k \in \mathbb{N}^*$ an appropriate search direction \mathbf{d}_k is determined via solution of an optimization problem with special structure. At iterate $(\mathbf{x}_k, \boldsymbol{\lambda}_k, \boldsymbol{\mu}_k)$ the search direction \mathbf{d}_k is defined as the

solution of

$$\begin{aligned} \max_{\mathbf{d} \in \mathbb{R}^n} \quad & \frac{1}{2} \mathbf{d}^T \nabla_{\mathbf{x}\mathbf{x}}^2 \mathcal{L}(\mathbf{x}_k, \boldsymbol{\lambda}_k, \boldsymbol{\mu}_k) \mathbf{d} + \nabla f(\mathbf{x}_k)^T \mathbf{d} \\ \text{s.t.} \quad & \nabla g_i(\mathbf{x}_k)^T \mathbf{d} + g_i(\mathbf{x}_k) \leq 0, \quad i = 1, \dots, m \\ & \nabla h_j(\mathbf{x}_k)^T \mathbf{d} + h_j(\mathbf{x}_k) = 0, \quad j = 1, \dots, p, \end{aligned} \quad (2.3)$$

where \mathcal{L} is the *Lagrangian function* defined as

$$\mathcal{L}(\mathbf{x}, \boldsymbol{\lambda}, \boldsymbol{\mu}) := f(\mathbf{x}) - \boldsymbol{\lambda}^T \mathbf{g}(\mathbf{x}) - \boldsymbol{\mu}^T \mathbf{h}(\mathbf{x}) \quad (2.4)$$

with *Lagrange multiplier* $\boldsymbol{\lambda} \in \mathbb{R}^m$ and $\boldsymbol{\mu} \in \mathbb{R}^p$.

If \mathbf{d}^* is the optimal solution of (2.3) with corresponding Lagrange multipliers $(\boldsymbol{\lambda}^*, \boldsymbol{\mu}^*)$ the new iterate is obtained via

$$\begin{pmatrix} \mathbf{x}_{k+1} \\ \boldsymbol{\lambda}_{k+1} \\ \boldsymbol{\mu}_{k+1} \end{pmatrix} = \begin{pmatrix} \mathbf{x}_k \\ \boldsymbol{\lambda}_k \\ \boldsymbol{\mu}_k \end{pmatrix} + \alpha_k \begin{pmatrix} \mathbf{d}^* \\ \boldsymbol{\lambda}^* - \boldsymbol{\lambda}_k \\ \boldsymbol{\mu}^* - \boldsymbol{\mu}_k \end{pmatrix}, \quad (2.5)$$

where α_k is an appropriate step length.

For a more detailed description of the implementation of SQP methods and step size control the reader is referred to Han (1977) and Powell (1978) for the origin of this method and Nocedal & Wright (2006) and Schittkowski (2011) for more recent work in this field.

2.2. Multi-criteria optimization

The field of multi-criteria optimization (MCO) deals with optimization problems where a best possible compromise should be found by evaluating a number of conflicting objectives. In this section, the mathematical principles of multi-criteria are presented and techniques for deterministic multi-criteria optimization are introduced, which are in part also used within the scope of this thesis. For more details on multi-criteria optimization the reader is referred to, e.g. Steuer (1989), Hillier & Miettinen (1998), Ehrgott (2005), Rangaiah (2009).

A *multi-criteria optimization problem* in its general form can be formulated as follows:

$$\begin{aligned} \min_{\mathbf{x} \in \mathbb{R}^n} \quad & (f_1(\mathbf{x}), f_2(\mathbf{x}), \dots, f_k(\mathbf{x})) \\ \text{s.t.} \quad & \mathbf{x} \in S. \end{aligned} \tag{2.6}$$

We consider $k \geq 2$ different *objective functions* $f_i : \mathbb{R}^n \rightarrow \mathbb{R}$, which should be minimized. Furthermore, $\mathbf{x} \in \mathbb{R}^n$ are the *decision variables* from the nonempty *feasible region* $S \subseteq \mathbb{R}^n$.

Definition 2.1 (Ehrgott (2005), p.24). *A feasible solution $\hat{\mathbf{x}} \in S$ is called efficient or Pareto optimal if there is no other $\mathbf{x} \in S$ such that $f_i(\mathbf{x}) \leq f_i(\hat{\mathbf{x}})$ for all $i = 1, \dots, k$. If $\hat{\mathbf{x}}$ is efficient, $\mathbf{f}(\hat{\mathbf{x}})$ is called nondominated point. The set of all efficient solutions is called the efficient set or Pareto set.*

Best compromises are supposed to be found among the set of Pareto optimal solutions. In the following, two strategies for finding Pareto optimal solutions are presented.

Weighting method

When applying the *weighting method* (Gass & Saaty, 1955; Zadeh, 1963) the following single-objective optimization problem is solved using appropriate techniques:

$$\begin{aligned} \min_{\mathbf{x} \in \mathbb{R}^n} \quad & \sum_{i=1}^k \omega_i f_i(\mathbf{x}) \\ \text{s.t.} \quad & \mathbf{x} \in S, \end{aligned} \tag{2.7}$$

where $\omega_i \geq 0$ for all $i = 1, \dots, k$ and $\sum_{i=1}^k \omega_i = 1$.

One weakness of the weighting method is the fact that not all Pareto optimal solutions can be found unless the problem is convex. Conditions under which the whole Pareto optimal set can be generated by the above method are presented in Censor (1977).

ε -constraint method

Within the scope of the *ε -constraint method* (Haimes et al., 1971), one of the objective functions is optimized in the following way:

$$\begin{aligned} \min_{\mathbf{x} \in \mathbb{R}^n} \quad & f_l(\mathbf{x}) \\ \text{s.t.} \quad & f_j(\mathbf{x}) \leq \varepsilon_j, \quad j = 1, \dots, l-1, l+1, \dots, k, \\ & \mathbf{x} \in S, \end{aligned} \tag{2.8}$$

with $\varepsilon_j \in \mathbb{R}$ upper bounds for the objectives $j \neq l$.

In contrast to the weighting methods, the ε -constraint method is able to find all Pareto optimal points even if the problem is not convex.

There exist more elaborate approaches that facilitate efficient approximation of the Pareto set and techniques that help finding the best compromise. The work of Bortz et al. (2014) uses some of these concepts in order to deal with MCO in chemical engineering and decision support.

2.3. Ordinary differential equations and the shooting method

Ordinary differential equations (ODEs) arise frequently in the context of engineering and science. In the general case, we are looking for an n -dimensional differentiable function

$$\mathbf{y}(x) := \begin{pmatrix} y_1(x) \\ \vdots \\ y_n(x) \end{pmatrix}, \tag{2.9}$$

which is a function of x and fulfills

$$\mathbf{y}'(x) = \mathbf{f}(x, \mathbf{y}(x)), \tag{2.10}$$

where \mathbf{f} is an n -dimensional function of the form

$$\mathbf{f}(x, \mathbf{y}(x)) := \begin{pmatrix} f_1(x, \mathbf{y}(x)) \\ \vdots \\ f_n(x, \mathbf{y}(x)) \end{pmatrix}. \tag{2.11}$$

We call (2.10) an ODE in explicit form. In general, there exist infinitely many functions \mathbf{y} that solve (2.10). The solution space can be restricted by additionally imposing an *initial value* of the form

$$\mathbf{y}(x_0) = \mathbf{y}_0. \quad (2.12)$$

Equation (2.10) together with (2.12) is called an *initial value problem* (IVP).

Apart from IVPs for systems of ODEs, real-life applications often deal with *boundary value problems* (BVPs). For this class of problems, the solution \mathbf{y} is supposed to fulfill a *boundary condition* of the most general form

$$\mathbf{r}(\mathbf{y}(a), \mathbf{y}(b)) = 0, \quad (2.13)$$

where $a \neq b$ and \mathbf{r} is an n -dimensional function of $2n$ unknowns.

In contrast to IVPs that are usually uniquely solvable for an arbitrary initial value (cf. Stoer & Bulirsch (2005, Theorem (7.1.1))), BVPs might also have no solution or multiple solutions depending on the choice of the boundary conditions.

A well-known solution strategy for BVPs is the *shooting method*. This approach attempts to find a solution of the IVP

$$\mathbf{y}'(x) = \mathbf{f}(x, \mathbf{y}(x)), \quad \mathbf{y}(a) = \mathbf{s}, \quad (2.14)$$

with $\mathbf{s} \in \mathbb{R}^n$ such that $\mathbf{y}(x) := \mathbf{y}(x; \mathbf{s})$ fulfills the boundary conditions (2.13)

$$\mathbf{r}(\mathbf{y}(a; \mathbf{s}), \mathbf{y}(b; \mathbf{s})) \equiv \mathbf{r}(\mathbf{s}, \mathbf{y}(b; \mathbf{s})) = 0. \quad (2.15)$$

In order to solve BVPs using the shooting method, we can reformulate this task as finding the root of a function $\mathbf{F}(\mathbf{s})$ with

$$\mathbf{F}(\mathbf{s}) := \mathbf{r}(\mathbf{s}, \mathbf{y}(b; \mathbf{s})), \quad (2.16)$$

for example by using Newton's method.

We illustrate the shooting method with an example (see also Stoer & Bulirsch (2005, Chap. 7.3.1)). Let the following one-dimensional BVP be given:

$$y'(x) = y(x), \quad y(0) = s, \quad y(1) = 3. \quad (2.17)$$

In this example, the boundary conditions are given in separated form. The IVP

$$y'(x) = y(x), \quad y(0) = s \quad (2.18)$$

will in general have a unique solution $y(x) \equiv y(x; s)$ that depends on the choice of s . The goal is now to determine s^* in such a way that it holds

$$y(1) \equiv y(1; s^*) = 3 \quad (2.19)$$

or in other words to find a root of the function

$$F(s) := y(1; s) - 3. \quad (2.20)$$

The evaluation of the function F requires the solution of the IVP (2.18). In this simple example, it is possible to derive the analytical solution of (2.18). In the general case, the solution of the IVP can only be obtained by numerical integration as described for example in Hairer et al. (1993). The function $y(x; s)$ is depicted in Figure 2.1 for different choices of s , including the root of F which is at $s^* = 1.1036$ in this example.

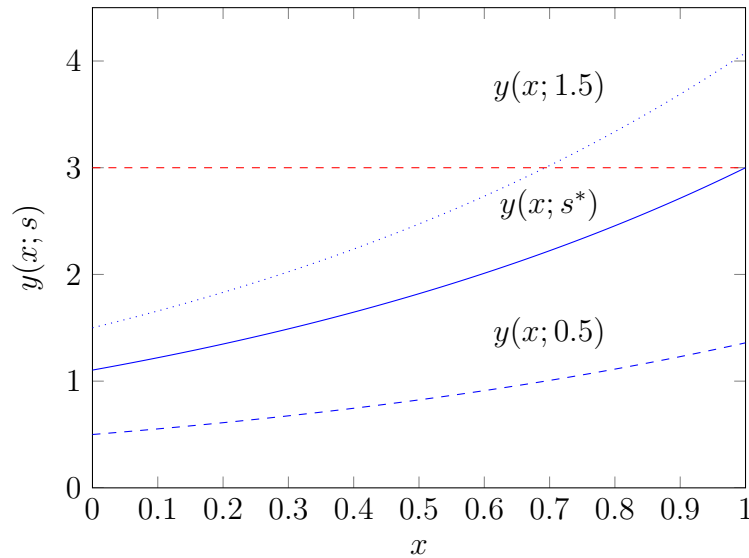


Figure 2.1.: Plot of $y(x; s)$ for different choices of s . The dashed curve represents $s = 0.5$, the dotted curve $s = 1.5$, and the solid curve depicts the choice of s such that (2.19) is fulfilled. The horizontal line at $y(x) = 3$ indicates the desired boundary value at $x = 1$.

2. *Mathematical principles*

For a more detailed review on the mathematical theory and solution strategies for ODEs and BVPs we refer the reader to Grüne & Junge (2009), Teschl (2012), Deuffhard & Bornemann (2008), Hairer et al. (1993), and Stoer & Bulirsch (2005).

Embedding process simulation in an optimization problem

Commercial flowsheet simulators generally require the specification of fixed values for every degree of freedom and try to solve the resulting square system of nonlinear equations in a subsequent step. At this point, flowsheet simulators still encounter problems with regard to the numerical stability of solution strategies for the underlying system of nonlinear equations. This fact potentially turns process simulation into a tedious task. For process optimization the situation is even worse, as it requires a convergent simulation run as a starting point and repeatedly calls the process simulation during its execution.

In this chapter, a new approach is presented, which embeds the process simulation in an optimization problem with a small number of optimization variables and constraints. Hence, large-scale solvers are not needed. The question which process variables and model equations should be included explicitly in the optimization problem and which process variables can be determined via simulation in a guaranteed way using the remaining model equations has to be answered individually for each unit model. To illustrate the new approach, we present tailored strategies for a simple flash unit and a distillation column. Especially the strategy for distillation columns was strongly inspired by the asymptotic limiting cases of distillation columns with an infinite number of stages and infinite reflux ratio. The presented approach facilitates simultaneous flowsheet simulation and optimization. Moreover, an arbitrary number of specifications in the form of equalities

or inequalities can be incorporated in the problem formulation. This matches the process engineering demands usually much better than specifying a given quantity of fixed numbers, when fixing the degrees of freedom.

3.1. General idea

The new approach described in this work is based on solving the MESH equations by formulating this task as an optimization problem. Whenever process simulation is formulated as an optimization problem, it is possible to incorporate an arbitrary number of additional inequality and equality constraints which represent the specifications of the process. This leads to significantly more flexibility in terms of problem formulation. However, not all process variables are incorporated in the optimization problem as optimization variables and not all MESH equations are included as constraints. The approach is particularly attractive when it is possible to obtain solutions for the equations which are not incorporated in the optimization problem as constraints in a robust manner.

For the following considerations we define \mathcal{I}_{eq} to be the set of indices for the model equations and \mathcal{I}_{var} to be the set of indices for the process variables with $|\mathcal{I}_{\text{eq}}| =: N_{\text{eq}}$ and $|\mathcal{I}_{\text{var}}| =: N_{\text{var}}$. The number of degrees of freedom is $N_{\text{dof}} = N_{\text{var}} - N_{\text{eq}}$. We introduce the notation $\mathbf{x}_{\text{var}} := (x_j)_{j \in \mathcal{I}_{\text{var}}} \in \mathbb{R}^{N_{\text{var}}}$ and $\mathbf{x}_{\text{opt}} := (x_j)_{j \in \mathcal{I}_{\text{opt}}} \in \mathbb{R}^{N_{\text{opt}}}$ for the process variables and optimization variables, respectively. Furthermore, we write

$$\mathbf{g}_{\text{eq}}(\mathbf{x}_{\text{var}}) := (g_j(\mathbf{x}_{\text{var}}))_{j \in \mathcal{I}_{\text{eq}}} \in \mathbb{R}^{N_{\text{eq}}}, \quad (3.1)$$

with $g_j : \mathbb{R}^{N_{\text{var}}} \rightarrow \mathbb{R}$, $j \in \mathcal{I}_{\text{eq}}$. The model equations are formulated in such a way that $\mathbf{g}_{\text{eq}}(\mathbf{x}_{\text{var}}) = \mathbf{0}$. \mathcal{S}_{eq} and $\mathcal{S}_{\text{ineq}}$ are the sets of indices for the desired specifications which are formulated as equalities or inequalities, respectively. The number of specifications given as equalities $|\mathcal{S}_{\text{eq}}|$ as well as the number of specifications given as inequalities $|\mathcal{S}_{\text{ineq}}|$ is arbitrary and thus not referred to in the following discussion. To solve the flowsheet problem, an optimization problem is formulated in the following general form:

Definition 3.1 (General optimization problem for process simulation). *Let $\mathbf{x}_{\text{var}} \in \mathbb{R}^{N_{\text{var}}}$ be the vector of process variables and $\mathbf{x}_{\text{opt}} \in \mathbb{R}^{N_{\text{opt}}}$ be the vector of optimization variables. Furthermore, let $\mathcal{I}_{\text{constr}} \subseteq \mathcal{I}_{\text{eq}}$ be a set of indices for the model equations that serve as constraints and $\mathcal{I}_{\text{opt}} \subseteq \mathcal{I}_{\text{var}}$ a set of indices for the optimization variables. The general*

optimization problem for process simulation is defined as

$$\begin{aligned}
 \min_{\mathbf{x}_{opt}} \quad & f(\mathbf{x}_{var}) & (3.2) \\
 \text{s.t.} \quad & g_j(\mathbf{x}_{var}) = 0, & j \in \mathcal{I}_{constr} \\
 & s_k(\mathbf{x}_{var}) = 0, & k \in \mathcal{S}_{eq} \\
 & s_l(\mathbf{x}_{var}) \leq 0, & l \in \mathcal{S}_{ineq},
 \end{aligned}$$

with the objective function $f : \mathbb{R}^{N_{var}} \rightarrow \mathbb{R}$, and the constraints $g_j : \mathbb{R}^{N_{var}} \rightarrow \mathbb{R}$, $j \in \mathcal{I}_{constr}$ and $s_j : \mathbb{R}^{N_{var}} \rightarrow \mathbb{R}$, $j \in \mathcal{S}_{eq} \cup \mathcal{S}_{ineq}$.

One possibility is to choose $\mathcal{I}_{constr} = \mathcal{I}_{eq}$ and $\mathcal{I}_{opt} = \mathcal{I}_{var}$ which means that all process variables are regarded as optimization variables and all model equations are included explicitly as constraints in the optimization problem. This typically leads to an optimization problem with hundreds or thousands of optimization variables and constraints and requires a large-scale optimization solver. Within the scope of this work, we do not consider large-scale optimization strategies but want to focus on small optimization problems. Hence, $N_{constr} := |\mathcal{I}_{constr}|$ is supposed to be much smaller than N_{eq} and N_{opt} is supposed to be much smaller than N_{var} .

The novel approach presented in this work incorporates only a small number of model equations explicitly as constraints and only few well selected process variables are used as optimization variables, i.e. we suitably choose a set of indices for the constraints $\mathcal{I}_{constr} \subset \mathcal{I}_{eq}$ and a set of indices for the optimization variables $\mathcal{I}_{opt} \subset \mathcal{I}_{var}$. Thereby the number of optimization variables N_{opt} equals the number of the constraints N_{constr} plus the number of degrees of freedom N_{dof} , i.e.:

$$\begin{aligned}
 N_{opt} &= |\mathcal{I}_{opt}| \\
 &= |\mathcal{I}_{constr}| + |\mathcal{I}_{eq}| - |\mathcal{I}_{var}| \\
 &= N_{constr} + N_{dof}.
 \end{aligned} \tag{3.3}$$

The optimization solver ensures that the model equations included as constraints

$$g_j(\mathbf{x}_{var}) = 0, \quad j \in \mathcal{I}_{constr} \tag{3.4}$$

are solved when a solution is found.

3. Embedding process simulation in an optimization problem

The remaining $N_{\text{eq}} - N_{\text{constr}}$ model equations are not considered explicitly as constraints:

$$g_j(\mathbf{x}_{\text{var}}) = 0, \quad j \in \mathcal{I}_{\text{eq}} \setminus \mathcal{I}_{\text{constr}}. \quad (3.5)$$

A key idea of the present approach is to choose $\mathcal{I}_{\text{constr}}$ and \mathcal{I}_{opt} so that (3.5) can be solved for the process variables $\mathbf{x}_{\text{dep}} := (x_j)_{j \in \mathcal{I}_{\text{var}} \setminus \mathcal{I}_{\text{opt}}} \in \mathbb{R}^{N_{\text{var}} - N_{\text{opt}}}$ for given values of the optimization variables \mathbf{x}_{opt} by numerically robust solution strategies and without observing convergence failures. These strategies are tailor-made for the different unit models. Hence, it is possible to determine \mathbf{x}_{dep} as a function of \mathbf{x}_{opt} within each iteration and we can write $\mathbf{x}_{\text{dep}}(\mathbf{x}_{\text{opt}})$. Thus, the vector of process variables \mathbf{x}_{var} is composed by \mathbf{x}_{opt} and \mathbf{x}_{dep} . By construction, the number of process variables that are not chosen as optimization variables equals the number of remaining model equations, i.e.:

$$\begin{aligned} |\mathcal{I}_{\text{var}} \setminus \mathcal{I}_{\text{opt}}| &= N_{\text{var}} - N_{\text{constr}} - N_{\text{dof}} \\ &= N_{\text{eq}} - N_{\text{constr}} \\ &= |\mathcal{I}_{\text{eq}} \setminus \mathcal{I}_{\text{constr}}|. \end{aligned} \quad (3.6)$$

Hence, in a solution of (3.2) all N_{eq} equations of the original problem are solved. N_{constr} of them are incorporated as constraints in the optimization problem and the remaining $N_{\text{eq}} - N_{\text{constr}}$ equations are incorporated in the robust solution of the subproblem (3.5).

The objective function of the optimization problem (3.2) can be chosen as a constant function (e.g. 0). In that case, the optimization algorithm will try to find a solution that fulfills all MESH equations \mathbf{g}_{eq} and specifications $s_k(\mathbf{x}_{\text{var}}) = 0$, $k \in \mathcal{S}_{\text{eq}}$ and $s_l(\mathbf{x}_{\text{var}}) \leq 0$, $l \in \mathcal{S}_{\text{ineq}}$. Depending on the number of specifications and the choice of inequalities or equalities, there exists no solution (over-specification), exactly one solution, or there exist infinitely many solutions (under-specification). If there exist infinitely many solutions, then an optimization problem with constant objective function will output the first solution found, which usually depends on the starting values for the optimization variables and the optimization algorithm that is applied. However, it is also possible to choose the objective function to be a non-constant function depending on the process variables, which means that the obtained solution is optimal with respect to the objective function and enables simultaneous simulation and optimization. This point is discussed in detail in Section 3.4.

The described approach is illustrated with the examples of a simple flash calculation in Section 3.2 and the calculation of a distillation column in Section 3.3, which is an extremely important unit model in process simulation. An algorithm that facilitates numerically

robust calculation of \mathbf{x}_{dep} for simple distillation columns is presented in Chapter 4. The ideas are extended to general columns with an arbitrary number of feed streams and side-draws in Chapter 5.

3.2. Flash units

Consider the flash unit depicted in Figure 3.1. The model comprises the feed, the vapor and the liquid stream which have molar flow rates F , V , and L , respectively. The liquid and vapor mole fractions are $\mathbf{x} = (x_1, \dots, x_{N_C})$ and $\mathbf{y} = (y_1, \dots, y_{N_C})$, respectively, where N_C is the number of components in the system. The index i denotes the different components. The state of the feed stream is assumed to be completely defined, i.e. the feed flow rate and the mole fractions x_i^F , $i = 1, \dots, N_C$, are known and, in this example, the feed is assumed to be liquid boiling at a given pressure p^F . The pressure and temperature in the flash unit are denoted by p and T respectively, and the heat duty is denoted by \dot{Q} .

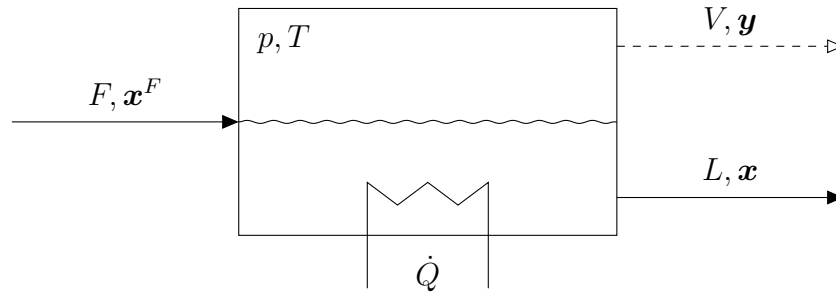


Figure 3.1.: Schematic model of a flash unit.

The flash unit is described by the following model equations:

- Material balances

$$F x_i^F = L x_i + V y_i, \quad i = 1, \dots, N_C. \quad (3.7)$$

- Equilibrium conditions

Extended Raoult's law is used here to describe the vapor-liquid equilibrium (VLE) (see also Appendix A.2):

$$p_i^S(T) x_i \gamma_i(\mathbf{x}, T) = p y_i, \quad \text{for } i = 1, \dots, N_C, \quad (3.8)$$

where $p_i^S(T)$ is the vapor pressure of the pure component i at temperature T and $\gamma_i(\mathbf{x}, T)$ is the activity coefficient of component i for the composition \mathbf{x} of the liquid phase at temperature T . We assume that for given pressure and composition of one of the phases in equilibrium the extended Raoult's law can be solved without any convergence failures. It is assumed that no second liquid phase (no LLE split) occurs along the column.

- Summation equations

$$\sum_{i=1}^{N_C} x_i = 1, \quad \text{and} \quad \sum_{i=1}^{N_C} y_i = 1. \quad (3.9)$$

- Energy balance (see also Appendix A.2)

$$\dot{Q} = Lh^l(\mathbf{x}, T) + Vh^v(\mathbf{y}, T) - Fh^l(\mathbf{x}^F, T^F), \quad (3.10)$$

with $h^l(\mathbf{x}, T)$ and $h^v(\mathbf{y}, T)$ being the enthalpies of the liquid and vapor phase, respectively, which depend on the composition and the temperature of the stream. In this work, the enthalpy h_i^v in the vapor phase of each component i at 298 K is set to 0 kJ/mol and the enthalpy of mixing is neglected in both phases, as well as the pressure dependence of the enthalpy.

Alternatively, it would also be possible to omit Equation (3.9) assuming implicitly that it is always fulfilled and to specify only $(N_C - 1)$ liquid and vapor mole fractions.

Under the above assumption of a completely defined feed stream, we obtain a system with $N_{\text{eq}} = (2N_C + 3)$ equations and $N_{\text{var}} = (2N_C + 5)$ unknowns, which has $N_{\text{dof}} = N_{\text{var}} - N_{\text{eq}} = 2$ degrees of freedom.

As already mentioned, there exist different possibilities of conducting process simulation. Following the classical Newton approach of solving square nonlinear systems of equations one could specify two unknowns and try to solve the resulting equation system.

As sketched in Section 3.1, we can also formulate process simulation as an optimization problem. Our goal is to choose the set $\mathcal{I}_{\text{constr}}$ small while it is still possible to solve for \mathbf{x}_{dep} in an easy and numerically robust manner.

An exemplary strategy is presented now to solve the flash unit problem where $N_{\text{constr}} = N_C$. As optimization variables p , $\dot{\mathbf{n}}^L := L\mathbf{x}$, and \dot{Q} are used, i.e. $N_{\text{opt}} = (N_C + 2)$. It is possible to compute the remaining variables based on the knowledge of these optimization

variables without using all model equations: Fixing values for $\dot{\mathbf{n}}^L$ uniquely determines L and \mathbf{x} . Furthermore, the temperature T and the composition vector of the vapor phase \mathbf{y} that is in equilibrium with \mathbf{x} can be determined by using the equilibrium equations and the summation equation for \mathbf{y} . The enthalpy equation can thereafter be used to determine the vapor flow rate V . In order to emphasize that the calculated values for T , \mathbf{y} , and V depend on the specific choice of the optimization variables p , $\dot{\mathbf{n}}^L$, and \dot{Q} we write $T(p, \dot{\mathbf{n}}^L, \dot{Q})$, $\mathbf{y}(p, \dot{\mathbf{n}}^L, \dot{Q})$, and $V(p, \dot{\mathbf{n}}^L, \dot{Q})$. At this point, values for all remaining unknowns have been determined using $N_{\text{eq}} - N_{\text{constr}} = (N_C + 3)$ model equations but the N_C material balance equations have not been used. They are included as constraints in the optimization problem, i.e. $N_{\text{constr}} = N_C$:

$$\begin{aligned} \min_{p, \dot{\mathbf{n}}^L, \dot{Q}} \quad & 0 \\ \text{s.t.} \quad & F\mathbf{x}^F = \dot{\mathbf{n}}^L + V(p, \dot{\mathbf{n}}^L, \dot{Q})\mathbf{y}(p, \dot{\mathbf{n}}^L, \dot{Q}). \end{aligned} \tag{3.11}$$

The equilibrium, summation and energy equations are not explicitly incorporated in the optimization problem as constraints as they are already enforced during the calculation of the remaining process variables at any iteration step of the optimization algorithm. The fact that the process variables cannot only be calculated for feasible but also for infeasible choices of values for the optimization variables facilitates the embedding of process simulation in an optimization problem. Although (3.11) is formulated as an optimization problem this approach basically solves the underlying system of MESH equations due to the fact that the constant objective 0 is incorporated here. Thus, the solution to (3.11) is typically not unique. Depending on the starting values for the optimization variables and the specific implementation of the optimization algorithm, the first feasible solution found by the optimization algorithm will be the final result.

The exemplary optimization problem (3.11) for a flash unit comprises $(N_C + 2)$ optimization variables and N_C constraints. The number of optimization variables is larger than the number of degrees of freedom, which need to be fixed for the classical Newton approach, but for systems with a moderate number of components this still results in a small optimization problem.

The optimization problem (3.11) can be regarded as an example for the more general case (3.2). However, one could also think of other examples by varying the number and choice of optimization variables and constraints. In this work, our goal is to find an

optimization problem with a small number of optimization variables that still enables solving for the remaining unknown process variables in a robust manner. As described above, this is the case here for Equations (3.8)–(3.10) in the variables p , $\dot{\mathbf{n}}^L$, and \dot{Q} .

3.3. Distillation columns in combination with the shooting method

The advantages of the presented method become evident when considering units with many process variables such as a distillation column. As depicted in Figure 3.2, the distillation column is modeled here as a cascade of equilibrium stages with a reboiler with duty $\dot{Q}_R > 0$ kW at the bottom and a total condenser with duty $\dot{Q}_C < 0$ kW at the top. N_S denotes the number of stages in the column with corresponding index n counted from the bottom. For simplicity, a distillation column with one single feed on stage N_F ($N_F = 2$ in the example in Figure 3.2) and without side-draws is considered. As in the previous example (cf. Section 3.2) the feed is assumed to be completely defined. Each stage n has liquid and vapor streams flowing from it (with total molar flow rate L^n and V^n) and onto it (with total molar flow rate L^{n+1} and V^{n+1}) and is therefore connected to the stages above and below. The reflux ratio R is defined as the ratio of the liquid molar flow rate L^R returned to the column divided by the molar flow rate of the distillate D , i.e. $R = L^R/D$. The MESH equations for an arbitrary control volume of the column can be easily derived using the MESH equations for a flash unit (cf. Section 3.2) or the MESH equations for an equilibrium stage (cf. Appendix A) as an example. Assuming constant pressure on all stages yields $N_{\text{var}} = N_S \cdot (2N_C + 3) + 3$ and $N_{\text{eq}} = N_S \cdot (2N_C + 3)$, which means that three degrees of freedom remain for the combined MESH system.

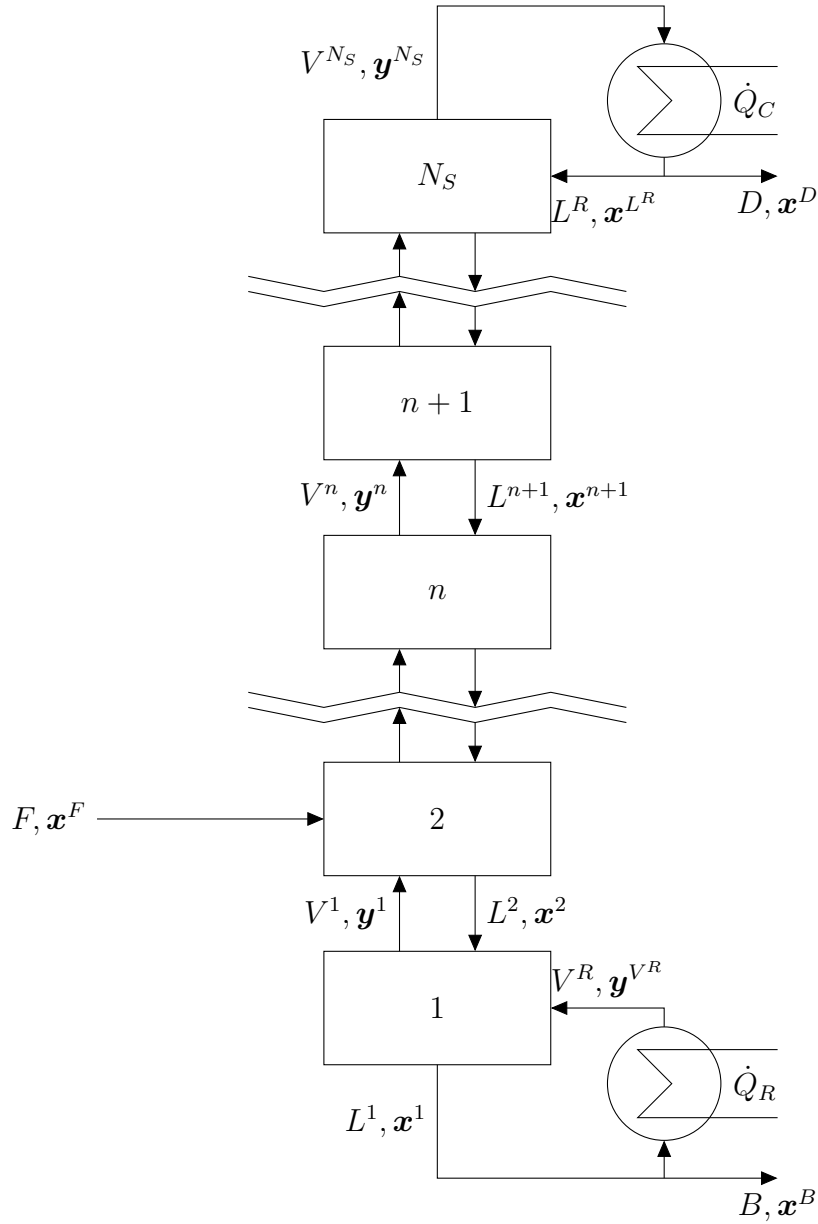


Figure 3.2.: Schematic of an equilibrium stage model of a distillation column with a single feed on stage $N_F = 2$, total condenser and reboiler.

For a distillation column a numerically robust algorithm is required that determines the unknown process variables for a wide range of choices for the fixed variables without observing convergence failures. In this thesis, we employ numerically stable stage-to-stage calculations based on the solution of a fixed-point problem on every stage. The transition from one stage to the next has guaranteed convergence if the input variables for stage-to-

stage calculations are chosen in a suitable way as described in Chapter 4 and 5. These chapters are devoted to the development of stage-to-stage strategies for simple column with one feed and two product streams and general columns with an arbitrary number of feed streams and side-draws. The approach is sketched briefly here: For an upward calculation of the column, the values for p , $\dot{\mathbf{n}}^B := B\mathbf{x}$, and \dot{Q}_R have to be given. In a first step, the system of MESH equations for a control volume that comprises the reboiler and the lowest stage of the column are derived and reformulated as a fixed-point problem as presented in detail in Section 4.2. The unknowns in this problem are the liquid and vapor streams connecting the first and the second stage of the column. This fixed-point problem can be solved by applying fixed-point iteration. The control volume is extended by a stage and in that way one can proceed upward a column by solving a fixed-point problem on each stage. In an analogous way it is also possible to proceed downward the column. For the asymptotic limiting case of a column with an infinite reflux ratio, convergence of the fixed-point iteration is immediately guaranteed. Based on this asymptotic limiting case, we want to answer the question how small the reflux ratio, and the heat duty respectively, can be chosen in order to still be able to guarantee convergence of the fixed-point iteration. A detailed analysis of the existence and uniqueness of fixed points and the convergence properties of the corresponding fixed-point iteration for columns with finite reflux can be found in Section 4.3.

When calculating a distillation column starting from the reboiler upward, based on given input variables p , $\dot{\mathbf{n}}^B$, and \dot{Q}_R , we proceed until we have solved the fixed-point problem for stage $(N_S - 1)$. This gives the concentration vector \mathbf{x}^{N_S} from which the composition of the corresponding vapor phase \mathbf{y}^{N_S} in equilibrium with the liquid phase can be calculated. Due to the total condenser at the top of the column the following relation holds:

$$\mathbf{y}^{N_S} = \mathbf{x}^D. \quad (3.12)$$

Again we write $\mathbf{x}^D(p, \dot{\mathbf{n}}^B, \dot{Q}_R)$ in order to stress the dependence of this composition vector on the choice of p , $\dot{\mathbf{n}}^B$, and \dot{Q}_R . The component material balance for the entire distillation column is not necessarily enforced during upward calculation of the distillation column, i.e. $\mathbf{x}^D(p, \dot{\mathbf{n}}^B, \dot{Q}_R)$ will not necessarily fulfill:

$$F\mathbf{x}^F = B\mathbf{x}^B + (F - B)\mathbf{x}^D(p, \dot{\mathbf{n}}^B, \dot{Q}_R), \quad (3.13)$$

where the relation $F = B + D$ was used. In order to obtain a feasible column design p , $\dot{\mathbf{n}}^B$, and \dot{Q}_R have to be adapted in a way such that Equation (3.13) is fulfilled.

There is an analogy between the problem described above and boundary value problems (BVP) (Stoer & Bulirsch, 2005, Chap. 7.3) that arise in the context of ordinary differential equations (ODE). The parameters p , $\dot{\mathbf{n}}^B$, and \dot{Q}_R , which are imposed at the bottom of the column, correspond to the initial values of the ODE. The analogy is further strengthened by the fact that a difference equation is solved by calculating the distillation column upward, which is strongly related to the solution of an ODE with fixed step size. The aspired boundary value corresponds to the result for \mathbf{x}^D that can be calculated a priori using the overall component material balance:

$$\mathbf{x}^D = \frac{F\mathbf{x}^F - B\mathbf{x}^B}{F - B}. \quad (3.14)$$

A method for solving such BVP is the (single) shooting method (Stoer & Bulirsch, 2005, Chap. 7.3.1). For more details see also Section 2.3. One way of transferring the ideas of this method to our problem of finding a feasible column design is to formulate the problem as an optimization problem of the following form:

$$\begin{aligned} \min_{p, \dot{\mathbf{n}}^B, \dot{Q}_R} \quad & 0 \\ \text{s.t.} \quad & Fx_i^F = Bx_i^B + (F - B)x_i^D(p, \dot{\mathbf{n}}^B, \dot{Q}_R), \quad i = 1, \dots, N_C - 1. \end{aligned} \quad (3.15)$$

This optimization problem is very similar to the optimization problem for a flash unit and again of size $N_{\text{opt}} = (N_C + 2)$ in terms of optimization variables. The number of constraints in (3.15) is $N_{\text{constr}} = (N_C - 1)$ (the component material balance for the component N_C is fulfilled by construction in case the component material balances for the $(N_C - 1)$ remaining components are fulfilled). The fact that the number of constraints remains small, although the total number of process variables and the size of the MESH equation system is much larger for a distillation column than the MESH equation system for a flash unit, is remarkable. Those MESH equations that are not incorporated explicitly as constraints in the optimization problem are already enforced during the upward or downward calculation of the distillation column, which is needed in any iteration step of the optimization algorithm in order to determine all process variables. In Chapter 4 and 5 we show that stage-to-stage calculations typically have guaranteed convergence for values of

the input variables chosen in a wide region, which we can quantify, including also infeasible choices and not only feasible ones. This allows the embedding of process simulation in an optimization problem and it is possible to use suitable nonlinear optimization algorithms to find a solution in a targeted manner.

The optimization problem (3.15) again has a constant objective function. This means that the optimization algorithm will output the first feasible column found, analogously to (3.11) for a flash unit. A non-constant objective function usually leads to a unique solution. In the general case, it is also possible to impose additional equality or inequality constraints, for example desired product purities.

Along the same lines, it is possible to formulate an optimization problem when calculating a feasible distillation column starting from the condenser downward. For the sake of brevity this is not discussed in detail.

Figure 3.3 depicts the different building blocks for process simulation or optimization of a distillation column, which were discussed in this section and will be topic of the next chapters, in a flow diagram.

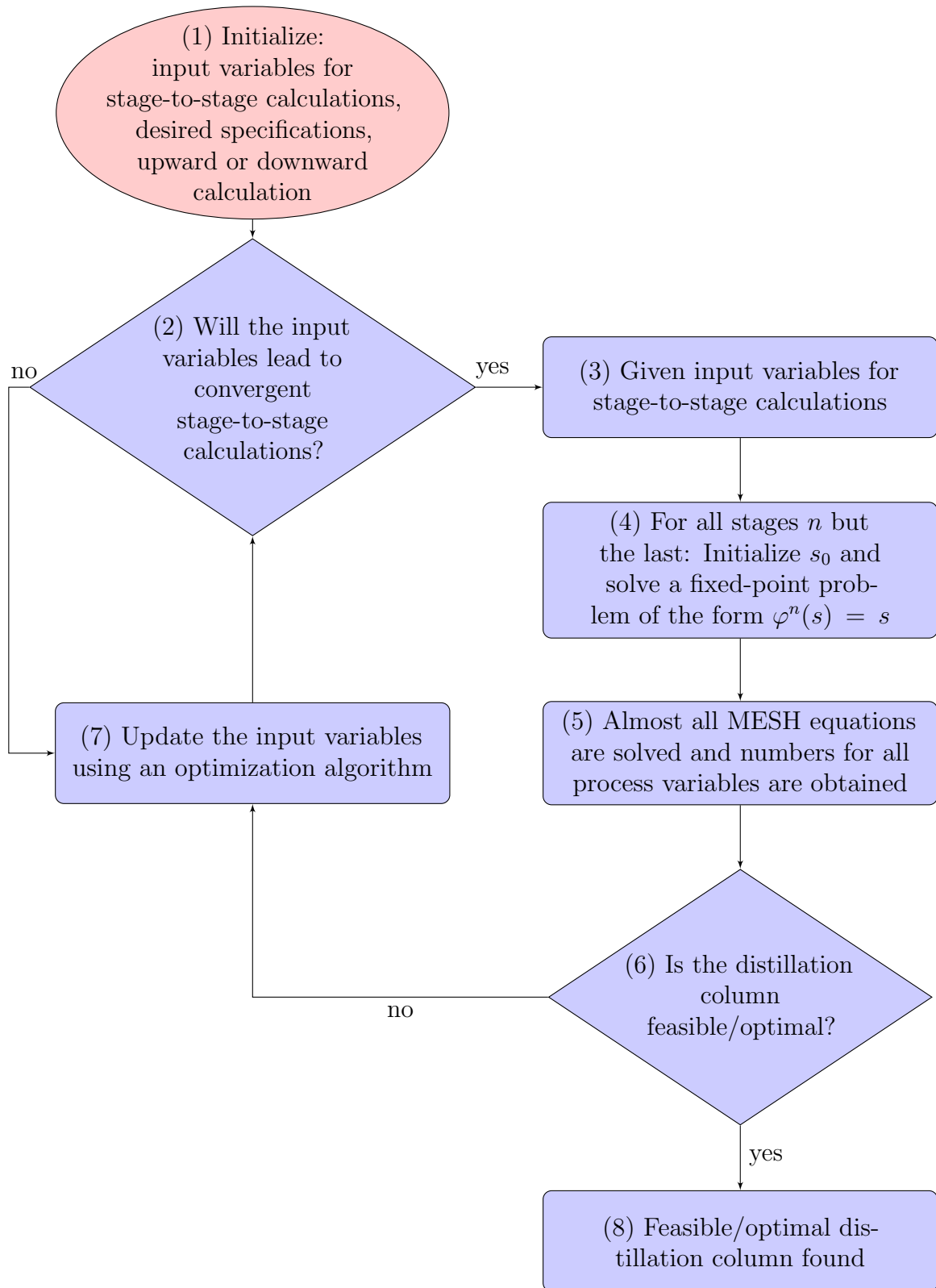


Figure 3.3.: A flow diagram for process simulation or optimization of a distillation column embedded in an optimization problem.

3.4. Simultaneous process simulation and optimization

In the previous section, process simulation was embedded in an optimization problem aiming for a feasible design. However, in many cases we are not only interested in an arbitrary feasible design but a design which is optimal in some sense. In order to perform process optimization it is only necessary to replace the constant objective function in the optimization problem (3.11) or (3.15) by an objective function of interest. It is of big advantage that for optimizing a process there is no need for a feasible column design as a starting point and hence it is not necessary to perform process simulation in advance.

In case we are not sure that the desired specifications can actually be met, process simulation and optimization can be combined by incorporating suitable objective functions. One possibility is to include the specified process variable as objective function, which should be minimized or maximized. By that approach, the lower or upper bound of the feasible interval for the considered process variable can be determined. If a certain desired target value should be achieved for a process variable, a corresponding distance function can be incorporated as objective function. Hence, the target value is feasible if the optimization problem outputs a feasible design with objective value equal to 0.

3.5. Starting values

So far, we did not comment on the starting values for the considered optimization problems. In principle, the pressure p can be used as an optimization variable. However, the designer usually has some idea about the pressure and in many cases it is specified to a fixed value.

Conceptual methods for distillation-based flowsheets that determine feasible column products can be used to generate starting values for one of the product stream, which is used as optimization variable. Examples for such methods are the boundary value method (Levy et al., 1985; Van Dongen & Doherty, 1985; Levy & Doherty, 1986), the rectification body method (Bausa et al., 1998), the shortest stripping line method (Lucia et al., 2006, 2008), or ∞/∞ -analysis developed by Petlyuk & Avet'yan (1971) and Serafimov et al. (1973), which was used to predict multiple steady states in azeotropic distillation (Bekiaris et al., 1993, 1996; Bekiaris & Morari, 1996; Güttinger & Morari, 1997) and for conceptual process design (Ryll et al., 2012, 2013).

In this work, ∞/∞ -analysis is used, which can be derived as the limiting case of the equilibrium stage model for columns with an infinite number of stages and infinite reflux. In this limiting case, the number of degrees of freedom is decreased and the flowsheet can be solved with guaranteed convergence (Ryll et al., 2012, 2013). The resulting solution provides excellent starting values for B and \mathbf{x}^B , and thus also for $\dot{\mathbf{n}}^B$. Note that, in case ∞/∞ -analysis outputs a composition vector \mathbf{x}^B containing zero elements, we slightly correct this vector by adding a small δ to the zero component and subtracting the same δ from a non-zero component. By doing so, we move the starting value for the composition vector to the interior of the ternary diagram, as its boundary can only be attained in the asymptotic limiting case where separation is optimal.

Besides ∞/∞ -analysis, starting values for B and \mathbf{x}^B could also be generated via solving only the overall component material balances. Clearly, this approach does not necessarily take into consideration the thermodynamic properties of the analyzed multi-component system, but still the starting values can be a good initial guess.

The starting value for \dot{Q}_R can be chosen in such a way that the derived fixed-point problem for the upward calculation of a distillation column has Lipschitz constant strictly smaller than 1, which implies that the stage-to-stage calculations of the column in the flowsheet have guaranteed convergence in the fixed-point iterations. This essential result of the thesis is derived and proven in detail in Section 4.3 and 5.3. Without conducting further analysis, it is always a good choice to start with a very large heat duty, as we know that in the limiting case of infinitely large heat duty stage-to-stage calculations have guaranteed convergence. The large starting value for the heat duty could then be minimized during optimization by incorporating it as objective in the optimization problem.

As discussed above, there exist several strategies that generate good starting values for the optimization variables. In this regard, especially ideas from conceptual design such as the ∞/∞ -analysis perfectly match the choice of optimization variables and the structure of the optimization problem. However, we will show in Chapter 7 that the optimization problems are usually quite robust with respect to poor starting values.

3.6. Extensions of the presented approach

We have presented an approach for embedding process simulation in an optimization problem with the examples of a flash unit and a simple distillation column. It can be easily extended in several ways.

First, it is not only possible to consider simple distillation columns but one could also think of more complex distillation columns, for example with an arbitrary number of feed streams on different stages. Furthermore, intermediate reboilers or condensers can be included in the problem formulation, where every intermediate reboiler or condenser leads to one additional optimization variable. Additional side-draws could also be incorporated. Each side-draw results in N_C additional optimization variables. Clearly, the approach can be applied to systems with an arbitrary number of components N_C .

Tailored strategies that determine the remaining process variables for simple distillation columns and distillation columns with an arbitrary number of feed streams and side-draws are derived and analyzed with respect to convergence of the fixed-point iteration in Chapter 4 and 5, respectively.

Furthermore, the presented ideas in this chapter will be extended to flowsheets consisting of several units of the same type or of different types in Chapter 6.

Another possible extension is to include the number of stages of a distillation column as well as the feed stages in the problem formulation as integer optimization variables. The optimization problem then turns into a mixed-integer nonlinear optimization problem. A corresponding numerical example is shown in Section 7.3.1. If we use the number of stages of a distillation column as optimization variable, it is possible to choose a column with a large reboiler duty and a large number of stages as starting point. This mimics the asymptotic limiting case considered in ∞/∞ -analysis. From this starting point it is empirically easier to initialize a column and during simultaneous simulation and optimization we can decrease the reboiler duty and the number of stages to sound values.

The presented approach for process simulation via formulation of an optimization problem of small size could also be extended to other (simple and stage-based) unit operations such as splitters, reactors, heat exchangers, decanters, extraction columns, absorption columns, or even Petlyuk distillation columns (Wolff & Skogestad, 1995). As prerequisite, suitable algorithms are needed for the different units that facilitate the calculation of all process variables. The number of additional optimization variables and constraints depends on the specific unit. Absorption columns and Petlyuk distillation

columns can be modeled as a special case of a distillation column, or the connection of distillation columns respectively, and can therefore be easily incorporated. There exist other units, however, which require more preliminary work.

In recent studies, distillation-based flowsheets including also splitters and decanters have been simulated. The splitter with two product streams can be modeled in a very simple and straight-forward way by including the split ratio as one additional optimization variable in the optimization problem. No additional constraints have to be added and process simulation of this unit does not require the solution of a system of equations. The decanter was treated in a similar way as the flash unit described in Section 3.2 replacing the equations for the vapor-liquid equilibrium with the equations for the liquid-liquid equilibrium (LLE). However, efficient algorithms for example for the computation of extractive columns still need to be developed and require a sound analysis. From our point of view it would also be worthwhile to include reactions in our approach.

In case we want to consider competing objective functions for process optimization, strategies for multi-criteria optimization can be applied in the context of process simulation and optimization (Welke, 2013; Bortz et al., 2014). A numerical example with two competing objective functions is shown in Section 7.3.2.

Part II.

Solution approaches

Stage-to-stage calculations of simple distillation columns

In this chapter, a novel approach for stage-to-stage calculations of distillation columns with one feed stream and two product streams based on the MESH equations is presented. No simplifying assumptions such as CMO are used. The transition from one stage to the next is formulated as a fixed-point problem, which can be solved by fixed-point iteration without computing derivatives. In the asymptotic limiting case of columns with infinite reflux ratio, convergence of the fixed-point iteration is guaranteed and we address the question how small the reflux ratio, or heat duty respectively, can be chosen to still have guaranteed convergence. Applying the Banach fixed-point theorem, bounds on the minimum energy requirement are derived. Within these bounds a solution to the fixed-point problem exists and convergence of the fixed-point iteration is guaranteed.

4.1. System of equations

The equilibrium stage model of a distillation column is schematically depicted in Figure 4.1 and was already introduced in Section 3.3. The MESH equations for an equilibrium stage are stated in detail in Appendix A. For simplicity, a distillation column with one single feed on stage N_F ($N_F = 2$ in the example of Figure 4.1) and without any side-draws is considered. The method described in the following will be extended to side-draws and multiple feeds in a straight forward manner in Chapter 5.

4. Stage-to-stage calculations of simple distillation columns

The state of the feed stream is assumed to be completely defined, i.e. the feed molar flow rate F , the pressure p^F , and the mole fractions x_i^F of each component i are known. Furthermore, it is assumed here that the feed stream is liquid boiling and the pressure of the feed stream p^F equals the pressure of the distillation column p . Also these assumptions are only used for simplicity and a generalization is possible.

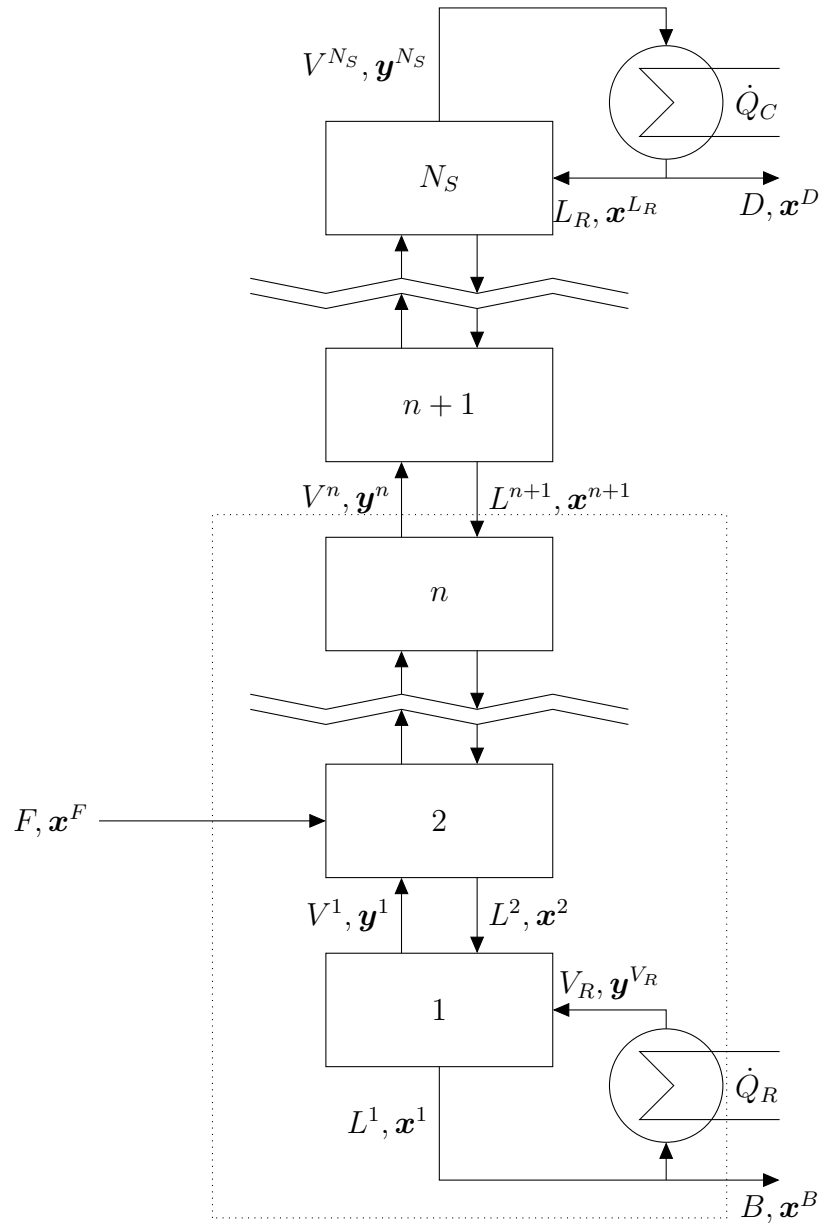


Figure 4.1.: Schematic of a stage-by-stage model of a distillation column with a single feed on stage $N_F = 2$, total condenser, and reboiler. The dotted box indicates a control volume.

Again, the extended Raoult's law is assumed to describe the VLE (see Section 3.2 and Appendix A.2). Furthermore, $h^l(\mathbf{x}, T)$ and $h^v(\mathbf{y}, T)$ denote the enthalpies of the liquid and vapor phase, respectively, which depend on the composition of the phase \mathbf{x} or \mathbf{y} , and the temperature T . We introduce some short notations that will be used in the following:

Definition 4.1. *Let the pressure p be given. For a liquid phase composition vector \mathbf{x} that is in equilibrium with the corresponding vapor phase we can determine the temperature T^{VLE} in equilibrium by using the extended Raoult's law. We define*

$$l(\mathbf{x}) := h^l(\mathbf{x}, T^{VLE}). \quad (4.1)$$

Analogously, for a vapor phase composition vector \mathbf{y} that is in equilibrium with the corresponding liquid phase we can determine T^{VLE} and define

$$v(\mathbf{y}) := h^v(\mathbf{y}, T^{VLE}). \quad (4.2)$$

Thus, $l(\mathbf{x})$ and $v(\mathbf{y})$ are short notations for the molar enthalpy of a given composition at liquid boiling and vapor dewing state, respectively.

For the subsequent results we assume the following to hold:

Assumption 4.2. *Internal streams among stages never vanish and mole fractions in the liquid and vapor phase are strictly larger than 0.*

Assumption 4.3. *Let the pressure p be given. For any composition vectors $\mathbf{x}, \mathbf{y} \in \mathbb{R}^{N_C}$ for which the summation equation holds it is assumed that*

$$v(\mathbf{y}) - l(\mathbf{x}) > 0. \quad (4.3)$$

For the general case, Assumption 4.3 cannot be proven, but it is plausible that it will hold for a big class of practical problems, cf. Appendix B.

4.2. Derivation of an equivalent fixed-point problem

A new approach is presented in which the full set of MESH equations is successively solved enabling a stage-wise calculation of distillation columns. It is either possible to calculate a column from the bottom to the top or the other way round. We elaborately describe the upward calculation of a distillation column and briefly describe downward calculation in this section.

For the following considerations, it is assumed that values for the variables p , $\dot{n}^B := B\mathbf{x}^B$, and \dot{Q}_R , as well as the specifications F and \mathbf{x}^F of the liquid boiling feed stream on stage N_F , are given in order to calculate a column from the bottom to the top. The given variables should fulfill the following assumption:

Assumption 4.4. *The values for B and \mathbf{x}^B are chosen in such a way that*

$$D := F - B \geq 0 \quad (4.4)$$

and

$$x_i^D := \frac{F x_i^F - B x_i^B}{F - B} > 0 \quad (4.5)$$

for all $i = 1, \dots, N_C$, i.e. the flow rate D and the composition \mathbf{x}^D of the distillate stream, which fulfills the material balance of the column, should be positive.

We proceed in the following way: We consider the MESH equations for a control volume including the reboiler and the first stage of the distillation column. The unknowns in the resulting system of equations are L^2 , \mathbf{x}^2 , V^1 , and \mathbf{y}^1 (upper case numbers always denote the stage in this work). The vapor stream leaving the first stage and the bottom stream, i.e. the liquid stream leaving the first stage, are in vapor-liquid equilibrium. Because the pressure p is given, the composition \mathbf{y}^1 of the vapor phase can immediately be calculated. The unknowns L^2 , \mathbf{x}^2 , and V^1 still need to be determined. For that purpose, the MESH equations for the considered control volume are reformulated as a fixed-point problem and solved by fixed-point iteration. This gives values for L^2 , \mathbf{x}^2 , and V^1 . The composition \mathbf{y}^2 can then be calculated by solving the vapor-liquid equilibrium and a new fixed-point problem for the transition from stage 2 to stage 3 can be derived by extending the control volume by the second stage. In this way we can proceed upward the column.

In the following, the fixed-point problem for the transition from an arbitrary stage n to stage $n + 1$ based on the MESH equations for a control volume including the reboiler and the lower part of the distillation column up to stage n as indicated by the dotted box in

Figure 4.1 is derived. The composition of the liquid phase \mathbf{x}^n on stage n is assumed to be given from the previous step which also determines the composition of the corresponding vapor phase \mathbf{y}^n . L^{n+1} , \mathbf{x}^{n+1} , and V^n are the unknown process variables, which have to be determined to proceed upward.

For the considered control volume shown in Figure 4.1 the following total material balance holds

$$F_{\text{up}}^n + L^{n+1} = V^n + B, \quad (4.6)$$

where

$$F_{\text{up}}^n := \begin{cases} 0 & \text{for } n < N_F, \\ F & \text{for } n \geq N_F. \end{cases} \quad (4.7)$$

Taking component material balances, we have that

$$F_{\text{up}}^n \mathbf{x}^F + L^{n+1} \mathbf{x}^{n+1} = V^n \mathbf{y}^n + B \mathbf{x}^B. \quad (4.8)$$

Dividing (4.8) by L^{n+1} and substituting (4.6) into (4.8), we get

$$\mathbf{x}^{n+1} = \frac{V^n}{V^n + B - F_{\text{up}}^n} \mathbf{y}^n + \frac{B}{V^n + B - F_{\text{up}}^n} \mathbf{x}^B - \frac{F_{\text{up}}^n}{V^n + B - F_{\text{up}}^n} \mathbf{x}^F. \quad (4.9)$$

Considering the same control volume the following enthalpy balance holds:

$$\dot{Q}_R + F_{\text{up}}^n l(\mathbf{x}^F) + L^{n+1} l(\mathbf{x}^{n+1}) = V^n v(\mathbf{y}^n) + B l(\mathbf{x}^B). \quad (4.10)$$

Substituting (4.6) into (4.10) and solving for V^n , we get

$$V^n = \frac{\dot{Q}_R + F_{\text{up}}^n l(\mathbf{x}^F) + (B - F_{\text{up}}^n) l(\mathbf{x}^{n+1}) - B l(\mathbf{x}^B)}{v(\mathbf{y}^n) - l(\mathbf{x}^{n+1})}. \quad (4.11)$$

For a feasible column design, the above equations have to be fulfilled. In particular, the above equations are fulfilled for a fixed point of the function φ_{up}^n , which is defined in the following way:

Definition 4.5 (Fixed-point problem for the transition from stage n to stage $n + 1$). *For the transition from stage n to stage $n + 1$, $n = 1, \dots, N_S - 1$, a fixed point of the function*

$$\varphi_{\text{up}}^n(s) := \frac{\dot{Q}_R + F_{\text{up}}^n l(\mathbf{x}^F) + (B - F_{\text{up}}^n) l(\mathbf{x}^{n+1}(s)) - B l(\mathbf{x}^B)}{v(\mathbf{y}^n) - l(\mathbf{x}^{n+1}(s))}, \quad (4.12)$$

4. Stage-to-stage calculations of simple distillation columns

where

$$\mathbf{x}^{n+1}(s) = \frac{s}{s+B-F_{up}^n} \mathbf{y}^n + \frac{B}{s+B-F_{up}^n} \mathbf{x}^B - \frac{F_{up}^n}{s+B-F_{up}^n} \mathbf{x}^F, \quad (4.13)$$

has to be found. Due to the fact that the auxiliary variable s is introduced, the MESH equations are decoupled and only in a fixed point s^* of φ_{up}^n we have $s^* = V^n$.

Hence, fixing p , B , \mathbf{x}^B , and \dot{Q}_R enables upward stage-to-stage calculations of a distillation column starting from the reboiler by solving a fixed-point problem on each stage.

Analogously, a sequence of fixed-point problems for the calculation of a distillation column from the condenser downward can be derived. In this case p , $\dot{\mathbf{n}}^D := D\mathbf{x}^D$, and \dot{Q}_C are fixed and the vapor composition \mathbf{y}^n on stage n is assumed to be given from which one can calculate the liquid composition \mathbf{x}^n in equilibrium. For downward calculation of a distillation column analogous conditions as stated in Assumption 4.4 should be fulfilled. The unknown values which have to be determined to proceed down the column are L^n and \mathbf{y}^{n-1} . These values can also be obtained by solving a fixed-point problem.

Definition 4.6 (Fixed-point problem for the transition from stage n to stage $n-1$). *For the transition from stage n to stage $n-1$, $n = 2, \dots, N_S$, a fixed point of the function*

$$\varphi_{down}^n(r) := \frac{\dot{Q}_C + F_{down}^n l(\mathbf{x}^F) + (D - F_{down}^n) v(\mathbf{y}^{n-1}(r)) - D l(\mathbf{x}^D)}{l(\mathbf{x}^n) - v(\mathbf{y}^{n-1}(r))}, \quad (4.14)$$

where

$$\mathbf{y}^{n-1}(r) = \frac{r}{r+D-F_{down}^n} \mathbf{x}^n + \frac{D}{r+D-F_{down}^n} \mathbf{x}^D - \frac{F_{down}^n}{r+D-F_{down}^n} \mathbf{x}^F \quad (4.15)$$

and

$$F_{down}^n := \begin{cases} 0 & \text{for } n > N_F, \\ F & \text{for } n \leq N_F, \end{cases} \quad (4.16)$$

has to be found. Again, the MESH equations are decoupled by introducing the auxiliary variable r . The solution of this fixed-point problem is $r^* = L^n$.

The following results are explained using the example of calculating a distillation column from bottom to the top. However, the results also hold for the opposite method unless specified otherwise.

4.3. Application of the Banach fixed-point theorem

In this section, the Banach fixed-point theorem is applied to the function φ_{up}^n introduced in Definition 4.5. This theorem provides the answer to the question whether there exists a fixed point and whether it is unique and it further provides a constructive way of finding this fixed point. In the following, the one-dimensional version of the Banach fixed-point theorem is used as stated in Forster (2013, p. 193):

Theorem 4.7 (Banach fixed-point theorem). *Let $I \subset \mathbb{R}$ be a closed interval and $f : I \rightarrow \mathbb{R}$ a differentiable function with $f(I) \subset I$. If there exists $0 \leq q < 1$ such that $|f'(x)| \leq q$ for all $x \in I$, the sequence $(x_n)_{n \in \mathbb{N}}$ defined by*

$$x_n := f(x_{n-1}), \quad n \geq 1 \quad (4.17)$$

converges towards the unique fixed point x^ of f with $f(x^*) = x^*$ for any $x_0 \in I$.*

Any value of q in the above theorem is called a Lipschitz constant for f . The goal is to provide insight how the process variables p , B , \mathbf{x}^B , and \dot{Q}_R have to be chosen in order to be able to apply the Banach fixed-point theorem.

4.3.1. Existence of a fixed point

In a first step, we show under which conditions at least one solution of the fixed-point problem can be guaranteed and under which conditions it is guaranteed that there exists no solution to the fixed-point problem. The uniqueness of the fixed point is discussed at a later point.

First of all, some properties of the derived fixed-point problems are discussed. This helps finding a suitable closed interval into which the function φ_{up}^n should map.

Lemma 4.8. *If s^* is a fixed point of φ_{up}^n it holds*

$$s^* > F_{\text{up}}^n - B. \quad (4.18)$$

Proof. For a valid column design we have $s^* = V^n$ and the following material balance holds for the considered control volume

$$F_{\text{up}}^n + L^{n+1} = V^n + B. \quad (4.19)$$

Solving for s^* leads to

$$s^* = V^n = F_{\text{up}}^n - B + \underbrace{L^{n+1}}_{>0}, \quad (4.20)$$

due to the fact that initial streams never vanish, cf. Assumption 4.2. \square

The subsequent results show which conditions have to hold in order to have strictly positive mole fractions in all streams during upward calculation of a column as requested in Assumption 4.2. There also exist solutions to the derived fixed-point problem, or the MESH system respectively, with zero or negative mole fractions. However, these solutions have only mathematical and no physical meaning, which is why we do not consider them in this work.

Lemma 4.9. *Let the composition vectors \mathbf{x}^B and \mathbf{y}^n be given. If $n < N_F$ and $s > -B$ it holds*

$$x_i^{n+1}(s) > 0, \quad i = 1, \dots, N_C \quad \iff \quad s > -B \min_{i=1, \dots, N_C} \left(\frac{x_i^B}{y_i^n} \right) \geq -B. \quad (4.21)$$

Proof.

$$\begin{aligned} & x_i^{n+1}(s) > 0, \quad i = 1, \dots, N_C \\ \iff & \frac{s}{s+B} y_i^n + \frac{B}{s+B} x_i^B > 0, \quad i = 1, \dots, N_C \\ \iff & s y_i^n + B x_i^B > 0, \quad i = 1, \dots, N_C \\ \iff & s > -B \underbrace{\min_{i=1, \dots, N_C} \left(\frac{x_i^B}{y_i^n} \right)}_{\leq 1}. \end{aligned}$$

\square

Lemma 4.10. *Let the composition vectors \mathbf{x}^D and \mathbf{y}^n be given. If $n \geq N_F$ and $s > D$ it holds*

$$x_i^{n+1}(s) > 0, \quad i = 1, \dots, N_C \quad \iff \quad s > D \max_{i=1, \dots, N_C} \left(\frac{x_i^D}{y_i^n} \right) \geq D. \quad (4.22)$$

Proof.

$$\begin{aligned}
 & x_i^{n+1}(s) > 0, \quad i = 1, \dots, N_C \\
 \Leftrightarrow & \frac{s}{s-D} y_i^n + \frac{B}{s-D} x_i^B - \frac{F}{s-D} x_i^F > 0, \quad i = 1, \dots, N_C \\
 \Leftrightarrow & s y_i^n + B x_i^B - F x_i^F > 0, \quad i = 1, \dots, N_C \\
 \Leftrightarrow & s y_i^n - D x_i^D > 0, \quad i = 1, \dots, N_C \\
 \Leftrightarrow & s y_i^n > D x_i^D, \quad i = 1, \dots, N_C \\
 \Leftrightarrow & s > D \underbrace{\max_{i=1, \dots, N_C} \left(\frac{x_i^D}{y_i^n} \right)}_{\geq 1}.
 \end{aligned}$$

□

We can conclude that a fixed point with not only mathematical but also physical meaning can only occur in

$$M_n := \begin{cases} (0; \infty) & \text{for } n < N_F, \\ (D m_n; \infty) & \text{for } n \geq N_F, \end{cases} \quad (4.23)$$

where

$$m_n := \max_{i=1, \dots, N_C} \left(\frac{x_i^D}{y_i^n} \right).$$

It always holds that $m_n \geq 1$ and if the mole fraction of a component in \mathbf{y}^n is much smaller than the mole fraction of the corresponding component in \mathbf{x}^D , the value for m_n gets large.

Lemma 4.11. *Let $n < N_F$. The function φ_{up}^n is bounded on $M_n := (0; \infty)$.*

Proof. The function φ_{up}^n is a continuous function on M_n . Hence, we only have to consider the behavior of φ_{up}^n at the boundaries of M_n . When considering the lower bound, we distinguish the following two cases:

Case 1: $B > 0$

We have that

$$\lim_{s \rightarrow 0} \mathbf{x}^{n+1}(s) = \mathbf{x}^B \quad (4.24)$$

and therefore

$$\lim_{s \rightarrow 0} |\varphi_{\text{up}}^n(s)| = \left| \frac{\dot{Q}_R}{v(\mathbf{y}^n) - l(\mathbf{x}^B)} \right| < \infty. \quad (4.25)$$

Case 2: $B = 0$

In this special case, we immediately get

$$\mathbf{x}^{n+1}(s) \equiv \mathbf{y}^n \quad (4.26)$$

and

$$|\varphi_{\text{up}}^n(s)| \equiv \left| \frac{\dot{Q}_R}{v(\mathbf{y}^n) - l(\mathbf{y}^n)} \right| < \infty. \quad (4.27)$$

For the limiting case $s \rightarrow \infty$ we do not have to consider two different cases but can conclude that

$$\lim_{s \rightarrow \infty} |\varphi_{\text{up}}^n(s)| = \left| \frac{\dot{Q}_R + Bl(\mathbf{y}^n) - Bl(\mathbf{x}^B)}{v(\mathbf{y}^n) - l(\mathbf{y}^n)} \right| < \infty \quad (4.28)$$

due to the fact that

$$\lim_{s \rightarrow \infty} \mathbf{x}^{n+1}(s) = \mathbf{y}^n. \quad (4.29)$$

This is exactly the definition of a distillation line. \square

Lemma 4.12. *Let $n \geq N_F$. The function φ_{up}^n is bounded on*

$$M_n := (Dm_n; \infty). \quad (4.30)$$

Proof. The function φ_{up}^n is a continuous function on M_n . Once again, we have to check the behavior of φ_{up}^n at the boundaries of M_n . For the lower bound, we have to consider two different cases:

Case 1: $\mathbf{x}^D \neq \mathbf{y}^n$

In this case we have that $m_n > 1$ and thus $Dm_n > D$, which yields

$$\lim_{s \rightarrow Dm_n} |\varphi_{\text{up}}^n(s)| < \infty. \quad (4.31)$$

Case 2: $\mathbf{x}^D = \mathbf{y}^n$

Using Equation (4.9) and the overall component material balance

$$F\mathbf{x}^F = B\mathbf{x}^B + D\mathbf{x}^D \quad (4.32)$$

leads to

$$\mathbf{x}^{n+1}(s) \equiv \mathbf{x}^D \quad (4.33)$$

and

$$\lim_{s \rightarrow D} |\varphi_{\text{up}}^n(s)| = \left| \frac{\dot{Q}_R + Fl(\mathbf{x}^F) - Dl(\mathbf{x}^D) - Bl(\mathbf{x}^B)}{v(\mathbf{x}^D) - l(\mathbf{x}^D)} \right| < \infty. \quad (4.34)$$

For the limiting case $s \rightarrow \infty$ we can conclude that

$$\lim_{s \rightarrow \infty} |\varphi_{\text{up}}^n(s)| = \left| \frac{\dot{Q}_R + Fl(\mathbf{x}^F) - Dl(\mathbf{y}^n) - Bl(\mathbf{x}^B)}{v(\mathbf{y}^n) - l(\mathbf{y}^n)} \right| < \infty \quad (4.35)$$

due to the fact that

$$\lim_{s \rightarrow \infty} \mathbf{x}^{n+1}(s) = \mathbf{y}^n. \quad (4.36)$$

□

For the limiting case $s \rightarrow \infty$ we end up with the same result for stages below and above the feed stage. This is plausible due to the fact that for internal streams of infinitely large flow rate the flow rate and composition of the feed stream vanishes in comparison to the internal streams.

In summary, the function φ_{up}^n always maps from M_n into the compact interval

$$I_n := \left[\inf_{s \in M_n} \varphi_{\text{up}}^n(s); \sup_{s \in M_n} \varphi_{\text{up}}^n(s) \right]. \quad (4.37)$$

Lemma 4.13. *Let $n < N_F$. If*

$$\dot{Q}_R > B(l(\mathbf{x}^B) - l(\mathbf{x}^{n+1}(s))) \quad (4.38)$$

for all $s \in M_n$ and in the limiting cases $s \rightarrow 0$ and $s \rightarrow \infty$ it holds that $\varphi_{\text{up}}^n(M_n) \subset M_n$.

Proof. In order to show that the function φ_{up}^n maps from M_n to itself it suffices to show that the interval I_n is a subset of M_n . As we have already shown that $\sup_{s \in M_n} \varphi_{\text{up}}^n(s) < \infty$ it remains to show that $\inf_{s \in M_n} \varphi_{\text{up}}^n(s) > 0$ if \dot{Q}_R fulfills the above condition. If it holds that

$$\dot{Q}_R + Bl(\mathbf{x}^{n+1}(s)) - Bl(\mathbf{x}^B) > 0 \quad (4.39)$$

for all $s \in M_n$ and in the limiting cases $s \rightarrow 0$ and $s \rightarrow \infty$ we can conclude that

$$\varphi_{\text{up}}^n(s) > 0 \quad (4.40)$$

4. Stage-to-stage calculations of simple distillation columns

for all $s \in M_n$ and in the limiting cases $s \rightarrow 0$ and $s \rightarrow \infty$. This immediately yields the claim. \square

The lower bound for \dot{Q}_R derived in Lemma 4.13 depends on B , \mathbf{x}^B , and on the current value of s , which usually changes during the fixed-point iteration. A more general bound on \dot{Q}_R can be derived as follows: Define

$$\mathcal{F}_{N_C} := \left\{ \mathbf{x} \in \mathbb{R}^{N_C} \left| \sum_{i=1}^{N_C} x_i = 1, x_i > 0, i = 1, \dots, N_C \right. \right\} \quad (4.41)$$

as the set of all physically meaningful compositions of a mixture. Assuming that $v(\mathbf{x})$ and $l(\mathbf{x})$ are bounded functions on \mathcal{F}_{N_C} we immediately get the following result:

Lemma 4.14. *Let $n < N_F$. If*

$$\dot{Q}_R > \dot{Q}_R^{LB1} \quad (4.42)$$

with

$$\dot{Q}_R^{LB1} := B \left(l(\mathbf{x}^B) - \min_{\mathbf{x} \in \mathcal{F}_{N_C}} l(\mathbf{x}) \right) \quad (4.43)$$

or alternatively if

$$\dot{Q}_R > \dot{Q}_R^{LB2} \quad (4.44)$$

with

$$\begin{aligned} \dot{Q}_R^{LB2} &:= B \left(\max_{\mathbf{x} \in \mathcal{F}_{N_C}} l(\mathbf{x}) - \min_{\mathbf{x} \in \mathcal{F}_{N_C}} l(\mathbf{x}) \right) \\ &\geq \dot{Q}_R^{LB1} \end{aligned} \quad (4.45)$$

it holds that $\varphi_{up}^n(M_n) \subset M_n$.

The bound \dot{Q}_R^{LB2} depends only on B and the physical properties of the specific components in the considered system at pressure p and is independent of the stage $n < N_F$. The maximum and minimum values of the liquid and vapor enthalpy functions for a system of substances only have to be calculated once, which can be done in a preprocessing step of process simulation. Enthalpy functions often exhibit only small changes on \mathcal{F}_{N_C} when compared to enthalpy changes between liquid and vapor phase. Thus the more general bound is expected to be close to the actual bound and not much more pessimistic.

Lemma 4.15. *Let $n \geq N_F$. If*

$$\dot{Q}_R > Bl(\mathbf{x}^B) - Fl(\mathbf{x}^F) + Dm_n v(\mathbf{y}^n) + D(1 - m_n) l(\mathbf{x}^{n+1}(s)) \quad (4.46)$$

or equivalently

$$\dot{Q}_C < D(l(\mathbf{x}^D) - m_n v(\mathbf{y}^n) + (m_n - 1) l(\mathbf{x}^{n+1}(s))) \quad (4.47)$$

for all $s \in M_n$ and in the limiting cases $s \rightarrow Dm_n$ and $s \rightarrow \infty$ it holds that $\varphi_{\text{up}}^n(M_n) \subset M_n$.

Proof. As before, it suffices to show that the interval I_n is a subset of M_n . Here, it remains to show that $\inf_{s \in M_n} \varphi_n(s) \geq Dm_n$ if \dot{Q}_R , or \dot{Q}_C respectively, fulfills the above condition.

If it holds that

$$\dot{Q}_R > Bl(\mathbf{x}^B) + Dl(\mathbf{x}^{n+1}(s)) - Fl(\mathbf{x}^F) + Dm_n(v(\mathbf{y}^n) - l(\mathbf{x}^{n+1}(s))) \quad (4.48)$$

for all $s \in M_n$ and in the limiting cases $s \rightarrow Dm_n$ and $s \rightarrow \infty$ we can conclude that

$$\varphi_{\text{up}}^n(s) > 0 \quad (4.49)$$

for all $s \in M_n$ and in the limiting cases $s \rightarrow Dm_n$ and $s \rightarrow \infty$. This immediately yields the claim.

The condition for \dot{Q}_C follows from the overall energy balance for the column. \square

More general bounds on \dot{Q}_R that do no longer depend on \mathbf{x}^F , \mathbf{x}^B , and the current value of s can be derived as follows:

Lemma 4.16. *Let $n \geq N_F$. If*

$$\dot{Q}_R > \dot{Q}_R^{LB1,n} \quad (4.50)$$

with

$$\dot{Q}_R^{LB1,n} := Bl(\mathbf{x}^B) - Fl(\mathbf{x}^F) + Dm_n v(\mathbf{y}^n) + D(1 - m_n) \min_{\mathbf{x} \in \mathcal{F}_{NC}} l(\mathbf{x}) \quad (4.51)$$

or alternatively if

$$\dot{Q}_R > \dot{Q}_R^{LB2,n} \quad (4.52)$$

with

$$\begin{aligned} \dot{Q}_R^{LB2,n} &:= B \left(\max_{\mathbf{x} \in \mathcal{F}_{NC}} l(\mathbf{x}) - \min_{\mathbf{x} \in \mathcal{F}_{NC}} l(\mathbf{x}) \right) + Dm_n \left(\max_{\mathbf{x} \in \mathcal{F}_{NC}} v(\mathbf{x}) - \min_{\mathbf{x} \in \mathcal{F}_{NC}} l(\mathbf{x}) \right) \\ &\geq \dot{Q}_R^{LB1,n} \end{aligned} \quad (4.53)$$

it holds that $\varphi_{up}^n(M_n) \subset M_n$.

The new bound $\dot{Q}_R^{LB2,n}$ depends only on F , B , m_n , and on the physical properties of the specific components in the considered system at pressure p . Unfortunately, the quotient m_n cannot be bounded from above due to the fact that y_i^n can be arbitrarily small and therefore it is not possible to derive a more general bound on \dot{Q}_R .

In an analogous way it is also possible to derive more general bounds for \dot{Q}_C using the overall energy balance of the distillation column. However, we will focus on bounds for \dot{Q}_R in the following.

Lemma 4.17. *If the function φ_{up}^n maps from M_n to itself it also maps from I_n to itself.*

Proof. Using the results of Lemma 4.13 and Lemma 4.15 we know that

$$\varphi_{up}^n(M_n) \subseteq I_n \subseteq M_n. \quad (4.54)$$

From this we can conclude

$$\varphi_{up}^n(I_n) \subseteq \varphi_{up}^n(M_n) \subseteq I_n. \quad (4.55)$$

□

Theorem 4.18 (Brouwer fixed-point theorem, see also Heuser (2008, p. 593)). *If the continuous function φ_{up}^n maps from the closed interval I_n to itself there exists at least one fixed point in the interval I_n .*

Proof. The claim can be proven by defining a function $g_n(s) := \varphi_{up}^n(s) - s$ on the interval I_n and applying the intermediate value theorem to this function in order to show that there exists some $s^* \in I_n$ such that $g_n(s^*) = 0$. □

The above results can be summarized in the following way:

Theorem 4.19 (Existence of a fixed point of φ_{up}^n in the interval I_n). *If $n < N_F$ and*

$$\dot{Q}_R > \dot{Q}_R^{LB2} \geq \dot{Q}_R^{LB1} \quad (4.56)$$

or $n \geq N_F$ and

$$\dot{Q}_R > \dot{Q}_R^{LB2,n} \geq \dot{Q}_R^{LB1,n} \quad (4.57)$$

it holds that $\varphi_{up}^n(I_n) \subset I_n$ and the existence of at least one fixed point in the closed interval I_n can be guaranteed.

The bounds in Theorem 4.19 that guarantee the existence of a fixed point depend on certain process variables and the physical properties of the multi-component system under consideration. It is clear that it is always possible to chose a very large \dot{Q}_R such that existence of a fixed point is guaranteed. In Section 4.4 these bounds will be evaluated for a binary example separation problem.

Remark 4.20. *It holds*

$$\dot{Q}_R^{LB2,n} \geq \dot{Q}_R^{LB2} \quad \text{for all } n \geq N_F. \quad (4.58)$$

This means that in order to be able to guarantee the existence of a fixed point for a tray $n \geq N_F$ we need at least the reboiler duty that is required to be able to guarantee a fixed point for a tray $n < N_F$.

So far, bounds on \dot{Q}_R , or \dot{Q}_C respectively, were derived such that the existence of at least one solution is guaranteed for the derived fixed-point problem. Similarly, one can show for which choices of \dot{Q}_R , respectively \dot{Q}_C , there exists no fixed point with physical meaning and thus no solution of the MESH system. The possibility of excluding a fixed point provides additional guidelines how the energy should be chosen.

Lemma 4.21. *Let $n < N_F$. If*

$$\dot{Q}_R \leq B (l(\mathbf{x}^B) - l(\mathbf{x}^{n+1}(s))) \quad (4.59)$$

for all $s \in M_n$ and in the limiting cases $s \rightarrow 0$ and $s \rightarrow \infty$ the function φ_{up}^n has no fixed point in M_n .

Proof. A way to guarantee that there exists no fixed point is to assure that $I_n \cap M_n = \emptyset$. Requiring that

$$\sup_{s \in M_n} \varphi_{up}^n(s) \leq 0$$

yields the claim. □

Again, a more general bound on \dot{Q}_R can be derived:

Lemma 4.22. *Let $n < N_F$. If*

$$\dot{Q}_R \leq \dot{Q}_R^{UB1} \quad (4.60)$$

with

$$\dot{Q}_R^{UB1} := B \left(l(\mathbf{x}^B) - \max_{\mathbf{x} \in \mathcal{F}_{NC}} l(\mathbf{x}) \right) \quad (4.61)$$

or alternatively if

$$\dot{Q}_R \leq \dot{Q}_R^{UB2} \quad (4.62)$$

with

$$\begin{aligned} \dot{Q}_R^{UB2} &:= B \left(\min_{\mathbf{x} \in \mathcal{F}_{NC}} l(\mathbf{x}) - \max_{\mathbf{x} \in \mathcal{F}_{NC}} l(\mathbf{x}) \right) \\ &\leq \dot{Q}_R^{UB1} \end{aligned} \quad (4.63)$$

the function φ_{up}^n has no fixed point in M_n .

Remark 4.23. *Note that it always holds $\dot{Q}_R^{UB1} < 0$ and $\dot{Q}_R^{UB2} < 0$. Hence, these bounds are redundant for our considerations as we have already required $\dot{Q}_R > 0$.*

Lemma 4.24. *Let $n \geq N_F$. If*

$$\dot{Q}_R \leq B l(\mathbf{x}^B) - F l(\mathbf{x}^F) + D m_n v(\mathbf{y}^n) + D(1 - m_n) l(\mathbf{x}^{n+1}(s)) \quad (4.64)$$

or equivalently

$$\dot{Q}_C \geq D(l(\mathbf{x}^D) - m_n v(\mathbf{y}^n) + (m_n - 1) l(\mathbf{x}^{n+1}(s))) \quad (4.65)$$

for all $s \in M_n$ and in the limiting cases $s \rightarrow D m_n$ and $s \rightarrow \infty$ the function φ_{up}^n has no fixed point in M_n .

Proof. Analogous to the proof for a stage below the feed stage. \square

Again, more general bounds on \dot{Q}_R that do no longer depend on \mathbf{x}^F and \mathbf{x}^B can be derived:

Lemma 4.25. *Let $n \geq N_F$. If*

$$\dot{Q}_R \leq \dot{Q}_R^{UB1,n} \quad (4.66)$$

with

$$\dot{Q}_R^{UB1,n} := Bl(\mathbf{x}^B) - Fl(\mathbf{x}^F) + Dm_n v(\mathbf{y}^n) + D(1 - m_n) \max_{\mathbf{x} \in \mathcal{F}_{N_C}} l(\mathbf{x}) \quad (4.67)$$

or alternatively if

$$\dot{Q}_R \leq \dot{Q}_R^{UB2,n} \quad (4.68)$$

with

$$\begin{aligned} \dot{Q}_R^{UB2,n} &:= B \left(\min_{\mathbf{x} \in \mathcal{F}_{N_C}} l(\mathbf{x}) - \max_{\mathbf{x} \in \mathcal{F}_{N_C}} l(\mathbf{x}) \right) + Dm_n \left(\min_{\mathbf{x} \in \mathcal{F}_{N_C}} v(\mathbf{x}) - \max_{\mathbf{x} \in \mathcal{F}_{N_C}} l(\mathbf{x}) \right) \\ &\leq \dot{Q}_R^{UB1,n} \end{aligned} \quad (4.69)$$

the function φ_{up}^n has no fixed point in M_n .

It is even possible to formulate a similar result independently of the quotient m_n :

Lemma 4.26. *Let $n \geq N_F$. If*

$$\dot{Q}_R \leq \dot{Q}_R^{UB3,n} \quad (4.70)$$

with

$$\dot{Q}_R^{UB3,n} := Bl(\mathbf{x}^B) - Fl(\mathbf{x}^F) + Dv(\mathbf{y}^n) \quad (4.71)$$

or equivalently

$$\dot{Q}_C \geq D(l(\mathbf{x}^D) - v(\mathbf{y}^n)) \quad (4.72)$$

for all $s \in M_n$ and in the limiting cases $s \rightarrow Dm_n$ and $s \rightarrow \infty$ the function φ_{up}^n has no fixed point in M_n .

Proof. For the proof we use the fact that

$$\begin{aligned} & B(l(\mathbf{x}^B) - l(\mathbf{x}^{n+1}(s))) + D \underbrace{m_n}_{\geq 1} \underbrace{(v(\mathbf{y}^n) - l(\mathbf{x}^{n+1}(s)))}_{> 0} \\ & + F(l(\mathbf{x}^{n+1}(s)) - l(\mathbf{x}^F)) \\ & \geq B(l(\mathbf{x}^B) - l(\mathbf{x}^{n+1}(s))) + D(v(\mathbf{y}^n) - l(\mathbf{x}^{n+1}(s))) \\ & + F(l(\mathbf{x}^{n+1}(s)) - l(\mathbf{x}^F)) \\ & = Bl(\mathbf{x}^B) - Fl(\mathbf{x}^F) + Dv(\mathbf{y}^n). \end{aligned}$$

□

As argued above, more general bounds can also be derived:

Lemma 4.27. *Let $n \geq N_F$. If*

$$\dot{Q}_R \leq \dot{Q}_R^{UB4} \quad (4.73)$$

with

$$\begin{aligned} \dot{Q}_R^{UB4} &:= B \left(\min_{\mathbf{x} \in \mathcal{F}_{NC}} l(\mathbf{x}) - \max_{\mathbf{x} \in \mathcal{F}_{NC}} l(\mathbf{x}) \right) + D \left(\min_{\mathbf{x} \in \mathcal{F}_{NC}} v(\mathbf{x}) - \max_{\mathbf{x} \in \mathcal{F}_{NC}} l(\mathbf{x}) \right) \\ &\leq \dot{Q}_R^{UB3,n} \end{aligned} \quad (4.74)$$

the function φ_{up}^n has no fixed point in M_n .

As a final result we want to summarize our findings with regard to the existence of no fixed point for the function φ_{up}^n :

Theorem 4.28 (Existence of no fixed point of φ_{up}^n in the interval M_n). *For stages $n < N_F$ and strictly positive \dot{Q}_R it is not possible to exclude the existence of a fixed point a priori. For stages $n \geq N_F$ and*

$$\dot{Q}_R \leq \dot{Q}_R^{UB4} \leq \dot{Q}_R^{UB3,n}, \dot{Q}_R^{UB2,n} \leq \dot{Q}_R^{UB1,n} \quad (4.75)$$

there exists no fixed point for the function φ_{up}^n in the interval M_n .

Remark 4.29. *For the sake of completeness we can also state that for $n < N_F$ and*

$$0 < \dot{Q}_R \leq \dot{Q}_R^{LB1} \leq \dot{Q}_R^{LB2} \quad (4.76)$$

it is neither possible to guarantee nor to exclude the existence of a fixed point. A similar result can be derived for $n \geq N_F$ and

$$\dot{Q}_R^{UB4} \leq \dot{Q}_R^{UB3,n}, \dot{Q}_R^{UB2,n} \leq \dot{Q}_R^{UB1,n} < \dot{Q}_R \leq \dot{Q}_R^{LB1,n} \leq \dot{Q}_R^{LB2,n}. \quad (4.77)$$

The lower and upper bounds on \dot{Q}_R in Remark 4.29 for a stage $n \geq N_F$ define intervals for which we cannot state anything about the existence of a fixed point. However, these intervals are usually very small. For a stage $n \geq N_F$ it holds

$$\dot{Q}_R^{LB1,n} - \dot{Q}_R^{UB1,n} = D(m_n - 1) \left(\max_{\mathbf{x} \in \mathcal{F}_{NC}} l(\mathbf{x}) - \min_{\mathbf{x} \in \mathcal{F}_{NC}} l(\mathbf{x}) \right). \quad (4.78)$$

4.3.2. Uniqueness of the fixed point and convergence of the fixed-point iteration

So far, the existence of a fixed point in the interval I_n with $\varphi_{\text{up}}^n(I_n) \subset I_n$ was discussed. If one can additionally show that there exists some $0 \leq q < 1$ such that

$$|(\varphi_{\text{up}}^n)'(s)| \leq q \quad (4.79)$$

for all $s \in I_n$, the fixed point $s^* \in I_n$ is unique and the sequence $(s_k)_{k \in \mathbb{N}}$ defined by $s_k := \varphi_{\text{up}}^n(s_{k-1})$, $k \geq 1$ converges to this fixed point for any $s_0 \in I_n$ by application of the Banach fixed-point theorem.

In a first step we derive an expression for the derivative of φ_{up}^n :

$$(\varphi_{\text{up}}^n)'(s) = (\varphi_{\text{up}}^n(s) + B - F_{\text{up}}^n) \frac{\nabla l(\mathbf{x}^{n+1}(s))(\mathbf{x}^{n+1})'(s)}{v(\mathbf{y}^n) - l(\mathbf{x}^{n+1}(s))}. \quad (4.80)$$

Inserting

$$(\mathbf{x}^{n+1})'(s) = \frac{1}{s + B - F_{\text{up}}^n} (\mathbf{y}^n - \mathbf{x}^{n+1}(s)) \quad (4.81)$$

into Equation (4.80) yields

$$(\varphi_{\text{up}}^n)'(s) = \frac{\varphi_{\text{up}}^n(s) + B - F_{\text{up}}^n}{s + B - F_{\text{up}}^n} \cdot \frac{\nabla l(\mathbf{x}^{n+1}(s)) (\mathbf{y}^n - \mathbf{x}^{n+1}(s))}{v(\mathbf{y}^n) - l(\mathbf{x}^{n+1}(s))}. \quad (4.82)$$

Before considering the general case we want to discuss three special cases.

Case a) $n < N_F$ and $B = 0$:

It follows that $\mathbf{x}^{n+1}(s) \equiv \mathbf{y}^n$ and

$$\varphi_{\text{up}}^n(s) \equiv \frac{\dot{Q}_R}{v(\mathbf{y}^n) - l(\mathbf{y}^n)}. \quad (4.83)$$

From this we can conclude that $(\varphi_{\text{up}}^n)'(s) \equiv 0$.

Case b) $n \geq N_F$ and $B = F$:

Analogously to a) we can conclude that $(\varphi_{\text{up}}^n)'(s) \equiv 0$.

Case c) The asymptotic limiting case $\dot{Q}_R \rightarrow \infty$:

In this case we have

$$\varphi_{\text{up}}^n(s) = \mathcal{O}(\dot{Q}_R) \quad (4.84)$$

and hence also

$$\inf_{s \in M_n} \varphi_{\text{up}}^n(s) = \mathcal{O}(\dot{Q}_R) \quad (4.85)$$

and

$$\sup_{s \in M_n} \varphi_{\text{up}}^n(s) = \mathcal{O}(\dot{Q}_R). \quad (4.86)$$

This yields

$$\lim_{\dot{Q}_R \rightarrow \infty} \max_{s \in I_n} |(\varphi_{\text{up}}^n)'(s)| = 0 \quad (4.87)$$

due to the fact that

$$\lim_{\dot{Q}_R \rightarrow \infty} \max_{s \in I_n} |x_i^{n+1}(s) - y_i^n| = 0 \quad \text{for all } i = 1, \dots, N_C. \quad (4.88)$$

Theorem 4.30 (Uniqueness of the fixed point for three special cases). *In each special case discussed above $(\varphi_{\text{up}}^n)'$ is bounded by 0, i.e. the Lipschitz constant is 0. Thus, the fixed point is unique in I_n and the fixed point is obtained after the first iteration as the function φ_{up}^n is a constant function.*

Due to continuity reasons we can deduce that in case a) there exists $\varepsilon > 0$ such that for all $B < \varepsilon$ we have that $|(\varphi_{\text{up}}^n)'(s)| \leq q < 1$. Similar results can also be derived for b). However, for many separation tasks the choice of B is not completely arbitrary and thus it is not possible to choose B in such a way that a contraction mapping is guaranteed. The most interesting special case is c) from which we can conclude that we can always get an arbitrarily small upper bound on $(\varphi_{\text{up}}^n)'$, i.e. an arbitrary small Lipschitz constant, by increasing \dot{Q}_R due to the fact that we have $(\varphi_{\text{up}}^n)'(s) \equiv 0$ for the asymptotic limiting case. Note that we have already shown in Section 4.3.1 that the existence of a fixed point can also be guaranteed by increasing \dot{Q}_R . Analogously to the approach in the previous section, we want to investigate how small the reboiler duty can be chosen in order to be able to guarantee uniqueness of the fixed point.

We now want to consider the general case and derive bounds on \dot{Q}_R such that the bound $|(\varphi_{\text{up}}^n)'(s)| \leq q < 1$ holds. Once again, we discuss the cases $n < N_F$ and $n \geq N_F$ separately.

Case 1: $n < N_F$

Here, Equation (4.82) simplifies to

$$(\varphi_{\text{up}}^n)'(s) = \frac{\varphi_{\text{up}}^n(s) + B}{s + B} \cdot \frac{\nabla l(\mathbf{x}^{n+1}(s))(\mathbf{y}^n - \mathbf{x}^{n+1}(s))}{v(\mathbf{y}^n) - l(\mathbf{x}^{n+1}(s))}. \quad (4.89)$$

We assume $B > 0$ as we have already discussed $B = 0$ in case a) and furthermore we require \dot{Q}_R to be large enough so that φ_{up}^n maps from I_n to itself (cf. Lemma 4.13). In order to bound (4.89) we start by deriving a bound on the first part of $(\varphi_{\text{up}}^n)'$:

$$\begin{aligned} \left| \frac{\varphi_{\text{up}}^n(s) + B}{s + B} \right| &= \frac{\varphi_{\text{up}}^n(s) + B}{s + B} \\ &\leq \frac{\sup_{s \in M_n} \varphi_{\text{up}}^n(s) + B}{\inf_{s \in M_n} \varphi_{\text{up}}^n(s) + B} \\ &= \sup_{s \in M_n} \left(\frac{\dot{Q}_R + Bl(\mathbf{x}^{n+1}(s)) - Bl(\mathbf{x}^B)}{v(\mathbf{y}^n) - l(\mathbf{x}^{n+1}(s))} + B \right) \\ &\quad \cdot \inf_{s \in M_n} \left(\frac{\dot{Q}_R + Bl(\mathbf{x}^{n+1}(s)) - Bl(\mathbf{x}^B)}{v(\mathbf{y}^n) - l(\mathbf{x}^{n+1}(s))} + B \right)^{-1} \\ &= \sup_{s \in M_n} \left(\frac{\dot{Q}_R + Bv(\mathbf{y}^n) - Bl(\mathbf{x}^B)}{v(\mathbf{y}^n) - l(\mathbf{x}^{n+1}(s))} \right) \\ &\quad \cdot \inf_{s \in M_n} \left(\frac{\dot{Q}_R + Bv(\mathbf{y}^n) - Bl(\mathbf{x}^B)}{v(\mathbf{y}^n) - l(\mathbf{x}^{n+1}(s))} \right)^{-1} \\ &\leq \frac{\min_{\mathbf{x} \in \mathcal{F}_{N_C}} v(\mathbf{x}) - \min_{\mathbf{x} \in \mathcal{F}_{N_C}} l(\mathbf{x})}{\min_{\mathbf{x} \in \mathcal{F}_{N_C}} v(\mathbf{x}) - \max_{\mathbf{x} \in \mathcal{F}_{N_C}} l(\mathbf{x})}. \end{aligned}$$

This bound only depends on the physical properties of the multi-component mixture at pressure p . Obviously, the denominator of the second fraction can be bounded by

$$\left| \frac{1}{v(\mathbf{y}^n) - l(\mathbf{x}^{n+1}(s))} \right| \leq \frac{1}{\min_{\mathbf{x} \in \mathcal{F}_{N_C}} v(\mathbf{x}) - \max_{\mathbf{x} \in \mathcal{F}_{N_C}} l(\mathbf{x})}. \quad (4.90)$$

Using Equation (4.13) we can derive the following expression

$$y_i^n - x_i^{n+1}(s) = \frac{B}{s + B} (y_i^n - x_i^B), \quad i = 1, \dots, N_C \quad (4.91)$$

from which we can conclude that

$$|y_i^n - x_i^{n+1}(s)| = \frac{B}{s+B} |y_i^n - x_i^B|, \quad i = 1, \dots, N_C. \quad (4.92)$$

If we additionally require $\inf_{s \in M_n} \varphi_{\text{up}}^n(s) \geq \hat{c} \cdot B > 0$ with parameter $\hat{c} > 0$ we get

$$|y_i^n - x_i^{n+1}(s)| \leq \frac{1}{\hat{c} + 1} |y_i^n - x_i^B|, \quad i = 1, \dots, N_C. \quad (4.93)$$

Lemma 4.31. *Let $n < N_F$. If*

$$\dot{Q}_R \geq \hat{c} \cdot B \left(\max_{\mathbf{x} \in \mathcal{F}_{N_C}} v(\mathbf{x}) - \min_{\mathbf{x} \in \mathcal{F}_{N_C}} l(\mathbf{x}) \right) + B \left(\max_{\mathbf{x} \in \mathcal{F}_{N_C}} l(\mathbf{x}) - \min_{\mathbf{x} \in \mathcal{F}_{N_C}} l(\mathbf{x}) \right) \quad (4.94)$$

$$\geq \hat{c} \cdot B (v(\mathbf{y}^n) - l(\mathbf{x}^{n+1}(s))) + B (l(\mathbf{x}^B) - l(\mathbf{x}^{n+1}(s))), \quad (4.95)$$

for all $s \in M_n$ and in the limiting cases $s \rightarrow Dm_n$ and $s \rightarrow \infty$ it holds that $\inf_{s \in M_n} \varphi_{\text{up}}^n(s) \geq \hat{c} \cdot B > 0$.

The following computations yield a bound for the remaining nominator:

$$|\nabla l(\mathbf{x}^{n+1}(s)) (\mathbf{y}^n - \mathbf{x}^{n+1}(s))| \quad (4.96)$$

$$= \left| \sum_{i=1}^{N_C} \frac{\partial l}{\partial x_i}(\mathbf{x}^{n+1}(s)) (y_i^n - x_i^{n+1}(s)) \right| \quad (4.97)$$

$$= \left| \sum_{i=2}^{N_C} \left(\frac{\partial l}{\partial x_i}(\mathbf{x}^{n+1}(s)) - \frac{\partial l}{\partial x_1}(\mathbf{x}^{n+1}(s)) \right) (y_i^n - x_i^{n+1}(s)) \right| \quad (4.98)$$

using the fact that

$$y_1^n - x_1^{n+1}(s) = - \sum_{i=2}^{N_C} (y_i^n - x_i^{n+1}(s)). \quad (4.99)$$

Triangle inequality gives us

$$\left| \sum_{i=2}^{N_C} \left(\frac{\partial l}{\partial x_i}(\mathbf{x}^{n+1}(s)) - \frac{\partial l}{\partial x_1}(\mathbf{x}^{n+1}(s)) \right) (y_i^n - x_i^{n+1}(s)) \right| \quad (4.100)$$

$$\leq \sum_{i=2}^{N_C} \left| \frac{\partial l}{\partial x_i}(\mathbf{x}^{n+1}(s)) - \frac{\partial l}{\partial x_1}(\mathbf{x}^{n+1}(s)) \right| |y_i^n - x_i^{n+1}(s)| \quad (4.101)$$

$$\leq \max_{1 \leq i < j \leq N_C} \left| \frac{\partial l}{\partial x_i}(\mathbf{x}^{n+1}(s)) - \frac{\partial l}{\partial x_j}(\mathbf{x}^{n+1}(s)) \right| \sum_{i=2}^{N_C} |y_i^n - x_i^{n+1}(s)|. \quad (4.102)$$

Inserting (4.93) into (4.102) and taking the maximum over all $\mathbf{x} \in \mathcal{F}_{N_C}$ yields

$$|\nabla l(\mathbf{x}^{n+1}(s)) (\mathbf{y}^n - \mathbf{x}^{n+1}(s))| \quad (4.103)$$

$$\leq \frac{1}{\hat{c} + 1} \max_{1 \leq i < j \leq N_C} \max_{\mathbf{x} \in \mathcal{F}_{N_C}} \left| \frac{\partial l}{\partial x_i}(\mathbf{x}) - \frac{\partial l}{\partial x_j}(\mathbf{x}) \right| \sum_{i=2}^{N_C} |y_i^n - x_i^B|. \quad (4.104)$$

For the considered system a bound for the term

$$\max_{1 \leq i < j \leq N_C} \max_{\mathbf{x} \in \mathcal{F}_{N_C}} \left| \frac{\partial l}{\partial x_i}(\mathbf{x}) - \frac{\partial l}{\partial x_j}(\mathbf{x}) \right| \quad (4.105)$$

can be obtained from a preprocessing step.

The derived upper bound in Equation (4.104) does no longer depend on the fixed-point variable s . In order to get an upper bound that is even independent of the concentration vectors \mathbf{x}^B and \mathbf{y}^n we can use the rather cautious bound

$$\sum_{i=1}^{N_C} |y_i^n - x_i^B| \leq 2 \quad (4.106)$$

which can be proven by using the summation equation for \mathbf{y}^n and \mathbf{x}^B . These results can be summarized in the following lemma:

Lemma 4.32. *Let $n < N_F$ and*

$$\dot{Q}_R > \dot{Q}_R^{LB1,n,unique} \quad \text{or} \quad \dot{Q}_R > \dot{Q}_R^{LB2,unique} \quad (4.107)$$

with

$$\begin{aligned} \dot{Q}_R^{LB1,n,unique} &:= \hat{c} \cdot B \left(v(\mathbf{y}^n) - \min_{\mathbf{x} \in \mathcal{F}_{N_C}} l(\mathbf{x}) \right) + B \left(l(\mathbf{x}^B) - \min_{\mathbf{x} \in \mathcal{F}_{N_C}} l(\mathbf{x}) \right) \\ &\geq \dot{Q}_R^{LB1} \end{aligned} \quad (4.108)$$

and

$$\begin{aligned} \dot{Q}_R^{LB2,unique} &:= \hat{c} \cdot B \left(\max_{\mathbf{x} \in \mathcal{F}_{N_C}} v(\mathbf{x}) - \min_{\mathbf{x} \in \mathcal{F}_{N_C}} l(\mathbf{x}) \right) + B \left(\max_{\mathbf{x} \in \mathcal{F}_{N_C}} l(\mathbf{x}) - \min_{\mathbf{x} \in \mathcal{F}_{N_C}} l(\mathbf{x}) \right) \\ &\geq \dot{Q}_R^{LB2}. \end{aligned} \quad (4.109)$$

Then it holds that

$$\begin{aligned}
 |(\varphi_{up}^n)'(s)| &= \left| \frac{\varphi_{up}^n(s) + B}{s + B} \cdot \frac{\nabla l(\mathbf{x}^{n+1}(s)) (\mathbf{y}^n - \mathbf{x}^{n+1}(s))}{v(\mathbf{y}^n) - l(\mathbf{x}^{n+1}(s))} \right| \\
 &\leq \frac{\min_{\mathbf{x} \in \mathcal{F}_{N_C}} v(\mathbf{x}) - \min_{\mathbf{x} \in \mathcal{F}_{N_C}} l(\mathbf{x})}{\left(\min_{\mathbf{x} \in \mathcal{F}_{N_C}} v(\mathbf{x}) - \max_{\mathbf{x} \in \mathcal{F}_{N_C}} l(\mathbf{x}) \right)^2} \\
 &\quad \cdot \frac{2}{\hat{c} + 1} \max_{1 \leq i < j \leq N_C} \max_{\mathbf{x} \in \mathcal{F}_{N_C}} \left| \frac{\partial l}{\partial x_i}(\mathbf{x}) - \frac{\partial l}{\partial x_j}(\mathbf{x}) \right| \\
 &=: q(\hat{c}).
 \end{aligned} \tag{4.110}$$

This bound only depends on \hat{c} and the physical properties of the multi-component mixture at pressure p . The value for \hat{c} can always be chosen in such a way that $|(\varphi_{up}^n)'(s)| \leq q(\hat{c}) < 1$. This leads to the following result:

Theorem 4.33 (Uniqueness of the fixed point for stages $n < N_F$). *Let $n < N_F$ and*

$$\dot{Q}_R > \dot{Q}_R^{LB1,n,unique} \quad \text{or} \quad \dot{Q}_R > \dot{Q}_R^{LB2,unique}.$$

If \hat{c} is chosen in a way that $|(\varphi_{up}^n)'(s)| \leq q(\hat{c}) < 1$ there exists a unique fixed point in I_n and convergence of the sequence $(s_k)_{k \in \mathbb{N}}$ defined by $s_k := \varphi_{up}^n(s_{k-1})$ towards this fixed point is guaranteed for any $s_0 \in I_n$.

The fixed-point iteration thus has guaranteed convergence if \dot{Q}_R is chosen above the derived limits $\dot{Q}_R^{LB1,n,unique}$ or $\dot{Q}_R^{LB2,unique}$. Both limits depend on the choice of B , \hat{c} and the physical properties of the considered system at pressure p , and evaluation of $\dot{Q}_R^{LB1,n,unique}$ additionally requires knowledge of the composition vectors \mathbf{y}^n and \mathbf{x}^B .

Note that the function $q(\hat{c})$ only serves as an upper bound for the actual Lipschitz constant for $(\varphi_{up}^n)'$ based on the physical properties of the considered system at pressure p . In case more information about the choice of process variables is known, it is also possible to evaluate the Lipschitz constant more precisely. Appropriate numerical examples are discussed in Section 4.4.

For completeness, we also want to discuss the second case.

Case 2: $n \geq N_F$

In this case, Equation (4.82) simplifies to

$$(\varphi_{\text{up}}^n)'(s) = \frac{\varphi_{\text{up}}^n(s) - D}{s - D} \cdot \frac{\nabla l(\mathbf{x}^{n+1}(s))(\mathbf{y}^n - \mathbf{x}^{n+1}(s))}{v(\mathbf{y}^n) - l(\mathbf{x}^{n+1}(s))}. \quad (4.111)$$

Analogously to case 1, we assume $D > 0$ as we have already discussed $D = 0$ in case b) and furthermore we require \dot{Q}_R to be large enough so that φ_{up}^n maps from I_n to itself (cf. Lemma 4.15). In order to bound (4.111) we start by deriving a bound on the first part of $(\varphi_{\text{up}}^n)'$:

$$\begin{aligned} \left| \frac{\varphi_{\text{up}}^n(s) - D}{s - D} \right| &= \frac{\varphi_{\text{up}}^n(s) - D}{s - D} \\ &\leq \frac{\sup_{s \in M_n} \varphi_{\text{up}}^n(s) - D}{\inf_{s \in M_n} \varphi_{\text{up}}^n(s) - D} \\ &= \sup_{s \in M_n} \left(\frac{\dot{Q}_R + Fl(\mathbf{x}^F) - Dl(\mathbf{x}^{n+1}(s)) - Bl(\mathbf{x}^B)}{v(\mathbf{y}^n) - l(\mathbf{x}^{n+1}(s))} - D \right) \\ &\quad \cdot \inf_{s \in M_n} \left(\frac{\dot{Q}_R + Fl(\mathbf{x}^F) - Dl(\mathbf{x}^{n+1}(s)) - Bl(\mathbf{x}^B)}{v(\mathbf{y}^n) - l(\mathbf{x}^{n+1}(s))} - D \right)^{-1} \\ &= \sup_{s \in M_n} \left(\frac{\dot{Q}_R + Fl(\mathbf{x}^F) - Dv(\mathbf{y}^n) - Bl(\mathbf{x}^B)}{v(\mathbf{y}^n) - l(\mathbf{x}^{n+1}(s))} \right) \\ &\quad \cdot \inf_{s \in M_n} \left(\frac{\dot{Q}_R + Fl(\mathbf{x}^F) - Dv(\mathbf{y}^n) - Bl(\mathbf{x}^B)}{v(\mathbf{y}^n) - l(\mathbf{x}^{n+1}(s))} \right)^{-1} \\ &\leq \frac{\min_{\mathbf{x} \in \mathcal{F}_{NC}} v(\mathbf{x}) - \min_{\mathbf{x} \in \mathcal{F}_{NC}} l(\mathbf{x})}{\min_{\mathbf{x} \in \mathcal{F}_{NC}} v(\mathbf{x}) - \max_{\mathbf{x} \in \mathcal{F}_{NC}} l(\mathbf{x})}. \end{aligned}$$

Furthermore, it holds:

$$\left| \frac{1}{v(\mathbf{y}^n) - l(\mathbf{x}^{n+1}(s))} \right| \leq \frac{1}{\min_{\mathbf{x} \in \mathcal{F}_{NC}} v(\mathbf{x}) - \max_{\mathbf{x} \in \mathcal{F}_{NC}} l(\mathbf{x})}. \quad (4.112)$$

Using Equation (4.13) the following expression can be derived

$$y_i^n - x_i^{n+1}(s) = \frac{D}{s - D} (x_i^D - y_i^n), \quad i = 1, \dots, N_C \quad (4.113)$$

from which we can conclude

$$|y_i^n - x_i^{n+1}(s)| = \frac{D}{s - D} |y_i^n - x_i^D|, \quad i = 1, \dots, N_C. \quad (4.114)$$

4. Stage-to-stage calculations of simple distillation columns

If we use this result and additionally require $\inf_{s \in M_n} \varphi_{\text{up}}^n(s) \geq \tilde{c} \cdot D > 0$ where we introduce the parameter $\tilde{c} > 1$ we get

$$|y_i^n - x_i^{n+1}(s)| \leq \frac{1}{\tilde{c} - 1} |y_i^n - x_i^D|, \quad i = 1, \dots, N_C. \quad (4.115)$$

From the following result it is possible to deduce under which conditions it holds that $\inf_{s \in M_n} \varphi_{\text{up}}^n(s) \geq \tilde{c} \cdot D > 0$:

Lemma 4.34. *Let $n \geq N_F$. If*

$$\begin{aligned} \dot{Q}_R &\geq B \left(\max_{\mathbf{x} \in \mathcal{F}_{N_C}} l(\mathbf{x}) - \min_{\mathbf{x} \in \mathcal{F}_{N_C}} l(\mathbf{x}) \right) + D\tilde{c} \left(\max_{\mathbf{x} \in \mathcal{F}_{N_C}} v(\mathbf{x}) - \min_{\mathbf{x} \in \mathcal{F}_{N_C}} l(\mathbf{x}) \right) \\ &\geq Bl(\mathbf{x}^B) - Fl(\mathbf{x}^F) + Dm_n v(\mathbf{y}^n) + D(1 - \tilde{c}) \min_{\mathbf{x} \in \mathcal{F}_{N_C}} l(\mathbf{x}) \end{aligned}$$

for all $s \in M_n$ and in the limiting cases $s \rightarrow Dm_n$ and $s \rightarrow \infty$ it holds that $\inf_{s \in M_n} \varphi_{\text{up}}^n(s) \geq \tilde{c} \cdot D > 0$.

Along the same lines as for the case $n < N_F$ we can proceed and summarize the final result:

Lemma 4.35. *Let $n \geq N_F$ and*

$$\dot{Q}_R > \dot{Q}_R^{\text{LB1},n,\text{unique}} \quad \text{or} \quad \dot{Q}_R > \dot{Q}_R^{\text{LB2},n,\text{unique}} \quad (4.116)$$

with

$$\begin{aligned} \dot{Q}_R^{\text{LB1},n,\text{unique}} &:= Bl(\mathbf{x}^B) - Fl(\mathbf{x}^F) + D \max(\tilde{c}, m_n) v(\mathbf{y}^n) \\ &\quad + D(1 - \max(\tilde{c}, m_n)) \max_{\mathbf{x} \in \mathcal{F}_{N_C}} l(\mathbf{x}) \\ &\geq \dot{Q}_R^{\text{LB1},n} \end{aligned} \quad (4.117)$$

and

$$\begin{aligned} \dot{Q}_R^{\text{LB2},n,\text{unique}} &:= B \left(\max_{\mathbf{x} \in \mathcal{F}_{N_C}} l(\mathbf{x}) - \min_{\mathbf{x} \in \mathcal{F}_{N_C}} l(\mathbf{x}) \right) \\ &\quad + D \max(\tilde{c}, m_n) \cdot \left(\max_{\mathbf{x} \in \mathcal{F}_{N_C}} v(\mathbf{x}) - \min_{\mathbf{x} \in \mathcal{F}_{N_C}} l(\mathbf{x}) \right) \\ &\geq \dot{Q}_R^{\text{LB2},n}. \end{aligned} \quad (4.118)$$

Then it holds that

$$\begin{aligned}
 |(\varphi_{up}^n)'(s)| &= \left| \frac{\varphi_{up}^n(s) - D}{s - D} \cdot \frac{\nabla l(\mathbf{x}^{n+1}(s)) (\mathbf{y}^n - \mathbf{x}^{n+1}(s))}{v(\mathbf{y}^n) - l(\mathbf{x}^{n+1}(s))} \right| \\
 &\leq \frac{\min_{\mathbf{x} \in \mathcal{F}_{N_C}} v(\mathbf{x}) - \min_{\mathbf{x} \in \mathcal{F}_{N_C}} l(\mathbf{x})}{\left(\min_{\mathbf{x} \in \mathcal{F}_{N_C}} v(\mathbf{x}) - \max_{\mathbf{x} \in \mathcal{F}_{N_C}} l(\mathbf{x}) \right)^2} \\
 &\quad \cdot \frac{2}{\tilde{c} - 1} \max_{1 \leq i < j \leq N_C} \max_{\mathbf{x} \in \mathcal{F}_{N_C}} \left| \frac{\partial l}{\partial x_i}(\mathbf{x}) - \frac{\partial l}{\partial x_j}(\mathbf{x}) \right| \\
 &=: q(\tilde{c}).
 \end{aligned} \tag{4.119}$$

The bound in (4.119) only depends on the parameter \tilde{c} and the physical properties of the multi-component mixture at given pressure p and again the value for \tilde{c} can always be chosen in such a way that $|(\varphi_{up}^n)'(s)| \leq q(\tilde{c}) < 1$. In summary we can conclude:

Theorem 4.36 (Uniqueness of the fixed point for stages $n \geq N_F$). *Let $n \geq N_F$ and*

$$\dot{Q}_R > \dot{Q}_R^{LB1,n,unique} \quad \text{or} \quad \dot{Q}_R > \dot{Q}_R^{LB2,n,unique}.$$

If \tilde{c} is chosen in a way that $|(\varphi_{up}^n)'(s)| \leq q(\tilde{c}) < 1$ there exists a unique fixed point in I_n and convergence of the sequence $(s_k)_{k \in \mathbb{N}}$ defined by $s_k := \varphi_{up}^n(s_{k-1})$ towards this fixed point is guaranteed for any $s_0 \in I_n$.

The fixed-point iteration thus has guaranteed convergence if \dot{Q}_R is chosen above the limits $\dot{Q}_R^{LB1,n,unique}$ or $\dot{Q}_R^{LB2,n,unique}$. Both limits depend on the choice of F , B , i.e. also D , the current value for m_n , the physical properties of the considered system at pressure p , and the parameter \tilde{c} . In addition, $\dot{Q}_R^{LB1,n,unique}$ requires the knowledge of the composition vectors \mathbf{x}^B , \mathbf{x}^F , and \mathbf{y}^n . As indicated in Lemma 4.35, the energy bounds that guarantee uniqueness of the fixed point might be more restrictive than those energy bounds that only guarantee the existence of at least one fixed point.

As in case 1, the bound $q(\tilde{c})$ on the Lipschitz constant only depends on \tilde{c} and the physical properties of the considered system at pressure p . The more information given on the choice of process variables, the more precisely the Lipschitz constant can be evaluated and numerical studies are presented in Section 4.4.

Remark 4.37. *In case we have $N_C \leq 3$ the factor 2 in (4.110) and (4.119) can be replaced by 1.*

4.3.3. Rate of convergence

In this section, the rate of convergence of the corresponding fixed-point iteration is considered. In case the parameter \hat{c} , or \tilde{c} respectively, is chosen in such a way that $|(\varphi_{\text{up}}^n)'(s)| \leq q < 1$ we know that the fixed-point iteration converges at least linearly. The question is now, whether higher order convergence can also be proven. We can state the following result:

Theorem 4.38 (Rate of convergence). *The rate of convergence for the considered fixed-point iteration of the function φ_{up}^n is generally linear.*

Proof. A necessary condition for convergence of order $p \geq 2$ is that for a fixed point s^* it holds:

$$(\varphi_{\text{up}}^n)^{(k)}(s^*) = 0 \quad \text{for all } k = 1, \dots, p - 1. \quad (4.120)$$

In the fixed point s^* we have

$$(\varphi_{\text{up}}^n)'(s^*) = \frac{\nabla l(\mathbf{x}^{n+1}(s^*)) (\mathbf{y}^n - \mathbf{x}^{n+1}(s^*))}{v(\mathbf{y}^n) - l(\mathbf{x}^{n+1}(s^*))}. \quad (4.121)$$

Hence, the derivative in the fixed point equals zero iff

$$\nabla l(\mathbf{x}^{n+1}(s^*)) (\mathbf{y}^n - \mathbf{x}^{n+1}(s^*)) = 0, \quad (4.122)$$

which is in general not the case and thus the rate of convergence is linear. \square

However, the actual Lipschitz constant is in general very small and the derived bound on $(\varphi_{\text{up}}^n)'$ can be shown to be strictly smaller than 1 for suitable \dot{Q}_R . This bound can be evaluated if only very basic information on the choice of variables is given and is quite pessimistic, which is especially due to the fact that we bound the differences of the composition vectors \mathbf{x}^B and \mathbf{y}^n , or \mathbf{y}^n and \mathbf{x}^D respectively, in the general case by 2.

4.4. A numerical example

In this section, we illustrate the theoretical results derived in this chapter with a numerical example. First, an example separation problem is introduced. Based on this problem it is possible to state minimal energy requirements that guarantee existence of a fixed

point and convergence towards this fixed point. Furthermore, we investigate the speed of convergence of the fixed-point iteration and determine the number of stages needed for the desired separation as well as the minimum energy needed.

4.4.1. Example separation problem

A binary mixture of acetone (AC) and chloroform (CF) is considered which exhibits a heavy-boiling azeotrope at

$$x_{AC}^{Azeo} = 0.3454 \text{ mol/mol} \quad (4.123)$$

for 1 bar. The physical property models used for the calculation including enthalpy data needed to derive the energy bounds are given in Appendix A.2. We specify the pressure p , the molar flow rate F and composition \mathbf{x}^F of the feed, the molar flow rate B and composition \mathbf{x}^B of the bottom product, the reboiler duty \dot{Q}_R , and the feed stage N_F . The parameters used in this example are given in Table 4.1.

Table 4.1.: Parameters used for stage-to-stage calculations of a distillation column for a binary mixture of acetone (AC) and chloroform (CF).

| Parameter | Value |
|----------------------------|--------------------|
| p / bar | 1 |
| F / (kmol/h) | 1 |
| \mathbf{x}^F / (mol/mol) | 0.5 AC 0.5 CF |
| B / (kmol/h) | 0.76 |
| \mathbf{x}^B / (mol/mol) | 0.35 AC 0.65 CF |
| \dot{Q}_R / kW | 25 |
| N_F | 30 |

Using the overall material balance for the parameters in Table 4.1 we obtain the molar flow rate $D = 0.24$ kmol/h, and composition $x_{AC}^D = 0.975$ mol/mol, $x_{CF}^D = 0.025$ mol/mol of the distillate. In this example, 0.975 mol/mol acetone is required as minimum purity of the distillate.

4.4.2. Energy bounds derived with the Banach fixed-point theorem

The energy bounds that have been derived in Section 4.3 can be applied to verify that the choice of \dot{Q}_R in Table 4.1 enables upward calculation of the column. Again we consider the two different cases $n < N_F$ and $n \geq N_F$.

In a first step we want to evaluate the energy bounds for an arbitrary stage $n < N_F$. Using the parameters from Table 4.1 we obtain using Equation (4.43)

$$\dot{Q}_R^{LB1} = 0.1431 \text{ kW} \quad (4.124)$$

and in case \mathbf{x}^B is not known we get using Equation (4.45)

$$\dot{Q}_R^{LB2} = 0.1477 \text{ kW}. \quad (4.125)$$

Note that in this exemplary case we need a very small reboiler duty in order to be able to proceed upward the column for stages below the feed stage. The lower bounds derived in Section 4.3.1 are negative and therefore not evaluated here. The physically relevant lower bound is $\dot{Q}_R > 0 \text{ kW}$.

Additionally, it is also possible to evaluate $\dot{Q}_R^{LB1,n,unique}$ and $\dot{Q}_R^{LB2,unique}$ for $n < N_F$. For that purpose, the parameter \hat{c} has to be chosen in an appropriate way such that $q(\hat{c}) < 1$. In order to determine \hat{c} , the function $q(\hat{c})$ (cf. Equation (4.110)) is plotted in Figure 4.2 for the system acetone and chloroform at 1 bar.

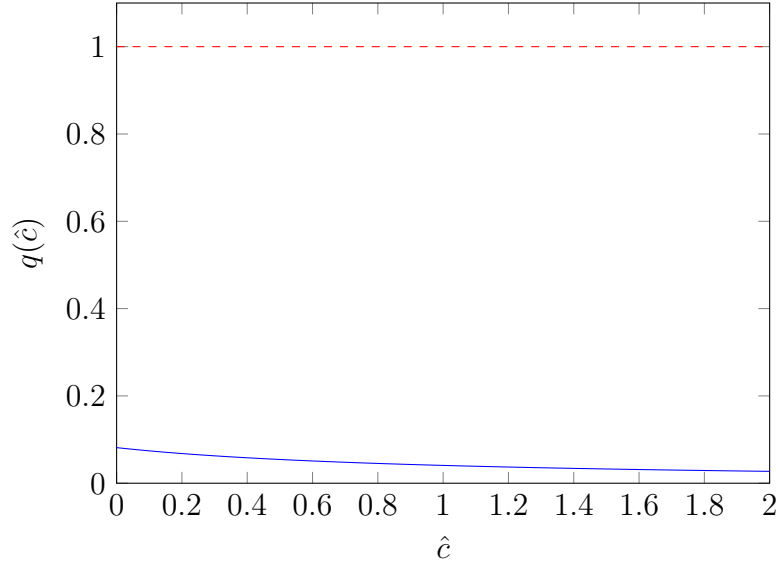


Figure 4.2.: Function $q(\hat{c})$ is plotted for the system acetone and chloroform at 1 bar. The dotted horizontal line at $q(\hat{c}) = 1$ indicates for which values of \hat{c} we can be sure to have a derivative which can be bounded by $q(\hat{c}) < 1$. The critical bound is the lower bound 0 as the function decreases for increasing \hat{c} as shown here for the exemplary interval $[0; 2]$.

From Figure 4.2 we can conclude that for each $\hat{c} > 0$ we can guarantee $q(\hat{c}) < 1$ which in turn gives uniqueness of the fixed point and convergence of the fixed-point iteration. With this information and by using Equation (4.108) and (4.109) we immediately get:

$$\dot{Q}_R^{LB1,n,unique} = \dot{Q}_R^{LB1} \quad (4.126)$$

and

$$\dot{Q}_R^{LB2,unique} = \dot{Q}_R^{LB2}. \quad (4.127)$$

In a next step, we observe how the bounds change for a stage $n \geq N_F$.

In the binary separation problem introduced above, the mole fraction of acetone in the vapor phase increases monotonously from stage to stage whereas the mole fraction of chloroform decreases for suitable choices of the reboiler duty due to the different boiling points. However, if the reboiler duty is chosen too small we obtain solutions that are only mathematically but not physically feasible as presented in a later example. For a feasible

column it holds

$$\frac{x_{AC}^D}{y_{AC}^n} \geq 1 \quad \text{and} \quad \frac{x_{CF}^D}{y_{CF}^n} \leq 1 \quad \text{for all } n = 1, \dots, N_S, \quad (4.128)$$

where $\mathbf{x}^D = \mathbf{y}^{N_S}$. The parameter $m_n = \max_{i=1, \dots, N_C} \left(\frac{x_i^D}{y_i^n} \right)$ attains its maximum at component $i = AC$ and as the mole fraction of acetone increases for increasing n , m_n takes its largest and thus most restrictive value on stage $n = 1$:

$$m_n \leq m_1 = \frac{x_{AC}^D}{y_{AC}^1} = 2.774 \quad (4.129)$$

for all $n \geq N_F$ and $y_{AC}^1 = 0.3515$ mol/mol, where \mathbf{y}^1 is calculated from \mathbf{x}^B and p by using the extended Raoult's law (cf. Appendix A.2).

By inserting the worst case values of m_n (cf. Equation (4.129)) and the vapor enthalpy of \mathbf{y}^n (cf. Table A.6) we obtain general bounds for all stages $n \geq N_F$ of the column. Using the parameters from Table 4.1 in Equation (4.51) we can conclude that

$$\dot{Q}_R^{LB1,n} \leq 5.502 \text{ kW} \quad \text{for all } n \geq N_F \quad (4.130)$$

and in case the composition vectors \mathbf{x}^F and \mathbf{x}^B are not known we still obtain

$$\dot{Q}_R^{LB2,n} \leq 5.697 \text{ kW} \quad \text{for all } n \geq N_F \quad (4.131)$$

using Equation (4.53).

The above bounds are derived without knowing the exact values for \mathbf{y}^n and m_n . Furthermore, we can also calculate values for $\dot{Q}_R^{UB3,n}$ and \dot{Q}_R^{UB4} using Equation (4.71) and (4.74) based on the parameters from Table 4.1. We get

$$\dot{Q}_R^{UB3,n} \geq 1.927 \text{ kW} \quad \text{for all } n \geq N_F \quad (4.132)$$

and

$$\dot{Q}_R^{UB4} = 1.779 \text{ kW} \quad (4.133)$$

if the composition vectors \mathbf{x}^F and \mathbf{x}^B are not known.

For choices of \dot{Q}_R below the above bounds $\dot{Q}_R^{UB3,n}$ and \dot{Q}_R^{UB4} there exists no fixed point for a stage $n \geq N_F$ and hence it is not possible to proceed upward the column. In order to calculate the remaining bounds $\dot{Q}_R^{UB1,n}$ and $\dot{Q}_R^{UB2,n}$, values for \mathbf{y}^n and m_n also have to be known.

The energy bounds derived so far are visualized in Figure 4.3. For values of \dot{Q}_R chosen between $\dot{Q}_R^{UB3,n}$ and $\dot{Q}_R^{LB1,n}$ it is not clear whether a fixed point exists or not.

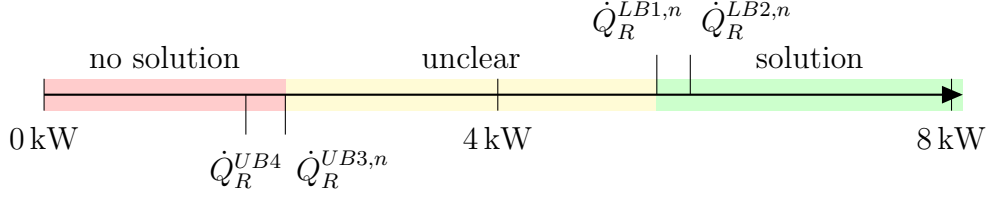


Figure 4.3.: Schematic visualization of the energy bounds that can be derived with the bound in Equation (4.129) and the parameters given in Table 4.1 but without knowing \mathbf{y}^n .

In a next step, one certain stage $n \geq N_F$ is considered for which \mathbf{y}^n is supposed to be given. In this exemplary case, we assume $y_{AC}^n = 0.6$ mol/mol. This gives $m_n = 1.625$. Based on these values and the parameters in Table 4.1 we can again evaluate the bounds $\dot{Q}_R^{LB1,n}$, $\dot{Q}_R^{LB2,n}$, and $\dot{Q}_R^{UB1,n} - \dot{Q}_R^{UB4}$ derived in Section 4.3. The results are given in Table 4.2.

In order to be able to evaluate $\dot{Q}_R^{LB1,n,unique}$ and $\dot{Q}_R^{LB2,n,unique}$ we need information about an appropriate choice of \tilde{c} . For that purpose, the function $q(\tilde{c})$ (cf. Equation (4.119)) is plotted in Figure 4.4 for the system acetone and chloroform at 1 bar.

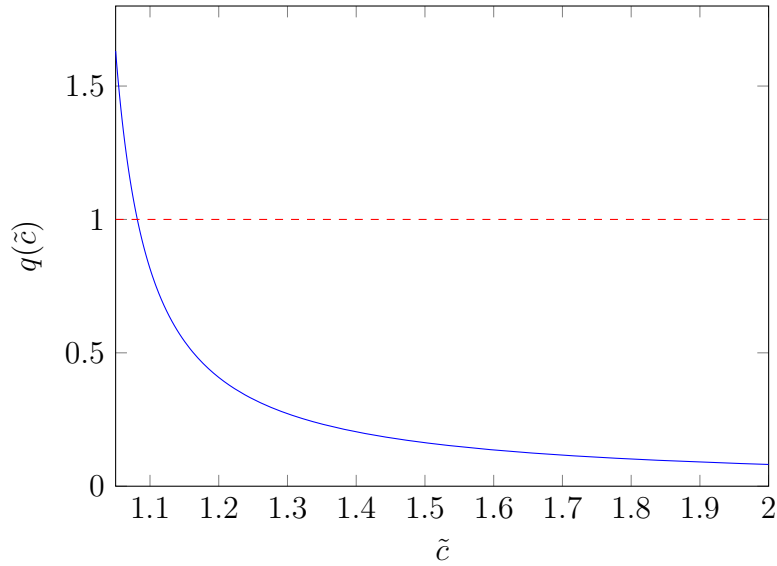


Figure 4.4.: Function $q(\tilde{c})$ is plotted for the system acetone and chloroform at 1 bar. The dotted horizontal line at $q(\tilde{c}) = 1$ indicates for which values of \tilde{c} we can be sure to have a derivative which can be bounded by $q(\tilde{c}) < 1$.

From Figure 4.4 we can conclude that $\tilde{c} \approx 1.09$ suffices in order to guarantee $q(\tilde{c}) < 1$ which gives us uniqueness of the fixed point and convergence of the fixed-point iteration. With this choice of \tilde{c} it is now possible to determine the two remaining energy bounds. In this exemplary case, we have

$$\max(\tilde{c}, m_n) \leq \max(\tilde{c}, m_1) = m_1 \quad \text{for all } n \geq N_F \quad (4.134)$$

and thus the energy bounds that guarantee uniqueness are not more restrictive than the bounds that guarantee existence of a fixed point, cf. Table 4.2 and Figure 4.5. Note that in this special case, where all information for the computation of $\dot{Q}_R^{LB1,n}$ and $\dot{Q}_R^{UB1,n}$ is available, the gap between $\dot{Q}_R^{LB1,n}$ and $\dot{Q}_R^{UB1,n}$, where we can neither guarantee, nor exclude a fixed point, becomes very small. For the value of \dot{Q}_R chosen in Table 4.1 a fixed point exists and stage-to-stage calculation of the column is possible with guaranteed convergence of the fixed-point iteration.

Table 4.2.: Energy bounds exemplarily evaluated for $y_{AC}^n = 0.6$ mol/mol and the parameters given in Table 4.1.

| Bound | Value / kW |
|--|------------|
| $\dot{Q}_R^{LB2,n} = \dot{Q}_R^{LB2,n,unique}$ | 3.399 |
| $\dot{Q}_R^{LB1,n} = \dot{Q}_R^{LB1,n,unique}$ | 3.201 |
| $\dot{Q}_R^{UB1,n}$ | 3.172 |
| $\dot{Q}_R^{UB2,n}$ | 2.983 |
| $\dot{Q}_R^{UB3,n}$ | 1.952 |
| \dot{Q}_R^{UB4} | 1.779 |

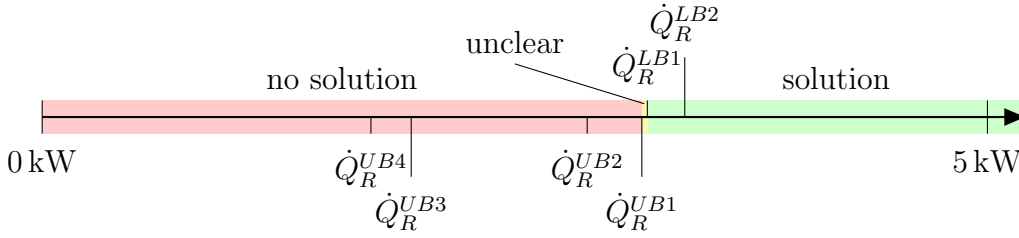


Figure 4.5.: Schematic visualization of the energy bounds for $y_{AC}^n = 0.6$ mol/mol, $m_n = 1.625$ and the parameters given in Table 4.1.

The energy bounds given in Table 4.2 can be graphically verified by plotting the function

$$\varphi_{\text{up}}^n(s) = \frac{\dot{Q}_R + Fl(\mathbf{x}^F) + (B - F)l(\mathbf{x}^{n+1}(s)) - Bl(\mathbf{x}^B)}{v(\mathbf{y}^n) - l(\mathbf{x}^{n+1}(s))} \quad (4.135)$$

for the parameters given in Table 4.1 and inserting $\dot{Q}_R^{LB1,n} = 3.201$ kW or $\dot{Q}_R^{UB1,n} = 3.172$ kW in the above function as reboiler duty. We expect that for $\dot{Q}_R^{LB1,n}$ the function $\varphi_{\text{up}}^n(s)$ intersects with the function $f(s) = s$, i.e. there exists a fixed point. The converse holds for $\dot{Q}_R^{UB1,n}$. Here, we expect that there exists no intersection between $\varphi_{\text{up}}^n(s)$ and $f(s) = s$ and thus also no fixed point. The result, which approves this behavior, is depicted in Figure 4.6 and 4.7 where the region of interest $(Dm_n; 0.4) = (0.39; 0.4)$ on the x -axis is enlarged.

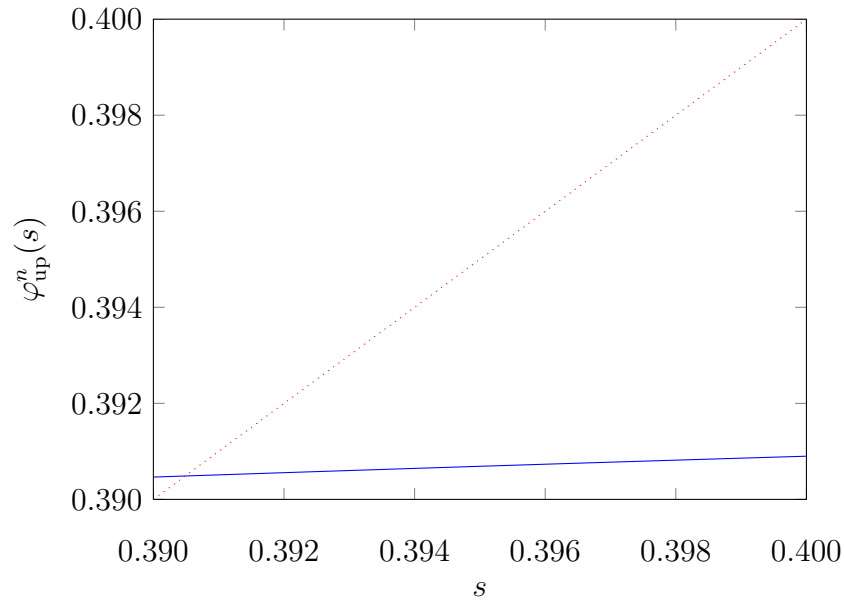


Figure 4.6.: φ_{up}^n is plotted for the region of interest $(Dm_n; 0.4) = (0.39; 0.4)$. The dotted line represents the function $f(s) = s$. We used $\dot{Q}_R^{LB1,n} = 3.201$ kW, $y_{\text{AC}}^n = 0.6$ mol/mol, $m_n = 1.625$ and the parameters given in Table 4.1.

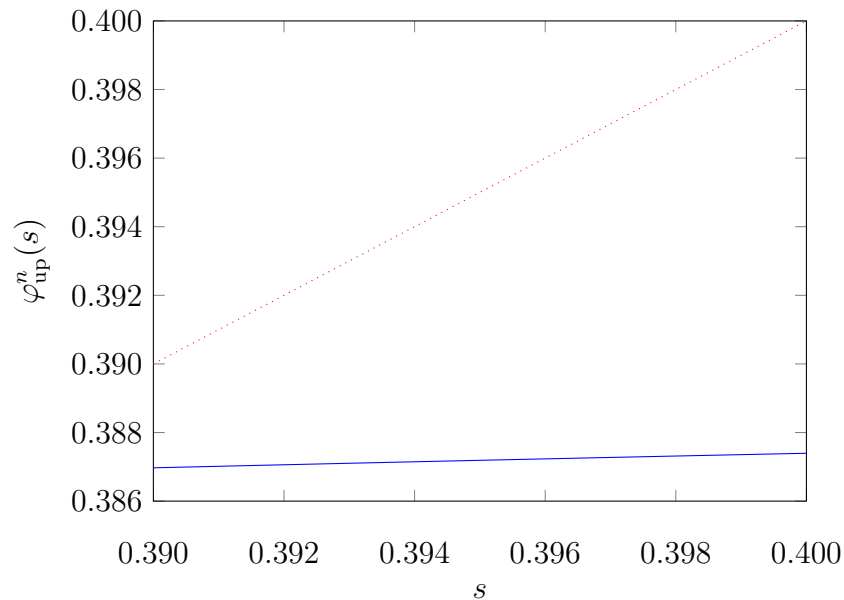


Figure 4.7.: φ_{up}^n is plotted for the region of interest $(Dm_n; 0.4) = (0.39; 0.4)$. The dotted line represents the function $f(s) = s$. We used $\dot{Q}_R^{UB1,n} = 3.172$ kW, $y_{\text{AC}}^n = 0.6$ mol/mol, $m_n = 1.625$ and the parameters given in Table 4.1.

4.4.3. Number of stages needed for the desired separation

For the parameters in Table 4.1 we can also determine the minimum number of stages needed for the desired separation. Stage-to-stage calculations are terminated if the mole fraction of acetone in the liquid phase exceeds 0.975 mol/mol. In this binary example 42 stages are required. The result is depicted in Figure 4.8.

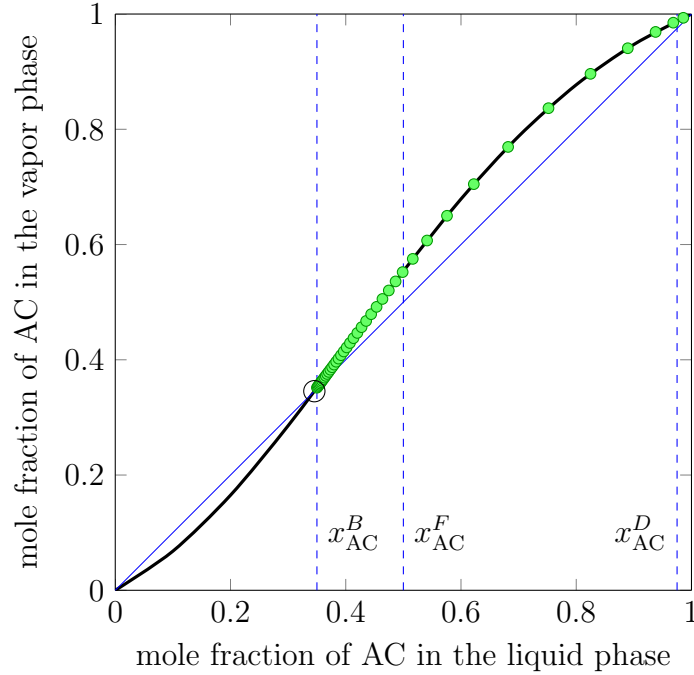


Figure 4.8.: Column profile depicted as green circles in a McCabe-Thiele plot (McCabe & Thiele, 1925) for the example in Table 4.1, $\dot{Q}_R = 25 \text{ kW}$. The large black circle depicts the azeotrope of the binary system and the vertical line on the right indicates the desired acetone purity in the distillate.

4.4.4. Speed of convergence of the fixed-point iteration

As mentioned above, the transition from one stage to the next is conducted via solution of a fixed-point problem. The rate of convergence is generally linear as shown in Section 4.3.3. Nevertheless, the fixed-point iteration converges very fast due to a small Lipschitz constant.

For the parameters in Table 4.1 and a stage $n < N_F$ only two fixed-point iterations are needed for the transition from stage 1 to stage 2 in order to obtain $|s_{k+1} - s_k| < 10^{-6}$. The iteration values are depicted in Table 4.3. The starting value s_0 is chosen to be $100 \in M_1$

in this example. Note that for practical purposes it is easier to choose $s_0 \in M_1$ than to choose $s_0 \in I_1$ due to the fact that further investigations are needed in order to determine the exact interval boundaries of I_1 . However, choosing $s_0 \in M_1$ guarantees $s_1 \in I_1$.

Table 4.3.: Iteration steps for the transition from stage 1 to stage 2 of a distillation column until it holds $|s_{k+1} - s_k| < 10^{-6}$. Parameter values can be obtained from Table 4.1.

| Iteration | Value |
|-----------|----------|
| s_0 | 100 |
| s_1 | 3.071837 |
| s_2 | 3.071834 |

In order to illustrate the speed of convergence for a stage $n < N_F$, the function

$$\varphi_{\text{up}}^1(s) = \frac{\dot{Q}_R + Bl(\mathbf{x}^2(s)) - Bl(\mathbf{x}^B)}{v(\mathbf{y}^1) - l(\mathbf{x}^2(s))} \quad (4.136)$$

is plotted for the parameters in Table 4.1 over the set $(0; 110) \subset M_1 = (0; \infty)$ in Figure 4.9 and in an enlarged region around the fixed point in Figure 4.10. The iterations for s are depicted as vertical dashed lines and labeled accordingly. The figures show that the range of φ_{up}^1 is extremely small. This is a typical characteristic of the function φ_{up}^n , independently of the current stage n and the considered multi-component mixture and as a consequence the corresponding fixed-point iteration converges very fast.

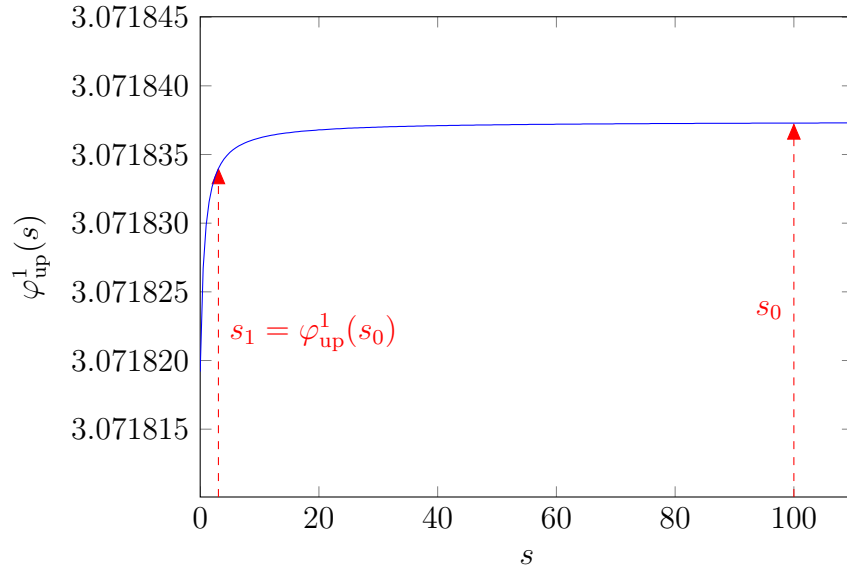


Figure 4.9.: Function φ_{up}^1 plotted for parameters in Table 4.1. The vertical dashed lines depict iteration s_0 and s_1 .

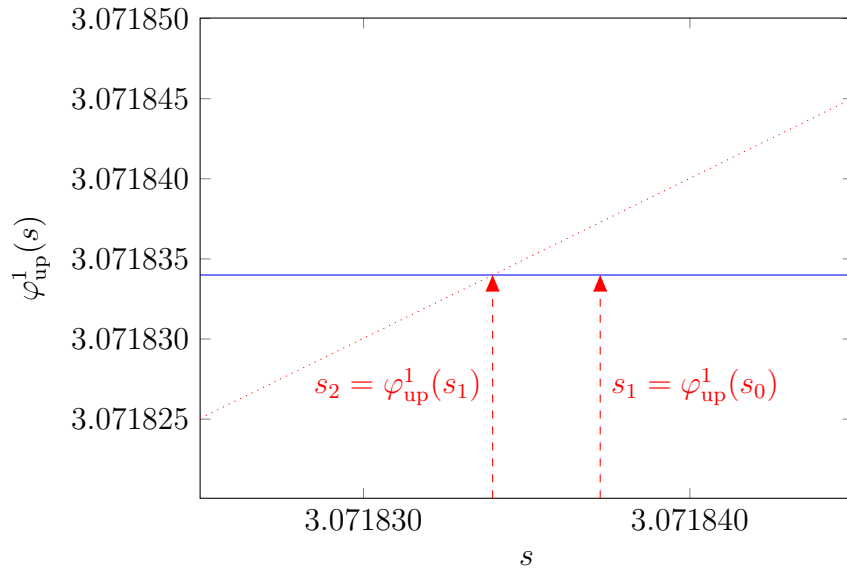


Figure 4.10.: Function φ_{up}^1 plotted for parameters in Table 4.1. The vertical dashed lines depict iteration s_1 and s_2 and the dotted line depicts the function $f(s) = s$.

In this exemplary study, we can also plot $(\varphi_{up}^1)'$ over the set $(0; 10) \subset M_1 = (0; \infty)$. The result is depicted in Figure 4.11 and from this figure we can conclude that the Lipschitz constant is in the order of magnitude 10^{-5} for the function φ_{up}^1 .

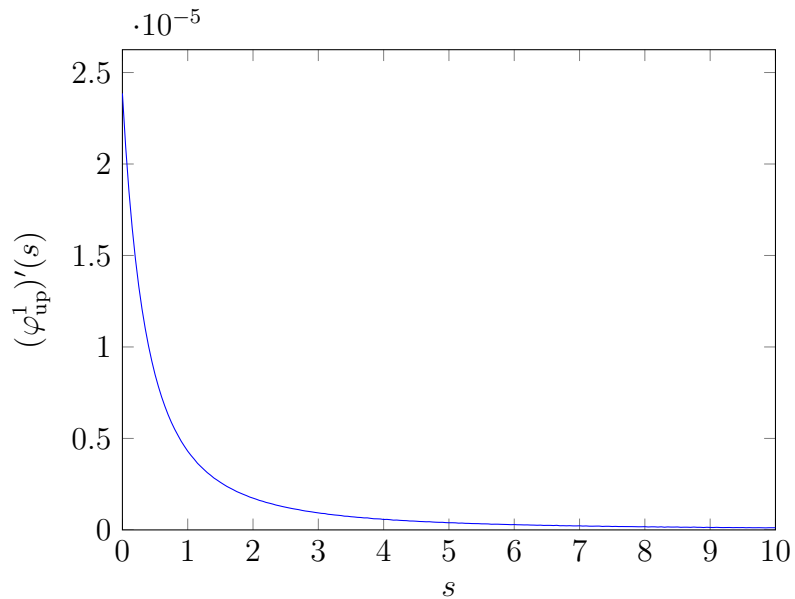


Figure 4.11.: Function $(\varphi_{up}^1)'$ plotted for parameters in Table 4.1.

In a second example for a stage $n \geq N_F$, three fixed-point iterations are needed for the transition from stage n to stage $n + 1$ in order to obtain $|s_{k+1} - s_k| < 10^{-6}$ where once again we assume $y_{AC}^n = 0.6$ mol/mol. The iterations are depicted in Table 4.4 with starting value s_0 chosen to be $100 \in M_n$.

Table 4.4.: Iteration steps for the transition from stage n to stage $n+1$ of a distillation column until it holds $|s_{k+1} - s_k| < 10^{-6}$. Parameter values can be obtained from Table 4.1 and $y_{AC}^n = 0.6$ mol/mol.

| Iteration | Value |
|-----------|----------|
| s_0 | 100 |
| s_1 | 3.065025 |
| s_2 | 3.067851 |
| s_3 | 3.067848 |

For the second example, we also plot the function

$$\varphi_{up}^n(s) = \frac{\dot{Q}_R + Fl(\mathbf{x}^F) + (B - F)l(\mathbf{x}^{n+1}(s)) - Bl(\mathbf{x}^B)}{v(\mathbf{y}^n) - l(\mathbf{x}^{n+1}(s))} \quad (4.137)$$

for the parameters in Table 4.1 over the set $(0.39; 110) \subset M_n = (Dm_n; \infty) = (0.39; \infty)$ in Figure 4.12 and in an enlarged region around the fixed point in Figure 4.13. The iterations for s are depicted as vertical dashed lines and labeled accordingly. The range of φ_{up}^n again is very small.

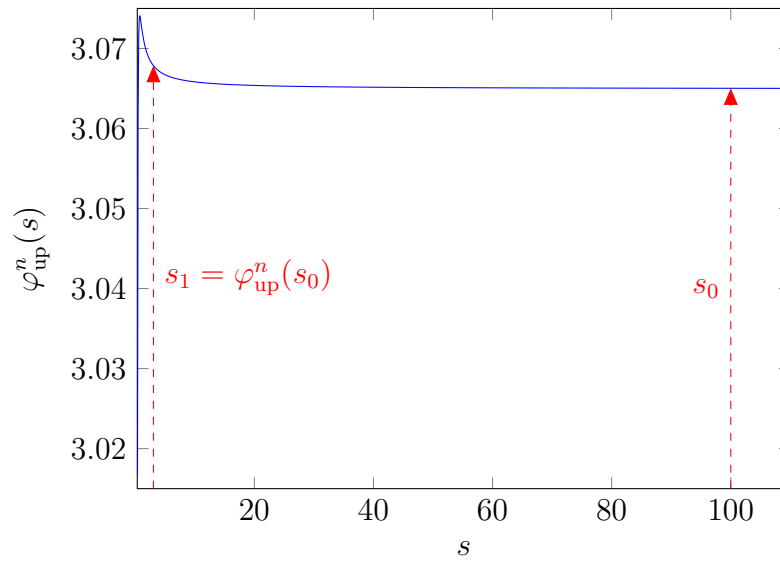


Figure 4.12.: Function φ_{up}^n plotted for parameters in Table 4.1 and $y_{\text{AC}}^n = 0.6$ mol/mol. The vertical dashed lines depict iteration s_0 and s_1 .

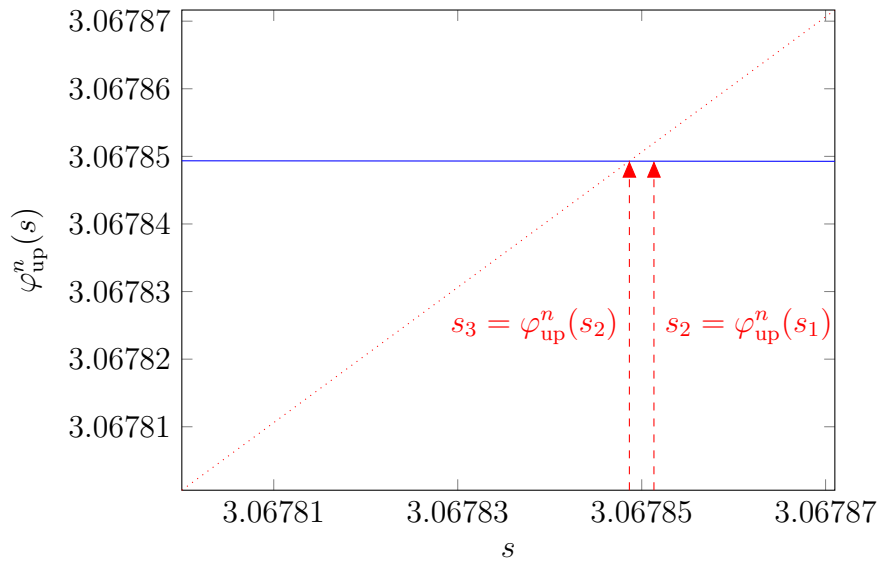


Figure 4.13.: Function φ_{up}^n plotted for parameters in Table 4.1 and $y_{AC}^n = 0.6$ mol/mol. The vertical dashed lines depict iteration s_2 and s_3 and the dotted line depicts the function $f(s) = s$.

Again, we can also plot $(\varphi_{up}^n)'$ over the set $(0.39; 10) \subset M_n = (Dm_n; \infty) = (0.39; \infty)$. The result is depicted in Figure 4.14 and we can conclude that the Lipschitz constant is strictly smaller than 1 for the function φ_{up}^n .

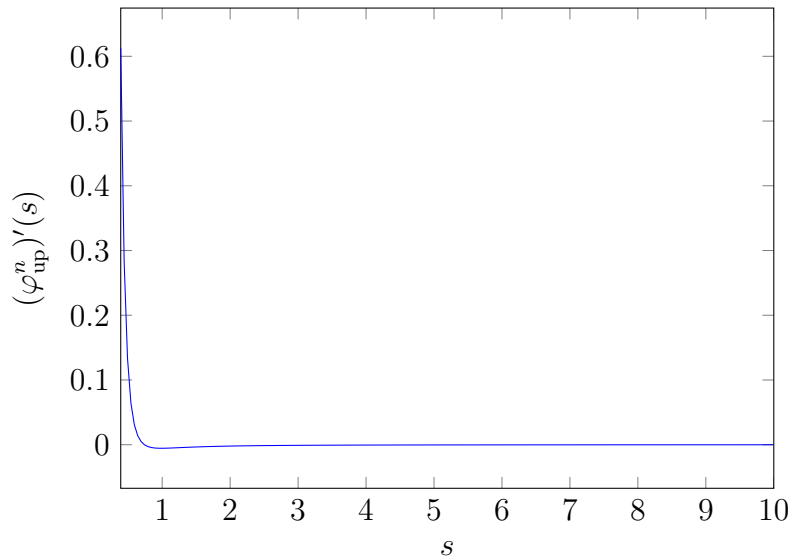


Figure 4.14.: Function $(\varphi_{up}^n)'$ plotted for parameters in Table 4.1 and $y_{AC}^n = 0.6$ mol/mol.

In Section 4.4.3 it was shown that 42 stages are needed to obtain a distillate with acetone purity greater than 0.975 mol/mol for stage-to-stage calculations based on the input variables given in Table 4.1. In Figure 4.15 the number of iterations steps that are needed in this example for the transition from stage n to stage $n + 1$ for $n = 1, \dots, 41$ are depicted. In the majority of all cases, only two iterations are needed and for a small number of transitions three iterations are conducted.

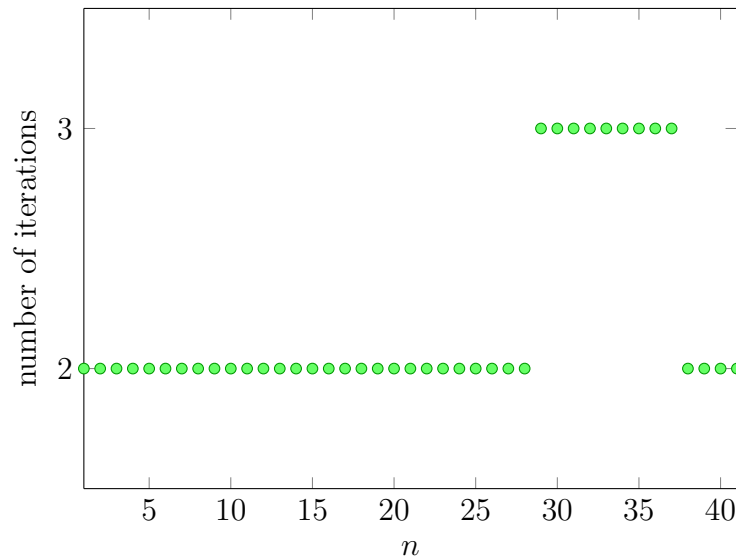


Figure 4.15.: Number of fixed-point iterations needed until a desired accuracy of 10^{-6} is reached, plotted as a function of the stage number n for which the transition to stage $n + 1$ is computed.

Clearly, the convergence properties of the fixed-point iteration, in general, depend on the considered example system. This means, that the Lipschitz constant could also be significantly larger and, hence, more iterations would be required. However, all example systems investigated so far have shown similar convergence properties as the example system presented here.

4.4.5. Minimum energy needed for the desired separation

Applying the McCabe-Thiele method (McCabe & Thiele, 1925) under the assumption of CMO to this binary example, the minimum energy that is needed in order to obtain the desired acetone purity in the distillate, using an infinite number of stages, is determined to be

$$\dot{Q}_{R,\min} = 17.35 \text{ kW}. \quad (4.138)$$

Comparing this result with the energy bounds derived in Table 4.2 we conclude that stage-to-stage calculations can be conducted for all physically relevant \dot{Q}_R due to the fact that $\dot{Q}_{R,\min}$ is significantly larger than the energy bounds in Table 4.2 that guarantee existence and uniqueness of the fixed point. Hence, the presented approach can also be used in order to determine $\dot{Q}_{R,\min}$. For that purpose we start stage-to-stage calculations at the bottom of the column and proceed without incorporating the feed stream until the composition vector in the liquid phase from one stage to the next changes less than some given threshold (here: 10^{-6}). Then we assume that we are in a pinch point. Now the feed stream is included in stage-to-stage calculations and we proceed until the desired acetone purity of 0.975 mol/mol in the liquid phase is obtained. For the subsequent numerical experiments the values for p , F , \mathbf{x}^F , B , and \mathbf{x}^B are taken from Table 4.1. In a first experiment we choose $\dot{Q}_R = 17.45 \text{ kW} > \dot{Q}_{R,\min}$. The column profile is depicted in Figure 4.16. A huge number of stages is needed to come from the bottom composition to the feed pinch. However, we can verify that this energy suffices in order to obtain the desired separation in a total of 316 stages.

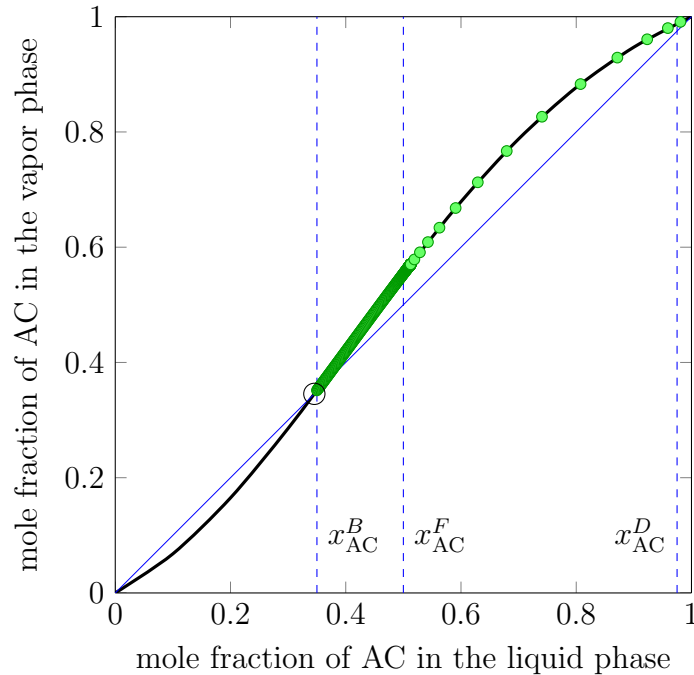


Figure 4.16.: Column profile depicted as green circles in a McCabe-Thiele plot for the example in Table 4.1, $\dot{Q}_R = 17.45 \text{ kW}$ and the feed placed at the pinch. The large black circle depicts the azeotrope of the binary system and the vertical line on the right indicates the desired acetone purity in the distillate.

In a next example, we choose $\dot{Q}_R = 17.25 \text{ kW} < \dot{Q}_{R,\min}$. The column profile is depicted in Figure 4.17. Again, a huge number of stages is needed to reach the feed pinch. However, the energy in this example does not suffice in order to obtain the desired separation. When incorporating the feed stream, the mole fraction of acetone in the column starts decreasing again using stage-to-stage calculations. Thus, the specified parameters are not feasible.

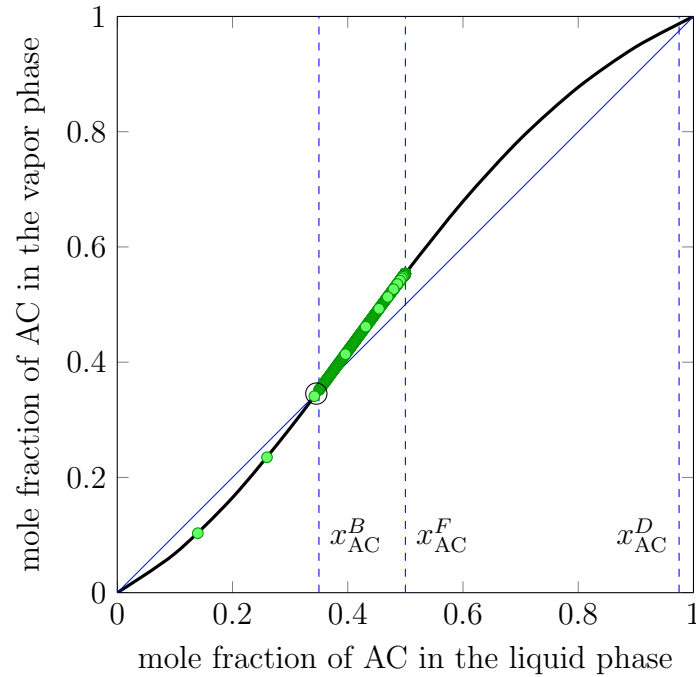


Figure 4.17.: Column profile depicted as green circles in a McCabe-Thiele plot for the example in Table 4.1, $\dot{Q}_R = 17.25 \text{ kW}$ and the feed placed at the pinch. The large black circle depicts the azeotrope of the binary system and the vertical line on the right indicates the desired acetone purity in the distillate.

Stage-to-stage calculations of general distillation columns

As an extension to Chapter 4, we consider in this chapter stage-to-stage calculations of distillation columns with an arbitrary number of feed streams and side-draws. Analogously to the approach for simple columns, the MESH equations are reformulated and the transition from one stage to the next is conducted via solution of a fixed-point problem. By applying the Banach fixed-point theorem we can derive lower bounds on the energy that guarantee the existence of a fixed point and convergence of the fixed-point iteration in this general case.

5.1. System of equations

In the following, distillation columns with $fs \geq 1$ feed streams and $sd \geq 1$ side-draws are considered. The feed streams enter the column on stages $N_{F_1} \leq \dots \leq N_{F_{fs}}$ with given molar flow rates F_k and composition vectors \mathbf{x}^{F_k} for $k = 1, \dots, fs$. Furthermore, all feed streams are assumed to be liquid boiling with pressure p . The side-draws leave the column liquid boiling on stages $N_{S_1} \leq \dots \leq N_{S_{sd}}$ with given molar flow rates S_l , compositions \mathbf{x}^{S_l} for $l = 1, \dots, sd$, and pressure p .

For a control volume that comprises the lower part of a the distillation column and the reboiler up to a certain stage n the following total material balance holds:

$$\sum_{k=1}^{k_{\text{act}}} F_k + L^{n+1} - V^n - B - \sum_{l=1}^{l_{\text{act}}} S_l = 0, \quad (5.1)$$

where

$$k_{\text{act}} := \max \{k \mid n \geq N_{F_k}\} \quad (5.2)$$

is the number of (active) feed streams that enter the considered control volume and

$$l_{\text{act}} := \max \{l \mid n \geq N_{S_l}\} \quad (5.3)$$

is the number of (active) side-draws that leave the considered control volume.

For the same control volume it is also possible to state the energy balance:

$$\dot{Q}_R + \sum_{k=1}^{k_{\text{act}}} F_k l(\mathbf{x}^{F_k}) + L^{n+1} l(\mathbf{x}^{n+1}) - V^n v(\mathbf{y}^n) - B l(\mathbf{x}^B) - \sum_{l=1}^{l_{\text{act}}} S_l l(\mathbf{x}^{S_l}) = 0. \quad (5.4)$$

5.2. Derivation of an equivalent fixed-point problem

Again, only the upward calculation of a general distillation column is discussed in detail. For the following considerations, it is assumed that values for the variables p , B , \mathbf{x}^B , and \dot{Q}_R are given. Furthermore, the specifications F_k and \mathbf{x}^{F_k} of the liquid boiling feed streams on stages $N_{F_1} \leq \dots \leq N_{F_{f_s}}$, and the specifications S_l and \mathbf{x}^{S_l} of the liquid boiling side-draws on stages $N_{S_1} \leq \dots \leq N_{S_{s_d}}$ are given in order to calculate a column from the bottom to the top. We assume the following to hold:

Assumption 5.1. *The values for B and \mathbf{x}^B are chosen in such a way that the flow rate D and the composition \mathbf{x}^D of the distillate stream, which fulfills the material balance of the column, should be positive.*

In an analogous way as presented in Chapter 4, the MESH equations for the transition from stage n to stage $n + 1$ are reformulated as a fixed-point problem of the following function:

Definition 5.2 (Fixed-point problem for the transition from stage n to stage $n + 1$). For the transition from state n to stage $n + 1$, $n = 1, \dots, N_S - 1$, a fixed point of the function

$$\begin{aligned} \varphi_{up}^n(s) := & \left(\dot{Q}_R + \sum_{k=1}^{k_{act}} F_k l(\mathbf{x}^{F_k}) + \left(- \sum_{k=1}^{k_{act}} F_k + B + \sum_{l=1}^{l_{act}} S_l \right) l(\mathbf{x}^{n+1}(s)) \right. \\ & \left. - Bl(\mathbf{x}^B) - \sum_{l=1}^{l_{act}} S_l l(\mathbf{x}^{S_l}) \right) \frac{1}{v(\mathbf{y}^n) - l(\mathbf{x}^{n+1}(s))}, \end{aligned} \quad (5.5)$$

where

$$\mathbf{x}^{n+1}(s) = \frac{1}{s - \sum_{k=1}^{k_{act}} F_k + B + \sum_{l=1}^{l_{act}} S_l} \left(s\mathbf{y}^n - \sum_{k=1}^{k_{act}} F_k \mathbf{x}^{F_k} + B\mathbf{x}^B + \sum_{l=1}^{l_{act}} S_l \mathbf{x}^{S_l} \right) \quad (5.6)$$

has to be found. Due to the fact that an auxiliary variable s is introduced, the MESH equations are decoupled and only in a fixed point s^* of φ_{up}^n it holds $s^* = V^n$.

Analogously, a sequence of fixed-point problems for the calculation of a general distillation column from the condenser downward can be derived.

5.3. Application of the Banach fixed-point theorem

In this section, the Banach fixed-point theorem (cf. Theorem 4.7) is applied to the function φ_{up}^n in Equation (5.5) for stage-to-stage calculations of a general distillation column. Using this theorem, it is possible to determine under which conditions there exists a fixed point and whether it is unique. In a first step, we discuss the existence of a fixed point. Conditions that guarantee uniqueness of the fixed point are derived in a second step.

5.3.1. Existence of a fixed point

Similar results as in Section 4.3.1 can be derived for distillation columns with an arbitrary number of feed streams and side-draws. In this section, most proofs are omitted due to the fact that they can be conducted in a very similar way as in Section 4.3.1.

Lemma 5.3. If s^* is a fixed point of φ_{up}^n it holds

$$s^* > \sum_{k=1}^{k_{act}} F_k - B - \sum_{l=1}^{l_{act}} S_l. \quad (5.7)$$

The results given below are derived under the assumption that

$$\sum_{k=1}^{k_{act}} F_k - B - \sum_{l=1}^{l_{act}} S_l \neq 0. \quad (5.8)$$

The special case where this assumption does not hold is discussed in a subsequent step.

Lemma 5.4. *If $s > \sum_{k=1}^{k_{act}} F_k - B - \sum_{l=1}^{l_{act}} S_l$ it holds*

$$x_i^{n+1}(s) > 0, \quad i = 1, \dots, N_C$$

iff

$$\begin{aligned} s &> \left(\sum_{k=1}^{k_{act}} F_k - B - \sum_{l=1}^{l_{act}} S_l \right) \left(\frac{\sum_{k=1}^{k_{act}} F_k x_i^{F_k} - B x_i^B - \sum_{l=1}^{l_{act}} S_l x_i^{S_l}}{\sum_{k=1}^{k_{act}} F_k - B - \sum_{l=1}^{l_{act}} S_l} \cdot \frac{1}{y_i^n} \right), \\ &\quad i = 1, \dots, N_C \\ &\geq \sum_{k=1}^{k_{act}} F_k - B - \sum_{l=1}^{l_{act}} S_l. \end{aligned}$$

For a general distillation column a fixed point with not only mathematical but also physical meaning can only occur in

$$M_n := \left(\max \left(0, \left(\sum_{k=1}^{k_{act}} F_k - B - \sum_{l=1}^{l_{act}} S_l \right) m_n \right); \infty \right), \quad (5.9)$$

where m_n is defined in the following way:

$$m_n := \max_{i=1, \dots, N_C} \left(\frac{\sum_{k=1}^{k_{act}} F_k x_i^{F_k} - B x_i^B - \sum_{l=1}^{l_{act}} S_l x_i^{S_l}}{\sum_{k=1}^{k_{act}} F_k - B - \sum_{l=1}^{l_{act}} S_l} \cdot \frac{1}{y_i^n} \right) \geq 1, \quad (5.10)$$

if

$$\sum_{k=1}^{k_{act}} F_k - B - \sum_{l=1}^{l_{act}} S_l > 0 \quad (5.11)$$

and

$$m_n := \min_{i=1, \dots, N_C} \left(\frac{\sum_{k=1}^{k_{act}} F_k x_i^{F_k} - B x_i^B - \sum_{l=1}^{l_{act}} S_l x_i^{S_l}}{\sum_{k=1}^{k_{act}} F_k - B - \sum_{l=1}^{l_{act}} S_l} \cdot \frac{1}{y_i^n} \right) \leq 1, \quad (5.12)$$

if

$$\sum_{k=1}^{k_{act}} F_k - B - \sum_{l=1}^{l_{act}} S_l < 0. \quad (5.13)$$

The lower and upper bound in Equation (5.10) and (5.12) for m_n can be obtained by using the fact that

$$\sum_{i=1}^{N_C} \left(\frac{\sum_{k=1}^{k_{act}} F_k x_i^{F_k} - B x_i^B - \sum_{l=1}^{l_{act}} S_l x_i^{S_l}}{\sum_{k=1}^{k_{act}} F_k - B - \sum_{l=1}^{l_{act}} S_l} \right) = 1. \quad (5.14)$$

Lemma 5.5. *The function φ_{up}^n is bounded on M_n .*

Lemma 5.6. *If*

$$\begin{aligned} \dot{Q}_R &> B l(\mathbf{x}^B) - \sum_{k=1}^{k_{act}} F_k l(\mathbf{x}^{F_k}) + \max \left(0, \left(\sum_{k=1}^{k_{act}} F_k - B - \sum_{l=1}^{l_{act}} S_l \right) m_n \right) v(\mathbf{y}^n) \\ &+ \left(\sum_{k=1}^{k_{act}} F_k - B - \sum_{l=1}^{l_{act}} S_l - \max \left(0, \left(\sum_{k=1}^{k_{act}} F_k - B - \sum_{l=1}^{l_{act}} S_l \right) m_n \right) \right) l(\mathbf{x}^{n+1}(s)) \\ &+ \sum_{l=1}^{l_{act}} S_l l(\mathbf{x}^{S_l}) \end{aligned} \quad (5.15)$$

for all $s \in M_n$ and in the limiting cases $s \rightarrow \max \left(0, \left(\sum_{k=1}^{k_{act}} F_k - B - \sum_{l=1}^{l_{act}} S_l \right) m_n \right)$ and $s \rightarrow \infty$ it holds that $\varphi_n^{up}(M_n) \subset M_n$.

It is also possible to derive a more general bound on \dot{Q}_R that does no longer depend on the current iterate at s and the specific compositions of entering feed streams and leaving side-draws. In order to derive this bound we use the following observation:

$$\left(\sum_{k=1}^{k_{act}} F_k - B - \sum_{l=1}^{l_{act}} S_l - \max \left(0, \left(\sum_{k=1}^{k_{act}} F_k - B - \sum_{l=1}^{l_{act}} S_l \right) m_n \right) \right) \leq 0. \quad (5.16)$$

This leads to a more general bound:

Lemma 5.7. *If*

$$\dot{Q}_R > \dot{Q}_R^{LB1,n} \quad (5.17)$$

with

$$\begin{aligned}
 \dot{Q}_R^{LB1,n} := & Bl(\mathbf{x}^B) - \sum_{k=1}^{k_{act}} F_k l(\mathbf{x}^{F_k}) + \max \left(0, \left(\sum_{k=1}^{k_{act}} F_k - B - \sum_{l=1}^{l_{act}} S_l \right) m_n \right) v(\mathbf{y}^n) \\
 & + \left(\sum_{k=1}^{k_{act}} F_k - B - \sum_{l=1}^{l_{act}} S_l - \max \left(0, \left(\sum_{k=1}^{k_{act}} F_k - B - \sum_{l=1}^{l_{act}} S_l \right) m_n \right) \right) \min_{\mathbf{x} \in \mathcal{F}_{NC}} l(\mathbf{x}) \\
 & + \sum_{l=1}^{l_{act}} S_l l(\mathbf{x}^{S_l})
 \end{aligned} \tag{5.18}$$

or alternatively if

$$\dot{Q}_R > \dot{Q}_R^{LB2,n} \tag{5.19}$$

with

$$\begin{aligned}
 \dot{Q}_R^{LB2,n} := & \left(B + \sum_{l=1}^{l_{act}} S_l \right) \left(\max_{\mathbf{x} \in \mathcal{F}_{NC}} l(\mathbf{x}) - \min_{\mathbf{x} \in \mathcal{F}_{NC}} l(\mathbf{x}) \right) \\
 & + \max \left(0, \left(\sum_{k=1}^{k_{act}} F_k - B - \sum_{l=1}^{l_{act}} S_l \right) m_n \right) \left(\max_{\mathbf{x} \in \mathcal{F}_{NC}} v(\mathbf{x}) - \min_{\mathbf{x} \in \mathcal{F}_{NC}} l(\mathbf{x}) \right) \\
 \geq & \dot{Q}_R^{LB1,n}
 \end{aligned} \tag{5.20}$$

it holds that $\varphi_{up}^n(M_n) \subset M_n$.

Using the rather technical Lemma 4.17 and Theorem 4.18 the above results can be summarized in the following way:

Theorem 5.8 (Existence of a fixed point of φ_{up}^n in the interval I_n). *If $\sum_{k=1}^{k_{act}} F_k - B - \sum_{l=1}^{l_{act}} S_l \neq 0$ and*

$$\dot{Q}_R > \dot{Q}_R^{LB2,n} \geq \dot{Q}_R^{LB1,n}$$

it holds that $\varphi_{up}^n(I_n) \subset I_n$ and the existence of at least one fixed point in the closed interval I_n can be guaranteed.

It is possible to conclude that \dot{Q}_R only has to be chosen large enough in order to guarantee the existence of a fixed point. So far, we derived conditions that guarantee the existence of a fixed point in the interval I_n . However, we also want to derive conditions that exclude the existence of a fixed point and, thus, can serve as guidelines for an appropriate choice of variables.

Lemma 5.9. *If*

$$\begin{aligned}
 \dot{Q}_R &\leq Bl(\mathbf{x}^B) - \sum_{k=1}^{k_{act}} F_k l(\mathbf{x}^{F_k}) + \max\left(0, \left(\sum_{k=1}^{k_{act}} F_k - B - \sum_{l=1}^{l_{act}} S_l\right) m_n\right) v(\mathbf{y}^n) \\
 &+ \left(\sum_{k=1}^{k_{act}} F_k - B - \sum_{l=1}^{l_{act}} S_l - \max\left(0, \left(\sum_{k=1}^{k_{act}} F_k - B - \sum_{l=1}^{l_{act}} S_l\right) m_n\right)\right) l(\mathbf{x}^{n+1}(s)) \\
 &+ \sum_{l=1}^{l_{act}} S_l l(\mathbf{x}^{S_l})
 \end{aligned} \tag{5.21}$$

for all $s \in M_n$ and in the limiting cases $s \rightarrow \max\left(0, \left(\sum_{k=1}^{k_{act}} F_k - B - \sum_{l=1}^{l_{act}} S_l\right) m_n\right)$ and $s \rightarrow \infty$ the function φ_n^{up} has no fixed point in M_n .

The result in Lemma 5.9 can also be formulated in a more general way:

Lemma 5.10. *If*

$$\dot{Q}_R \leq \dot{Q}_R^{UB1,n} \tag{5.22}$$

with

$$\begin{aligned}
 \dot{Q}_R^{UB1,n} &:= Bl(\mathbf{x}^B) - \sum_{k=1}^{k_{act}} F_k l(\mathbf{x}^{F_k}) + \max\left(0, \left(\sum_{k=1}^{k_{act}} F_k - B - \sum_{l=1}^{l_{act}} S_l\right) m_n\right) v(\mathbf{y}^n) \\
 &+ \left(\sum_{k=1}^{k_{act}} F_k - B - \sum_{l=1}^{l_{act}} S_l - \max\left(0, \left(\sum_{k=1}^{k_{act}} F_k - B - \sum_{l=1}^{l_{act}} S_l\right) m_n\right)\right) \max_{\mathbf{x} \in \mathcal{F}_{NC}} l(\mathbf{x}) \\
 &+ \sum_{l=1}^{l_{act}} S_l l(\mathbf{x}^{S_l})
 \end{aligned} \tag{5.23}$$

or alternatively if

$$\dot{Q}_R \leq \dot{Q}_R^{UB2,n} \tag{5.24}$$

with

$$\begin{aligned} \dot{Q}_R^{UB2,n} &:= \left(B + \sum_{l=1}^{l_{act}} S_l \right) \left(\min_{\mathbf{x} \in \mathcal{F}_{N_C}} l(\mathbf{x}) - \max_{\mathbf{x} \in \mathcal{F}_{N_C}} l(\mathbf{x}) \right) \\ &\quad + \max \left(0, \left(\sum_{k=1}^{k_{act}} F_k - B - \sum_{l=1}^{l_{act}} S_l \right) m_n \right) \left(\min_{\mathbf{x} \in \mathcal{F}_{N_C}} v(\mathbf{x}) - \max_{\mathbf{x} \in \mathcal{F}_{N_C}} l(\mathbf{x}) \right) \\ &\leq \dot{Q}_R^{UB1,n} \end{aligned} \quad (5.25)$$

the function φ_{up}^n has no fixed point in M_n .

We can summarize our insights in the following theorem:

Theorem 5.11 (Existence of no fixed point of the function φ_{up}^n in the interval M_n). *If $\sum_{k=1}^{k_{act}} F_k - B - \sum_{l=1}^{l_{act}} S_l \neq 0$ and*

$$\dot{Q}_R \leq \dot{Q}_R^{UB1,n} \leq \dot{Q}_R^{UB2,n} \quad (5.26)$$

the function φ_{up}^n has no fixed point in M_n and if

$$\dot{Q}_R^{UB1,n} \leq \dot{Q}_R^{UB2,n} < \dot{Q}_R \leq \dot{Q}_R^{LB1,n} \leq \dot{Q}_R^{LB2,n} \quad (5.27)$$

it is neither possible to exclude nor to guarantee a fixed point a priori.

For the sake of completeness we also discuss the case $\sum_{k=1}^{k_{act}} F_k - B - \sum_{l=1}^{l_{act}} S_l = 0$.

Lemma 5.12. *If $s > \sum_{k=1}^{k_{act}} F_k - B - \sum_{l=1}^{l_{act}} S_l = 0$ it holds*

$$x_i^{n+1}(s) > 0, \quad i = 1, \dots, N_C$$

iff

$$\begin{aligned} s &> \frac{\sum_{k=1}^{k_{act}} F_k x_i^{F_k} - B x_i^B - \sum_{l=1}^{l_{act}} S_l x_i^{S_l}}{y_i^n}, \quad i = 1, \dots, N_C \\ &\geq 0. \end{aligned}$$

A fixed point with not only mathematical but also physical meaning can only occur in

$$M_{n,0} := (m_{n,0}; \infty), \quad (5.28)$$

where $m_{n,0}$ is defined in the following way:

$$m_{n,0} := \max_{i=1,\dots,N_C} \left(\frac{\sum_{k=1}^{k_{\text{act}}} F_k x_i^{F_k} - B x_i^B - \sum_{l=1}^{l_{\text{act}}} S_l x_i^{S_l}}{y_i^n} \right) \geq 0. \quad (5.29)$$

The fact that $m_{n,0} \geq 0$ can be obtained by using the following relation:

$$\sum_{i=1}^{N_C} \left(\sum_{k=1}^{k_{\text{act}}} F_k x_i^{F_k} - B x_i^B - \sum_{l=1}^{l_{\text{act}}} S_l x_i^{S_l} \right) = 0. \quad (5.30)$$

Hence, the above sum consists of at least one non-negative element.

Lemma 5.13. *The function φ_{up}^n is bounded on $M_{n,0}$.*

Lemma 5.14. *If*

$$\dot{Q}_R > B l(\mathbf{x}^B) - \sum_{k=1}^{k_{\text{act}}} F_k l(\mathbf{x}^{F_k}) + \sum_{l=1}^{l_{\text{act}}} S_l l(\mathbf{x}^{S_l}) + m_{n,0} (v(\mathbf{y}^n) - l(\mathbf{x}^{n+1}(s))) \quad (5.31)$$

for all $s \in M_{n,0}$ and in the limiting cases $s \rightarrow m_{n,0}$ and $s \rightarrow \infty$ it holds that $\varphi_n^{\text{up}}(M_{n,0}) \subset M_{n,0}$.

Again, it is also possible to derive a more general bound on \dot{Q}_R :

Lemma 5.15. *If*

$$\dot{Q}_R > \dot{Q}_R^{LB1,n,0} \quad (5.32)$$

with

$$\dot{Q}_R^{LB1,n,0} := B l(\mathbf{x}^B) - \sum_{k=1}^{k_{\text{act}}} F_k l(\mathbf{x}^{F_k}) + \sum_{l=1}^{l_{\text{act}}} S_l l(\mathbf{x}^{S_l}) + m_{n,0} \left(v(\mathbf{y}^n) - \min_{\mathbf{x} \in \mathcal{F}_{N_C}} l(\mathbf{x}) \right) \quad (5.33)$$

or alternatively if

$$\dot{Q}_R > \dot{Q}_R^{LB2,n,0} \quad (5.34)$$

with

$$\begin{aligned} \dot{Q}_R^{LB2,n,0} &:= \left(B + \sum_{l=1}^{l_{act}} S_l \right) \left(\max_{\mathbf{x} \in \mathcal{F}_{NC}} l(\mathbf{x}) - \min_{\mathbf{x} \in \mathcal{F}_{NC}} l(\mathbf{x}) \right) \\ &\quad + m_{n,0} \left(\max_{\mathbf{x} \in \mathcal{F}_{NC}} v(\mathbf{x}) - \min_{\mathbf{x} \in \mathcal{F}_{NC}} l(\mathbf{x}) \right) \\ &\geq \dot{Q}_R^{LB1,n,0} \end{aligned} \quad (5.35)$$

it holds that $\varphi_{up}^n(M_{n,0}) \subset M_{n,0}$.

Using the same arguments as in Section 4.3.1 the above results can be summarized in the following way:

Theorem 5.16 (Existence of a fixed point of φ_{up}^n in the interval I_n). *If $\sum_{k=1}^{k_{act}} F_k - B - \sum_{l=1}^{l_{act}} S_l = 0$ and*

$$\dot{Q}_R > \dot{Q}_R^{LB2,n,0} \geq \dot{Q}_R^{LB1,n,0}$$

it holds that $\varphi_{up}^n(I_n) \subset I_n$ and the existence of at least one fixed point in the closed interval I_n can be guaranteed.

On the other hand, bounds on the reboiler duty can be stated below which there exists no fixed point.

Lemma 5.17. *If*

$$\dot{Q}_R \leq Bl(\mathbf{x}^B) - \sum_{k=1}^{k_{act}} F_k l(\mathbf{x}^{F_k}) + \sum_{l=1}^{l_{act}} S_l l(\mathbf{x}^{S_l}) + m_{n,0} (v(\mathbf{y}^n) - l(\mathbf{x}^{n+1}(s))) \quad (5.36)$$

for all $s \in M_{n,0}$ and in the limiting cases $s \rightarrow m_{n,0}$ and $s \rightarrow \infty$ the function φ_n^{up} has no fixed point in $M_{n,0}$.

This result can be formulated in a more general way:

Lemma 5.18. *If*

$$\dot{Q}_R \leq \dot{Q}_R^{UB1,n,0} \quad (5.37)$$

with

$$\dot{Q}_R^{UB1,n,0} := Bl(\mathbf{x}^B) - \sum_{k=1}^{k_{act}} F_k l(\mathbf{x}^{F_k}) + \sum_{l=1}^{l_{act}} S_l l(\mathbf{x}^{S_l}) + m_{n,0} \left(v(\mathbf{y}^n) - \max_{\mathbf{x} \in \mathcal{F}_{NC}} l(\mathbf{x}) \right) \quad (5.38)$$

or alternatively if

$$\dot{Q}_R \leq \dot{Q}_R^{UB2,n,0} \quad (5.39)$$

with

$$\dot{Q}_R^{UB2,n,0} := \left(B + \sum_{l=1}^{l_{act}} S_l \right) \left(\min_{\mathbf{x} \in \mathcal{F}_{NC}} l(\mathbf{x}) - \max_{\mathbf{x} \in \mathcal{F}_{NC}} l(\mathbf{x}) \right) \quad (5.40)$$

$$+ m_{n,0} \left(\min_{\mathbf{x} \in \mathcal{F}_{NC}} v(\mathbf{x}) - \max_{\mathbf{x} \in \mathcal{F}_{NC}} l(\mathbf{x}) \right) \quad (5.41)$$

$$\leq \dot{Q}_R^{UB1,n,0}$$

the function φ_{up}^n has no fixed point in $M_{n,0}$.

Last but not least we can state under which condition it is possible to exclude a fixed point and under which condition we have not enough information to come to a decision for the special case $\sum_{k=1}^{k_{act}} F_k - B - \sum_{l=1}^{l_{act}} S_l = 0$:

Theorem 5.19 (Existence of no fixed point of the function φ_{up}^n in the interval $M_{n,0}$). *If $\sum_{k=1}^{k_{act}} F_k - B - \sum_{l=1}^{l_{act}} S_l = 0$ and*

$$\dot{Q}_R \leq \dot{Q}_R^{UB1,n,0} \leq \dot{Q}_R^{UB2,n,0} \quad (5.42)$$

the function φ_{up}^n has no fixed point in $M_{n,0}$ and if

$$\dot{Q}_R^{UB1,n,0} \leq \dot{Q}_R^{UB2,n,0} < \dot{Q}_R \leq \dot{Q}_R^{LB1,n,0} \leq \dot{Q}_R^{LB2,n,0} \quad (5.43)$$

it is neither possible to exclude nor to guarantee a fixed point a priori.

5.3.2. Uniqueness of the fixed point and convergence of the fixed-point iteration

In this section, we derive conditions that guarantee the uniqueness of the fixed point and convergence of the fixed-point iteration. For a general distillation column with an arbitrary number of feed streams and side-draws the derivative of φ_{up}^n can be written as

$$(\varphi_{up}^n)'(s) = \frac{\varphi_{up}^n(s) - \sum_{k=1}^{k_{act}} F_k + B + \sum_{l=1}^{l_{act}} S_l}{s - \sum_{k=1}^{k_{act}} F_k + B + \sum_{l=1}^{l_{act}} S_l} \cdot \frac{\nabla l(\mathbf{x}^{n+1}(s))(\mathbf{y}^n - \mathbf{x}^{n+1}(s))}{v(\mathbf{y}^n) - l(\mathbf{x}^{n+1}(s))}. \quad (5.44)$$

As we pay special attention to the asymptotic limiting case $\dot{Q}_R \rightarrow \infty$ throughout this work, we discuss this special case in a first step. Following the arguments derived in Section 4.3.2 we can state:

Theorem 5.20 (Uniqueness of the fixed point for $\dot{Q}_R \rightarrow \infty$). *In this special case the function $(\varphi_{\text{up}}^n)'$ is bounded by 0, i.e. the Lipschitz constant is 0. Thus, the fixed point is unique in I_n and the fixed point is obtained after the first iteration as the function φ_{up}^n is a constant function.*

However, we are also interested in the bounds that guarantee uniqueness of a fixed point for finite \dot{Q}_R . These bounds will be investigated in the remainder of this chapter.

Analogously to the results in Section 4.3.2, a bound for the first part of Equation (5.44) can be derived:

$$\left| \frac{\varphi_{\text{up}}^n(s) - \sum_{k=1}^{k_{\text{act}}} F_k + B + \sum_{l=1}^{l_{\text{act}}} S_l}{s - \sum_{k=1}^{k_{\text{act}}} F_k + B + \sum_{l=1}^{l_{\text{act}}} S_l} \right| \leq \frac{\min_{\mathbf{x} \in \mathcal{F}_{N_C}} v(\mathbf{x}) - \min_{\mathbf{x} \in \mathcal{F}_{N_C}} l(\mathbf{x})}{\min_{\mathbf{x} \in \mathcal{F}_{N_C}} v(\mathbf{x}) - \max_{\mathbf{x} \in \mathcal{F}_{N_C}} l(\mathbf{x})}. \quad (5.45)$$

Again, we consider the case $\sum_{k=1}^{k_{\text{act}}} F_k - B - \sum_{l=1}^{l_{\text{act}}} S_l = 0$ separately in a subsequent step. If $\sum_{k=1}^{k_{\text{act}}} F_k - B - \sum_{l=1}^{l_{\text{act}}} S_l \neq 0$ we can derive the following expression:

$$y_i^n - x_i^{n+1}(s) = \frac{\sum_{k=1}^{k_{\text{act}}} F_k - B - \sum_{l=1}^{l_{\text{act}}} S_l}{s - \sum_{k=1}^{k_{\text{act}}} F_k + B + \sum_{l=1}^{l_{\text{act}}} S_l} \quad (5.46)$$

$$\begin{aligned} & \cdot \left(\frac{\sum_{k=1}^{k_{\text{act}}} F_k x_i^{F_k} - B x_i^B - \sum_{l=1}^{l_{\text{act}}} S_l x_i^{S_l}}{\sum_{k=1}^{k_{\text{act}}} F_k - B - \sum_{l=1}^{l_{\text{act}}} S_l} - y_i^n \right) \\ & = \frac{\sum_{k=1}^{k_{\text{act}}} F_k - B - \sum_{l=1}^{l_{\text{act}}} S_l}{s - \sum_{k=1}^{k_{\text{act}}} F_k + B + \sum_{l=1}^{l_{\text{act}}} S_l} y_i^n \\ & \cdot \left(\frac{\sum_{k=1}^{k_{\text{act}}} F_k x_i^{F_k} - B x_i^B - \sum_{l=1}^{l_{\text{act}}} S_l x_i^{S_l}}{\sum_{k=1}^{k_{\text{act}}} F_k - B - \sum_{l=1}^{l_{\text{act}}} S_l} \cdot \frac{1}{y_i^n} - 1 \right). \end{aligned} \quad (5.47)$$

This expression gives a bound for $|y_i^n - x_i^{n+1}(s)|$:

$$|y_i^n - x_i^{n+1}(s)| \leq \underbrace{\frac{\sum_{k=1}^{k_{\text{act}}} F_k - B - \sum_{l=1}^{l_{\text{act}}} S_l}{s - \sum_{k=1}^{k_{\text{act}}} F_k + B + \sum_{l=1}^{l_{\text{act}}} S_l}}_{\geq 0} y_i^n \cdot b_n, \quad (5.48)$$

with

$$b_n := \max \left\{ \max_{i=1, \dots, N_C} \left(\frac{\sum_{k=1}^{k_{\text{act}}} F_k x_i^{F_k} - B x_i^B - \sum_{l=1}^{l_{\text{act}}} S_l x_i^{S_l}}{\sum_{k=1}^{k_{\text{act}}} F_k - B - \sum_{l=1}^{l_{\text{act}}} S_l} \cdot \frac{1}{y_i^n} \right) - 1, \right. \\ \left. 1 - \min_{i=1, \dots, N_C} \left(\frac{\sum_{k=1}^{k_{\text{act}}} F_k x_i^{F_k} - B x_i^B - \sum_{l=1}^{l_{\text{act}}} S_l x_i^{S_l}}{\sum_{k=1}^{k_{\text{act}}} F_k - B - \sum_{l=1}^{l_{\text{act}}} S_l} \cdot \frac{1}{y_i^n} \right) \right\}, \quad (5.49)$$

if $\sum_{k=1}^{k_{\text{act}}} F_k - B - \sum_{l=1}^{l_{\text{act}}} S_l > 0$ and

$$b_n := \max \left\{ 1 - \max_{i=1, \dots, N_C} \left(\frac{\sum_{k=1}^{k_{\text{act}}} F_k x_i^{F_k} - B x_i^B - \sum_{l=1}^{l_{\text{act}}} S_l x_i^{S_l}}{\sum_{k=1}^{k_{\text{act}}} F_k - B - \sum_{l=1}^{l_{\text{act}}} S_l} \cdot \frac{1}{y_i^n} \right), \right. \\ \left. \min_{i=1, \dots, N_C} \left(\frac{\sum_{k=1}^{k_{\text{act}}} F_k x_i^{F_k} - B x_i^B - \sum_{l=1}^{l_{\text{act}}} S_l x_i^{S_l}}{\sum_{k=1}^{k_{\text{act}}} F_k - B - \sum_{l=1}^{l_{\text{act}}} S_l} \cdot \frac{1}{y_i^n} \right) - 1 \right\}, \quad (5.50)$$

if $\sum_{k=1}^{k_{\text{act}}} F_k - B - \sum_{l=1}^{l_{\text{act}}} S_l < 0$.

The right hand side of Equation (5.48) is positive as it holds

$$\left(\sum_{k=1}^{k_{\text{act}}} F_k - B - \sum_{l=1}^{l_{\text{act}}} S_l \right) b_n \geq 0. \quad (5.51)$$

Lemma 5.21. *Let $c_n \geq 1$. It holds*

$$\left(\sum_{k=1}^{k_{\text{act}}} F_k - B - \sum_{l=1}^{l_{\text{act}}} S_l \right) (c_n \cdot b_n + 1) \geq \left(\sum_{k=1}^{k_{\text{act}}} F_k - B - \sum_{l=1}^{l_{\text{act}}} S_l \right) m_n. \quad (5.52)$$

Proof. For the proof we use Equation (5.51) and the fact that $c_n \geq 1$. If $b_n \neq 0$ we can conclude

$$\left(\sum_{k=1}^{k_{\text{act}}} F_k - B - \sum_{l=1}^{l_{\text{act}}} S_l \right) (c_n \cdot b_n + 1) \geq \left(\sum_{k=1}^{k_{\text{act}}} F_k - B - \sum_{l=1}^{l_{\text{act}}} S_l \right) m_n \\ \iff \underbrace{\left(\sum_{k=1}^{k_{\text{act}}} F_k - B - \sum_{l=1}^{l_{\text{act}}} S_l \right)}_{\geq 0} \underbrace{b_n \left(c_n - \frac{\overbrace{m_n - 1}^{\leq 1}}{b_n} \right)}_{\geq 0} \geq 0.$$

If $b_n = 0$, it follows $m_n = 1$ and both sides of Equation (5.52) are identical. \square

5. Stage-to-stage calculations of general distillation columns

If we require that $\inf_{s \in M_n} \varphi_n^{\text{up}}(s) \geq \left(\sum_{k=1}^{k_{\text{act}}} F_k - B - \sum_{l=1}^{l_{\text{act}}} S_l \right) (c_n \cdot b_n + 1)$, where $c_n \geq 1$ we obtain the following result:

$$|y_i^n - x_i^{n+1}(s)| \leq \frac{\sum_{k=1}^{k_{\text{act}}} F_k - B - \sum_{l=1}^{l_{\text{act}}} S_l}{\left(\sum_{k=1}^{k_{\text{act}}} F_k - B - \sum_{l=1}^{l_{\text{act}}} S_l \right) c_n \cdot b_n} y_i^n \cdot b_n \quad (5.53)$$

$$= \frac{1}{c_n} y_i^n. \quad (5.54)$$

Along the same lines as in Section 4.3.2 we obtain:

$$\begin{aligned} & \left| \nabla l(\mathbf{x}^{n+1}(s)) (\mathbf{y}^n - \mathbf{x}^{n+1}(s)) \right| \\ &= \left| \sum_{i=1, i \neq i_0}^{N_C} \left(\frac{\partial l}{\partial x_i}(\mathbf{x}^{n+1}(s)) - \frac{\partial l}{\partial x_1}(\mathbf{x}^{n+1}(s)) \right) (y_i^n - x_i^{n+1}(s)) \right| \\ &\leq \max_{1 \leq i < j \leq N_C} \left| \frac{\partial l}{\partial x_i}(\mathbf{x}^{n+1}(s)) - \frac{\partial l}{\partial x_j}(\mathbf{x}^{n+1}(s)) \right| \sum_{i=1, i \neq i_0}^{N_C} |y_i^n - x_i^{n+1}(s)|, \end{aligned}$$

where i_0 can be arbitrarily chosen from $\arg \max_{i=1, \dots, N_C} y_i^n$. Using Equation (5.53) we end up with

$$\begin{aligned} \left| \nabla l(\mathbf{x}^{n+1}(s)) (\mathbf{y}^n - \mathbf{x}^{n+1}(s)) \right| &\leq \max_{1 \leq i < j \leq N_C} \max_{\mathbf{x} \in \mathcal{F}_{N_C}} \left| \frac{\partial l}{\partial x_i}(\mathbf{x}) - \frac{\partial l}{\partial x_j}(\mathbf{x}) \right| \left(\frac{1 - y_{i_0}^n}{c_n} \right) \\ &\leq \max_{1 \leq i < j \leq N_C} \max_{\mathbf{x} \in \mathcal{F}_{N_C}} \left| \frac{\partial l}{\partial x_i}(\mathbf{x}) - \frac{\partial l}{\partial x_j}(\mathbf{x}) \right| \left(\frac{1 - \frac{1}{N_C}}{c_n} \right). \end{aligned}$$

In summary, we can state the following lemma:

Lemma 5.22. *Let*

$$\dot{Q}_R > \dot{Q}_R^{LB1, n, \text{unique}} \quad \text{or} \quad \dot{Q}_R > \dot{Q}_R^{LB2, \text{unique}} \quad (5.55)$$

with

$$\begin{aligned}
 \dot{Q}_R^{LB1,n,unique} &:= Bl(\mathbf{x}^B) - \sum_{k=1}^{k_{act}} F_k l(\mathbf{x}^{F_k}) + \\
 &\quad \max \left(0, \left(\sum_{k=1}^{k_{act}} F_k - B - \sum_{l=1}^{l_{act}} S_l \right) (c_n \cdot b_n + 1) \right) v(\mathbf{y}^n) + \\
 &\quad \left(\sum_{k=1}^{k_{act}} F_k - B - \sum_{l=1}^{l_{act}} S_l - \max \left(0, \left(\sum_{k=1}^{k_{act}} F_k - B - \sum_{l=1}^{l_{act}} S_l \right) (c_n \cdot b_n + 1) \right) \right) \\
 &\quad \cdot \min_{\mathbf{x} \in \mathcal{F}_{N_C}} l(\mathbf{x}) + \sum_{l=1}^{l_{act}} S_l l(\mathbf{x}^{S_l}) \\
 &\geq \dot{Q}_R^{LB1,n}
 \end{aligned} \tag{5.56}$$

and

$$\begin{aligned}
 \dot{Q}_R^{LB2,n,unique} &:= \left(B + \sum_{l=1}^{l_{act}} S_l \right) \left(\max_{\mathbf{x} \in \mathcal{F}_{N_C}} l(\mathbf{x}) - \min_{\mathbf{x} \in \mathcal{F}_{N_C}} l(\mathbf{x}) \right) + \\
 &\quad \max \left(0, \left(\sum_{k=1}^{k_{act}} F_k - B - \sum_{l=1}^{l_{act}} S_l \right) (c_n \cdot b_n + 1) \right) \left(\max_{\mathbf{x} \in \mathcal{F}_{N_C}} v(\mathbf{x}) - \min_{\mathbf{x} \in \mathcal{F}_{N_C}} l(\mathbf{x}) \right) \\
 &\geq \dot{Q}_R^{LB2,n}.
 \end{aligned} \tag{5.57}$$

Then it holds that

$$\begin{aligned}
 |(\varphi_n^{up})'(s)| &= \left| \frac{\varphi_{up}^n(s) - \sum_{k=1}^{k_{act}} F_k + B + \sum_{l=1}^{l_{act}} S_l}{s - \sum_{k=1}^{k_{act}} F_k + B + \sum_{l=1}^{l_{act}} S_l} \cdot \frac{\nabla l(\mathbf{x}^{n+1}(s)) (\mathbf{y}^n - \mathbf{x}^{n+1}(s))}{v(\mathbf{y}^n) - l(\mathbf{x}^{n+1}(s))} \right| \\
 &\leq \frac{\min_{\mathbf{x} \in \mathcal{F}_{N_C}} v(\mathbf{x}) - \min_{\mathbf{x} \in \mathcal{F}_{N_C}} l(\mathbf{x})}{\left(\min_{\mathbf{x} \in \mathcal{F}_{N_C}} v(\mathbf{x}) - \max_{\mathbf{x} \in \mathcal{F}_{N_C}} l(\mathbf{x}) \right)^2} \\
 &\quad \cdot \max_{1 \leq i < j \leq N_C} \max_{\mathbf{x} \in \mathcal{F}_{N_C}} \left| \frac{\partial l}{\partial x_i}(\mathbf{x}) - \frac{\partial l}{\partial x_j}(\mathbf{x}) \right| \left(\frac{1 - \frac{1}{N_C}}{c_n} \right) \\
 &=: q(c_n).
 \end{aligned} \tag{5.58}$$

5. Stage-to-stage calculations of general distillation columns

This bound only depends on c_n and the physical properties of the multi-component mixture at pressure p . The value for c_n can always be chosen in such a way that $|(\varphi_{\text{up}}^n)'(s)| \leq q(c_n) < 1$.

Theorem 5.23 (Uniqueness of the fixed point). *Let $\sum_{k=1}^{k_{\text{act}}} F_k - B - \sum_{l=1}^{l_{\text{act}}} S_l \neq 0$ and*

$$\dot{Q}_R > \dot{Q}_R^{LB1,n,\text{unique}} \quad \text{or} \quad \dot{Q}_R > \dot{Q}_R^{LB2,n,\text{unique}}. \quad (5.59)$$

If c_n is chosen in a way that $|(\varphi_{\text{up}}^n)'(s)| \leq q(c_n) < 1$ there exists a unique fixed point in I_n and convergence of the sequence $(s_k)_{k \in \mathbb{N}}$ defined by $s_k := \varphi_{\text{up}}^n(s_{k-1})$ towards this fixed point is guaranteed for any $s_0 \in I_n$.

If $\sum_{k=1}^{k_{\text{act}}} F_k - B - \sum_{l=1}^{l_{\text{act}}} S_l = 0$ we get:

$$y_i^n - x_i^{n+1}(s) = \frac{1}{s} \cdot \left(\sum_{k=1}^{k_{\text{act}}} F_k x_i^{F_k} - B x_i^B - \sum_{l=1}^{l_{\text{act}}} S_l x_i^{S_l} - y_i^n \right) \quad (5.60)$$

$$= \frac{y_i^n}{s} \cdot \left(\frac{\sum_{k=1}^{k_{\text{act}}} F_k x_i^{F_k} - B x_i^B - \sum_{l=1}^{l_{\text{act}}} S_l x_i^{S_l}}{y_i^n} \right). \quad (5.61)$$

This expression gives a bound for $|y_i^n - x_i^{n+1}(s)|$:

$$|y_i^n - x_i^{n+1}(s)| \leq \underbrace{\frac{y_i^n}{s}}_{\geq 0} \cdot b_{n,0}, \quad (5.62)$$

with

$$b_{n,0} := \max \left\{ \max_{i=1, \dots, N_C} \left(\frac{\sum_{k=1}^{k_{\text{act}}} F_k x_i^{F_k} - B x_i^B - \sum_{l=1}^{l_{\text{act}}} S_l x_i^{S_l}}{y_i^n} \right), \right. \\ \left. - \min_{i=1, \dots, N_C} \left(\frac{\sum_{k=1}^{k_{\text{act}}} F_k x_i^{F_k} - B x_i^B - \sum_{l=1}^{l_{\text{act}}} S_l x_i^{S_l}}{y_i^n} \right) \right\}. \quad (5.63)$$

Lemma 5.24. *Let $c_{n,0} \geq 1$. It holds*

$$c_{n,0} \cdot b_{n,0} \geq m_{n,0}. \quad (5.64)$$

If we require that $\inf_{s \in M_{n,0}} \varphi_n^{\text{up}}(s) \geq c_{n,0} \cdot b_{n,0}$, where $c_{n,0} \geq 1$ we obtain the following result:

$$|y_i^n - x_i^{n+1}(s)| \leq \frac{1}{c_{n,0}} y_i^n. \quad (5.65)$$

Along the same lines as before we obtain:

$$\begin{aligned} |\nabla l(\mathbf{x}^{n+1}(s)) (\mathbf{y}^n - \mathbf{x}^{n+1}(s))| &\leq \max_{1 \leq i < j \leq N_C} \max_{\mathbf{x} \in \mathcal{F}_{N_C}} \left| \frac{\partial l}{\partial x_i}(\mathbf{x}) - \frac{\partial l}{\partial x_j}(\mathbf{x}) \right| \left(\frac{1 - y_{i_0}^n}{c_{n,0}} \right) \\ &\leq \max_{1 \leq i < j \leq N_C} \max_{\mathbf{x} \in \mathcal{F}_{N_C}} \left| \frac{\partial l}{\partial x_i}(\mathbf{x}) - \frac{\partial l}{\partial x_j}(\mathbf{x}) \right| \left(\frac{1 - \frac{1}{N_C}}{c_{n,0}} \right). \end{aligned}$$

Lemma 5.25. *Let*

$$\dot{Q}_R > \dot{Q}_R^{LB1,n,0,unique} \quad \text{or} \quad \dot{Q}_R > \dot{Q}_R^{LB2,n,0,unique} \quad (5.66)$$

with

$$\begin{aligned} \dot{Q}_R^{LB1,n,0,unique} &:= B l(\mathbf{x}^B) - \sum_{k=1}^{k_{act}} F_k l(\mathbf{x}^{F_k}) + \sum_{l=1}^{l_{act}} S_l l(\mathbf{x}^{S_l}) + c_{n,0} \cdot b_{n,0} \left(v(\mathbf{y}^n) - \min_{\mathbf{x} \in \mathcal{F}_{N_C}} l(\mathbf{x}) \right) \\ &\geq \dot{Q}_R^{LB1,n,0} \end{aligned} \quad (5.67)$$

and

$$\begin{aligned} \dot{Q}_R^{LB2,n,0,unique} &:= \left(B + \sum_{l=1}^{l_{act}} S_l \right) \left(\max_{\mathbf{x} \in \mathcal{F}_{N_C}} l(\mathbf{x}) - \min_{\mathbf{x} \in \mathcal{F}_{N_C}} l(\mathbf{x}) \right) \\ &\quad + c_{n,0} \cdot b_{n,0} \left(\max_{\mathbf{x} \in \mathcal{F}_{N_C}} v(\mathbf{x}) - \min_{\mathbf{x} \in \mathcal{F}_{N_C}} l(\mathbf{x}) \right) \\ &\geq \dot{Q}_R^{LB2,n,0}. \end{aligned} \quad (5.68)$$

Then it holds that

$$\begin{aligned}
 |(\varphi_n^{up})'(s)| &= \left| \frac{\varphi_{up}^n(s)}{s} \cdot \frac{\nabla l(\mathbf{x}^{n+1}(s)) (\mathbf{y}^n - \mathbf{x}^{n+1}(s))}{v(\mathbf{y}^n) - l(\mathbf{x}^{n+1}(s))} \right| \\
 &\leq \frac{\min_{\mathbf{x} \in \mathcal{F}_{N_C}} v(\mathbf{x}) - \min_{\mathbf{x} \in \mathcal{F}_{N_C}} l(\mathbf{x})}{\left(\min_{\mathbf{x} \in \mathcal{F}_{N_C}} v(\mathbf{x}) - \max_{\mathbf{x} \in \mathcal{F}_{N_C}} l(\mathbf{x}) \right)^2} \\
 &\quad \cdot \max_{1 \leq i < j \leq N_C} \max_{\mathbf{x} \in \mathcal{F}_{N_C}} \left| \frac{\partial l}{\partial x_i}(\mathbf{x}) - \frac{\partial l}{\partial x_j}(\mathbf{x}) \right| \left(\frac{1 - \frac{1}{N_C}}{c_{n,0}} \right) \\
 &=: q(c_{n,0}).
 \end{aligned} \tag{5.69}$$

Once again, the bound $q(c_{n,0})$ only depends on $c_{n,0}$ and the physical properties of the multi-component mixture at pressure p . The value for $c_{n,0}$ can always be chosen in such a way that $|(\varphi_{up}^n)'(s)| \leq q(c_{n,0}) < 1$. We can formulate the following theorem:

Theorem 5.26 (Uniqueness of the fixed point). *Let $\sum_{k=1}^{k_{act}} F_k - B - \sum_{l=1}^{l_{act}} S_l = 0$ and*

$$\dot{Q}_R > \dot{Q}_R^{LB1,n,0,unique} \quad \text{or} \quad \dot{Q}_R > \dot{Q}_R^{LB2,n,0,unique}. \tag{5.70}$$

If $c_{n,0}$ is chosen in a way that $|(\varphi_{up}^n)'(s)| \leq q(c_{n,0}) < 1$ there exists a unique fixed point in I_n and convergence of the sequence $(s_k)_{k \in \mathbb{N}}$ defined by $s_k := \varphi_{up}^n(s_{k-1})$ towards this fixed point is guaranteed for any $s_0 \in I_n$.

For the general distillation column discussed in this chapter, we can also summarize that the reboiler duty only needs to be increased sufficiently in order to be able to guarantee existence and uniqueness of a fixed point.

Distillation-based flowsheets comprising several unit operations

So far, the embedding of process simulation in an optimization problem was only presented for single units. However, typical flowsheets consist of several units of the same or different types, which are connected via streams. Analogously to the modular and the equation-oriented approach in classical process simulation (see also Biegler et al. (1997, Chap. 8), Biegler (2014), and Dowling & Biegler (2015)), the approach of the present work can also be realized in a modular or a simultaneous way. In this chapter, the two different alternatives are discussed and a graph theoretic algorithm is presented that determines the calculation order of units in a flowsheet within one iteration for the simultaneous approach.

6.1. The modular and the simultaneous approach

In the modular way, an optimization problem is formulated for each unit separately. The optimization problems are then solved in sequence. The sequence, in which the optimization problems are solved, can be determined completely analogous as for the classical modular flowsheeting methods. An advantage of this modular approach is that the resulting optimization problems are quite small. However, in case recycle streams are present in the considered flowsheet, this way of simulating flowsheets requires the introduction of tear streams and converging these tear stream on a higher level.

In the simultaneous approach the different constraints and optimization variables of each unit are gathered and a single optimization problem is formulated. For flowsheets with a moderate number of units N_U , the resulting optimization problem is still of moderate size ($\mathcal{O}(N_C \cdot N_U)$ optimization variables and constraints) and does not require large-scale optimization solvers. In contrast to that, the classical equation-oriented approach typically comprises hundreds or thousands of optimization variables and constraints for distillation-based flowsheets and requires sophisticated strategies in order to find appropriate starting values for the large number of optimization variables. Using the simultaneous approach in combination with the numerically robust stage-to-stage calculations of distillation columns as presented in Chapter 4 and 5, the unknown process variables can be easily determined based on the knowledge of a small number of optimization variables for distillation-based flowsheets. In this work, all numerical results are obtained by applying the simultaneous approach.

6.2. The simultaneous approach: Calculation order of units in a flowsheet within one iteration

When applying the simultaneous approach, all process variables have to be determined within every iteration of the optimization algorithm. In order to calculate the unknown process variables of a unit U_1 all of its feed streams have to be known. A feed stream can be known due to the fact that it is given as external stream or chosen as optimization variable and therefore also specified in each iteration. It is also possible, that the relevant stream can be computed robustly as output stream of another unit U_2 in the flowsheet. In this case, unit U_2 , which determines the relevant stream as output stream, clearly has to be calculated before unit U_1 and thus the calculation order within one iteration might not be arbitrary.

In the following, it is assumed that external input streams are completely specified. A calculation order for the units in the flowsheet within one iteration has to be determined and we have to decide which streams to choose as optimization variables. Note that the calculation order of units within one iteration should not be confused with the sequence in which the units are calculated in the modular flowsheet approach.

For flowsheets without recycle streams it is trivial to determine the calculation order of the units by proceeding through the flowsheet starting from a unit with given external feed streams. If recycle streams are present, it is not always obvious how the calculation order within one iteration should be chosen.

For distillation-based flowsheets (with and without recycle streams) consisting only of mixers and simple (one feed) distillation columns we prove that it is possible to choose the optimization variables for the distillation columns in such a way that all streams that serve as feed streams for a unit are determined either as external streams, as optimization variables, or computed as output streams of other units. Furthermore, we present an algorithm based on a graph-theoretical representation of the distillation-based flowsheet that determines the optimization variables in the flowsheet and gives a feasible calculation order of the units.

In a first step, a distillation-based flowsheet is regarded as a directed graph $G = (V, E)$ in the following way: Every distillation column is represented by a node $v \in V$ and an additional node is added as the sink $t \in V$ of the graph. Mixers are fused with the subsequent distillation column and hence neglected in the graph. Every stream is represented as a directed edge $e \in E$ pointing from the source unit to the target unit, except the external input streams which are neglected in the graph. Every effluent product stream ends in the sink t .

The construction of the graph-theoretical problems is illustrated by means of two exemplary distillation-based flowsheets. Figure 6.1 depicts the first flowsheet, which consists of two simple distillation columns C1 and C2 and one mixer M with two input streams. The external stream 1 is assumed to be fully specified.

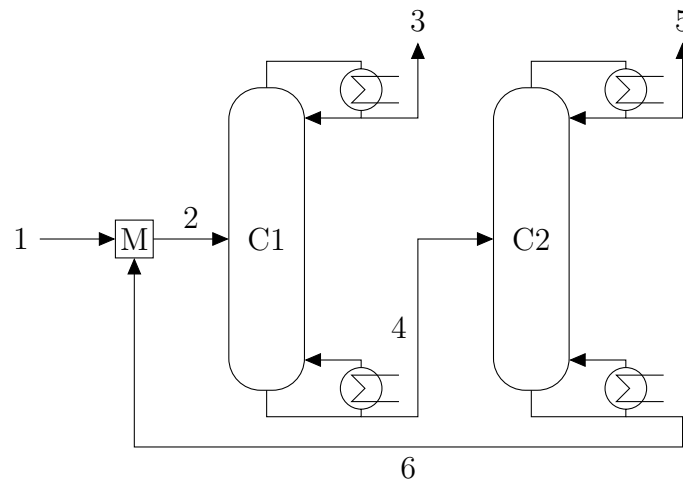


Figure 6.1.: Schematic representation of a flowsheet consisting of two simple columns and a mixer.

The second flowsheet consists of three simple columns and a mixer and is depicted in Figure 6.2. As in the previous example, stream 1 is assumed to be completely specified.

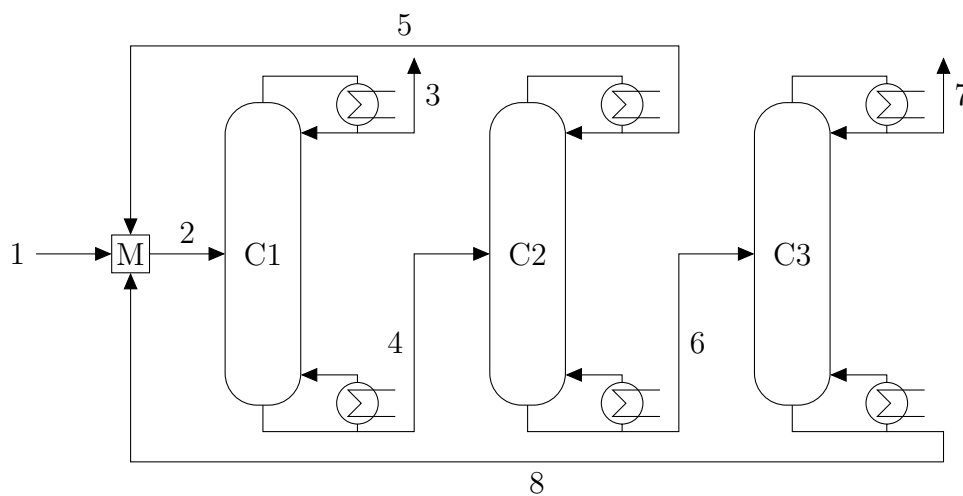


Figure 6.2.: Schematic representation of a flowsheet consisting of three simple columns and a mixer.

Figure 6.3 depicts the graph-theoretical representation of the flowsheets in Figure 6.1 and 6.2.

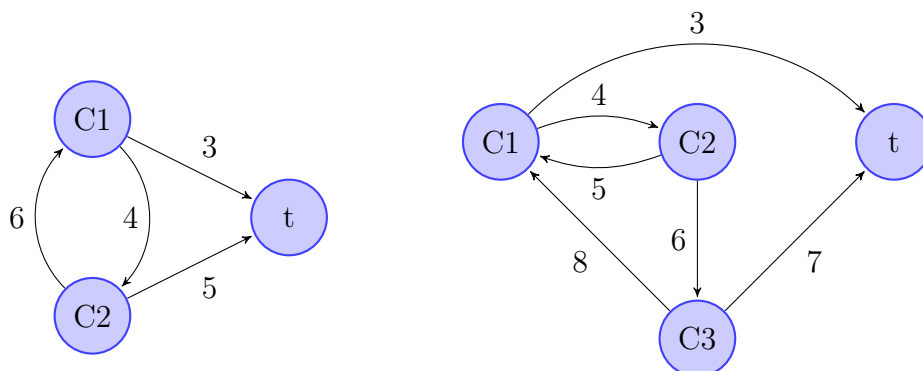


Figure 6.3.: Schematic representation of the flowsheets in Figure 6.1 (left) and 6.2 (right) as a graph $G = (V, E)$.

For the constructed graphs the following result holds:

Remark 6.1. *Due to its construction, the graph G is weakly connected, which means that replacing all directed edges with undirected edges yields a connected graph. Furthermore, it has no parallel edges. Every node $v \in V \setminus \{t\}$ has outdegree $\deg^+(v) = 2$ and every node is connected with the sink t via a directed path.*

In order to calculate a unit, all input streams have to be known. When we are trying to find the calculation order of the units within one iteration, directed circles consisting of unknown streams in the graph G pose a problem. However, it is possible to eliminate the directed circles from G , because for every distillation column either the bottom or the distillate stream is chosen as optimization variable depending on the choice of upward or downward calculation of the column. One of the product streams of a distillation column is therefore known in each iteration step and can be deleted from the set of edges E . The task is now to determine the streams that are optimization variables in such a way that the resulting graph \tilde{G} , whose edges represent only the unknown streams, contains no directed circles. This is conducted via the following Algorithms 1 and 2. The edges that are deleted from the set of edges during Algorithm 1 represent the streams that are chosen as optimization variables and thus known in each iteration.

Algorithm 1 Reduction of a graph G to obtain an acyclic graph \tilde{G}

Require: A directed graph $G = (V, E)$ with sink t and properties stated in Remark 6.1

Ensure: An acyclic directed graph $\tilde{G} = (V, \tilde{E})$

VISIT(t)

Algorithm 2 VISIT(v)

Require: A node $v \in V$

for all w that are predecessors of v **do**

 Keep the edge $e = (w, v)$ and delete the second outgoing edge.

 VISIT(w)

end for

Theorem 6.2. *Algorithm 1 correctly produces an acyclic graph in $\mathcal{O}(|V|)$.*

Proof. In a first step, we show that the resulting graph $\tilde{G} = (V \setminus \{t\}, \tilde{E})$ is weakly connected. To prove this by contradiction, we assume that V can be partitioned into two disjoint sets V_1, V_2 with no edge going from V_1 to V_2 or vice versa. W.l.o.g. assume that $t \in V_1$. Due to the properties of the original graph $G = (V, E)$ stated in Remark 6.1 there has to be an edge $e = (v, t) \in E$ with $v \in V_2$. However, this edge can never be deleted (see Algorithm 2). This contradicts our initial assumption and hence \tilde{G} is weakly connected. One can even conclude that in the reduced graph $\tilde{G} = (V, \tilde{E})$ there still exists a directed path from any node to the sink.

Furthermore, we claim that every node $v \in V$ is visited exactly once during Algorithm 1. After a node w has been visited from its successor v , the outdegree is reduced to $\deg^+(w) = 1$. Hence, a node can only be visited twice, iff the successor v is visited twice. Inductively, one can conclude that this is not possible. Along the same lines and using the fact that from any node there exists a directed path to the sink, one can conclude that every node is visited at least once. VISIT(v) is therefore called $|V| - 1$ times.

Finally, we shown that there exists no cycle in $\tilde{G} = (V, \tilde{E})$. Let us assume that there exists a cycle \mathcal{C} . Clearly, the sink t cannot be part of the cycle due to the fact that it has no outgoing edge. However, the nodes in the cycles have to be connected with t via a directed path pointing towards the sink. For every node $v \in V \setminus \{t\}$ it holds true that $\deg^+(v) = 1$ after the execution of Algorithm 1, so a cycle cannot exist. \square

We have shown that execution of Algorithm 1 always yields an acyclic graph. For this acyclic graph $\tilde{G} = (V, \tilde{E})$ it is possible to calculate a topological sorting $\sigma : V \rightarrow \{1, 2, \dots, |V|\}$ (see Krumke & Noltemeier, 2012, Chap. 3.2). The topological sorting can in turn serve as calculation order for the flowsheet within an iteration, which was the desired objective. Any mixer is calculated immediately before its target unit. The calculation

order will in general not be unique, but there usually exist several solutions. In case we can choose from several alternatives, it is always a good choice to calculate a distillation column in direction of a product stream with a desired high purity.

The exemplary graphs in Figure 6.3 are simplified to the graphs in Figure 6.4 using Algorithm 1.

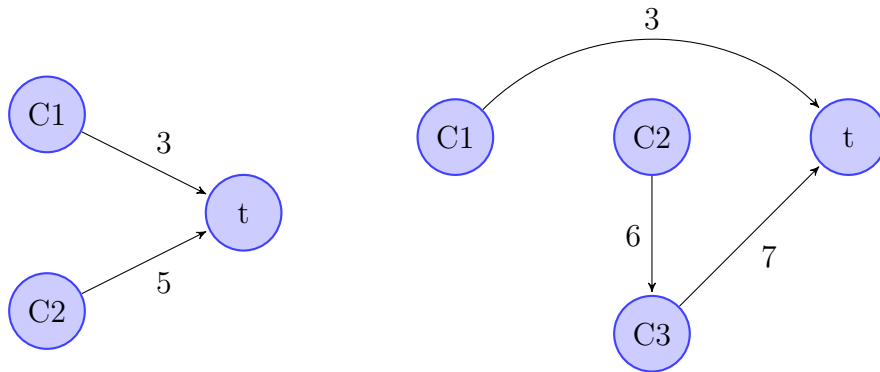


Figure 6.4.: Simplification of the graphs in Figure 6.3 after execution of Algorithm 1.

In the left graph the edges 4 and 6 have been deleted. This means that streams 4 and 6 are selected as optimization variables for the flowsheet in Figure 6.1, and the columns are calculated upward. A possible calculation order within one iteration is: C1, C2.

For the second flowsheet (right graph in Figure 6.4) the streams 4, 5, and 8 have been deleted. The molar flow rates of the streams 4, 5, and 8 are selected as optimization variables. Column C1 and C3 are calculated upward, C2 downward. A feasible calculation order within one iteration is: C1, C2, C3.

Graph theoretic methods are also applied in the context of data reconciliation in order to classify observable and redundant streams. Concepts for such classification based on overall flows have been developed by Václavek (1969) and Mah et al. (1976) and were extended by Václavek & Loučka (1976) to multi-component systems. For a brief overview and the algorithmic ideas behind the graph theoretic concepts the reader is referred to Narasimhan & Jordache (2000, pp. 72).

Part III.

Numerical analysis

CHAPTER 7

Numerical results

In this thesis, a novel approach that enables integrated process simulation and optimization was introduced. In this chapter, the approach is illustrated by numerical results. First, the performance of different optimization solvers is compared. In a subsequent step, typical examples for process simulation and optimization of single units and distillation-based flowsheets are presented that emphasize the advantages of the new approach.

7.1. Implementation details

Within the scope of this thesis, the novel approach for process simulation and optimization was implemented in C# in order to conduct numerical studies. The arising optimization problems are solved using either commercial optimization solvers or an in-house development.

Our code is not optimized for speed and therefore we will not focus on CPU times. However, the numerical results shown in this chapter are typically obtained within seconds for small examples or within a few minutes for large examples.

Our results have been checked for correctness by a comparison with the process simulator CHEMASIM (Hasse et al., 2006).

7.2. Comparison of optimization algorithms

In this section, different implementations of optimization algorithms are applied to the type of optimization problem that has been derived in Chapter 3. In order to compare the results a test problem is defined: The solver studies are conducted for a single distillation column with a ternary feed stream containing acetone, chloroform, and benzene. The column consists of 20 stages with feed on stage 10 and operates at 1 bar. Acetone is supposed to be withdrawn as distillate with a minimum purity of 0.99 mol/mol. Table 7.1 displays the specifications used in the test problem. The distillation column will be calculated upward. Using the ideas introduced in Section 3.3, this test problem can be formulated as an optimization problem with four optimization variables: the reboiler duty and the three molar flow rates of the bottom product.

Table 7.1.: Specifications for the distillation column used as test problem for solver comparison.

| Stream | Flow rate | Composition |
|------------|------------|--|
| Feed | 3.6 kmol/h | 0.4 mol/mol AC 0.3 mol/mol CF 0.3 mol/mol BE |
| Distillate | | ≥ 0.99 mol/mol AC |

The different implementations of the optimization algorithms considered in this thesis all aim at constrained nonlinear optimization. The following five commercial solvers and an in-house implementation will be compared:

- NLPQLP: A sequential quadratic programming algorithm using a line search method (monotone and non-monotone) (Schittkowski, 2009).
- ALTRA: A sequential quadratic programming algorithm using a trust region method (developed by Prof. Schittkowski and co-workers).
- MINNS: An adaptive gradient sampling solver (ALGLIB, 2016).
- MINNLC: An augmented Lagrangian solver (ALGLIB, 2016).
- IPOPT: An interior point solver (Wächter & Biegler, 2006).
- ITWMSQP: A sequential quadratic programming algorithm using a trust region method based on the quadratic programming algorithm of the ALGLIB.

In the solution, the algorithm requires that a final accuracy is not exceeded by the constraint violation. In the following examples, this final accuracy was chosen to be 10^{-6} . All solvers use derivative information that is approximated via numerical differentiation. In a first study, the performance of the optimization solvers using forward differences for numerical differentiation

$$\frac{\partial}{\partial x_i} f(\mathbf{x}) \approx \frac{1}{\eta_i} (f(\mathbf{x} + \eta_i \mathbf{e}_i) - f(\mathbf{x})) \quad (7.1)$$

is compared to the usage of central differences

$$\frac{\partial}{\partial x_i} f(\mathbf{x}) \approx \frac{1}{2\eta_i} (f(\mathbf{x} + \eta_i \mathbf{e}_i) - f(\mathbf{x} - \eta_i \mathbf{e}_i)), \quad (7.2)$$

where $\eta_i = \eta \max(|x_i|, 10^{-6})$ and \mathbf{e}_i is the i -th unit vector for all optimization variables $i = 1, \dots, N_{\text{opt}}$. For both cases, different step lengths η are applied. The subsequent test configurations are defined:

- (a) central differences, $\eta = 10^{-3}$
- (b) central differences, $\eta = 10^{-5}$
- (c) forward differences, $\eta = 10^{-4}$
- (d) forward differences, $\eta = 10^{-5}$

The initial values for the optimization variables, which are used in the following test scenarios, are derived by ∞/∞ -analysis and displayed in Table 7.2.

Table 7.2.: Initial values for the optimization variables.

| Optimization variable | Initial value |
|------------------------------------|---------------|
| \bar{Q}_R / kW | 100.00 |
| \dot{n}_{AC}^B / (kmol/h) | 0.1376 |
| \dot{n}_{CF}^B / (kmol/h) | 1.0800 |
| \dot{n}_{BE}^B / (kmol/h) | 1.0800 |

Table 7.3 shows the number of iterations needed for process simulation for the different test configurations and the different solver implementations, i.e. the algorithm terminates if an arbitrary feasible solution with the required product purity is found. In case no number is given in Table 7.3 the algorithm failed to find a feasible solution. NLPQLP

requires the smallest number of iterations, followed by ITWMSQP and ALTRA. MINNS performed poorly as it did not find a solution for configurations (a), (b), and (d) and MINNLC required a large number of iterations. The number of iterations required by IPOPT was larger than the number of iterations required for NLPQLP, ALTRA, and ITWMSQP for configurations (a)–(c) and for configuration (d) no solution was found.

Table 7.3.: Number of iterations needed for process simulation of a single distillation column with ternary feed stream for the different test configurations and the different solver implementations. A missing number means the algorithms did not find a solution.

| Configuration | Number of iterations | | | |
|---------------|----------------------|-----|-----|-----|
| | (a) | (b) | (c) | (d) |
| NLPQLP | 4 | 4 | 4 | 4 |
| ALTRA | 8 | 8 | 5 | 5 |
| MINNS | - | - | 477 | - |
| MINNLC | 1689 | 489 | 56 | 556 |
| IPOPT | 16 | 31 | 13 | - |
| ITWMSQP | 5 | 5 | 5 | 5 |

Table 7.4 shows the number of iterations required for process optimization where the reboiler duty of the distillation column is incorporated as objective function. The trivial solution with $D = 0$ kmol/h is prevented by the fact that we incorporate an additional constraint on the minimum acetone yield in the distillate: $\dot{n}_{AC}^D \geq 1.2$ kmol/h. As for process simulation of the test problem, NLPQLP, ALTRA, and ITWMSQP required a small number of iterations. MINNLC failed for configuration (b) and for all other configurations MINNLC and MINNS required significantly more iterations. IPOPT was not able to find an optimal solution. The number of iterations that are needed in order to obtain an optimal solution is in general larger than the number of iterations needed to find an arbitrary feasible solution.

Table 7.4.: Number of iterations needed for process optimization of a single distillation column with ternary feed stream for the different test configurations and the different solver implementations. A missing number means the algorithms did not find a solution.

| Configuration | Number of iterations | | | |
|---------------|----------------------|-----|-----|-----|
| | (a) | (b) | (c) | (d) |
| NLPQLP | 13 | 14 | 13 | 14 |
| ALTRA | 12 | 12 | 12 | 12 |
| MINNS | 126 | 119 | 156 | 139 |
| MINNLC | 62 | - | 84 | 82 |
| IPOPT | - | - | - | - |
| ITWMSQP | 18 | 18 | 18 | 18 |

In conclusion, especially for those solver implementations that performed well, there was no advantage in using central differences in order to approximate the derivative information. Furthermore, it is not clear which choice of η should be preferred and for NLPQLP, ALTRA, and ITWMSQP this choice had almost no influence on the number of iterations needed. For the following studies, forward differences are applied due to the fact that they need less function evaluations compared to central differences. The step length is chosen to be $\eta = 10^{-4}$.

In a next study, the robustness of the different solver implementations with respect to poor initial values is investigated. For this purpose, three poor initial values are defined in Table 7.5. The composition of the bottom product of "Initial value 1" even lies in a different distillation region than the desired distillate.

Table 7.5.: Different poor initial values for the optimization variables.

| Optimization variable | Initial value 1 | Initial value 2 | Initial value 3 |
|-----------------------------|-----------------|-----------------|-----------------|
| \dot{Q}_R / kW | 100.00 | 100.00 | 100.00 |
| \dot{n}_{AC}^B / (kmol/h) | 0.25 | 0.25 | 2.00 |
| \dot{n}_{CF}^B / (kmol/h) | 2.00 | 0.25 | 0.25 |
| \dot{n}_{BE}^B / (kmol/h) | 0.25 | 2.00 | 0.25 |

First, the distillation column in the test problem is simulated without including a non-constant objective function in the optimization problem. Table 7.6 shows the number of iterations needed until a feasible solution is found. Compared to the results for the initial values that are generated by ∞/∞ -analysis, it is harder for the optimization solver to find a feasible solution and the different solvers fail in about half the scenarios. The

best results are obtained by using NLPQLP, ALTRA, and MINNLC. If the results from NLPQLP and ALTRA are combined, a feasible solution can be found for all poor initial values defined in Table 7.2.

Table 7.6.: Number of iterations needed for process simulation of a single distillation column with ternary feed stream for different initial values and the different solver implementations. A missing number means the algorithms did not find a solution.

| Initial values | Number of iterations | | | |
|----------------|----------------------|-----|-----|-----|
| | IV _{∞/∞} | IV1 | IV2 | IV3 |
| NLPQLP | 4 | 6 | - | 30 |
| ALTRA | 5 | - | 4 | - |
| MINNS | 477 | - | - | - |
| MINNLC | 56 | 22 | 17 | - |
| IPOPT | 13 | - | - | - |
| ITWMSQP | 5 | - | - | - |

Process optimization, with the reboiler duty chosen as objective function, is also conducted for the poor initial values from Table 7.2. The results are summarized in Table 7.7. With a non-constant objective function NLPQLP and ALTRA always succeed in finding an optimal solution. MINNS also performs better when using the reboiler duty as objective function whereas MINNLC fails more often.

Table 7.7.: Number of iterations needed for process optimization of a single distillation column with ternary feed stream for different initial values and the different solver implementations. A missing number means the algorithms did not find a solution.

| Initial value | Number of iterations | | | |
|---------------|----------------------|-----|-----|-----|
| | IV _{∞/∞} | IV1 | IV2 | IV3 |
| NLPQLP | 13 | 21 | 12 | 13 |
| ALTRA | 12 | 10 | 9 | 9 |
| MINNS | 156 | 183 | 158 | 123 |
| MINNLC | 84 | - | - | - |
| IPOPT | - | - | - | - |
| ITWMSQP | 18 | - | - | - |

In summary, one can conclude that especially the solver implementations NLPQLP and ALTRA are robust in terms of poor initial values and perform even better in case the reboiler duty is incorporated as objective function.

For the subsequent numerical studies, we use NLPQLP or ALTRA as optimization solver. Derivative information is generated using forward differences and $\eta = 10^{-4}$, as described in test configuration (c).

7.3. Separation of acetone and chloroform

In a first study, we consider the separation of acetone and chloroform. This binary system exhibits a heavy-boiling azeotrope.

7.3.1. Single distillation column

A simple distillation column is considered with a defined binary feed containing acetone (AC) and chloroform (CF) as depicted in Figure 7.1. Acetone is obtained as distillate. The distillation column operates at 1 bar and has 20 stages. The feed stage is stage 10 counted from bottom. This example comprises 182 process variables. Assuming that the pressure is given and the feed is fully defined, there remain two degrees of freedom.

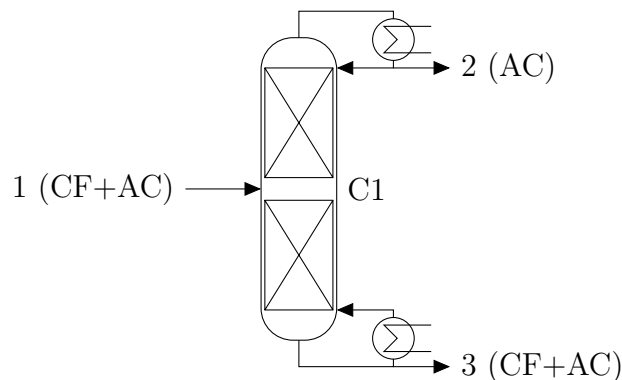


Figure 7.1.: Schematic distillation column with binary feed containing acetone (AC) and chloroform (CF).

Process simulation

The required minimum purity of acetone in the distillate is 0.99 mol/mol. There are no further requirements. This specification and the specifications of the feed stream are summarized in Table 7.8.

Table 7.8.: Specifications for the distillation column shown in Figure 7.1.

| Stream | Flow rate | Composition |
|--------|-----------|----------------------------------|
| 1 | 1 kmol/h | 0.5 mol/mol AC 0.5 mol/mol CF |
| 2 | | ≥ 0.99 mol/mol AC |

If only the specifications in Table 7.8 are required, there will clearly not exist a unique solution to the problem but infinitely many solutions due to the fact that we did not fix the two degrees of freedom. Even if we include two specifications, which are formulated as inequalities, the solution will in general not be unique. The optimization algorithm will output the first feasible solution that is found depending on starting values for the optimization variables and the choice of internal parameters for the optimization algorithm.

In order to simulate the distillation column using commercial systems, all degrees of freedom have to be specified. An obvious specification is to fix the mole fraction of acetone in stream 2 to be 0.99 mol/mol. However, this specification significantly restricts the solution space compared to incorporating the required purity via an inequality constraint.

Using the method introduced in Chapter 3, we can formulate an optimization problem with three optimization variables \dot{Q}_R and \dot{n}^3 and include the desired acetone purity in stream 2 as an inequality constraint. In order to obtain the remaining process variables the distillation column is computed stage-wise starting from the bottom.

The system acetone, chloroform at 1 bar exhibits a heavy-boiling azeotrope at $x_{AC}^{Azeo} = 0.3454$ mol/mol. Given the feed on the acetone-rich side of the azeotrope, the fraction of acetone in the bottom product cannot fall below x_{AC}^{Azeo} . Therefore, the starting value for \mathbf{x}^3 is chosen to be the azeotropic composition. The starting value for the molar flow rate of stream 3 is calculated from the material balance assuming pure acetone in the distillate. The starting value for the reboiler duty can be chosen in a suitable way following the guidelines in Section 4.3.

In this example, a feasible distillation column that meets the specifications in Table 7.8 is calculated in four iterations. The obtained solution strongly depends on the choice of starting values for the optimization variables and internal parameters of the optimization algorithm and different solutions can vary strongly for example in terms of the reboiler duty. The initial values as well as the final values for the optimization variables are summarized in Table 7.9. The resulting mole fraction of acetone in stream 2 is 0.9996 mol/mol, which is also depicted in Table 7.10 (stream table).

Table 7.9.: Initial values and final values for the optimization variables.

| Optimization variable | Initial value | Final value |
|-----------------------------|---------------|-------------|
| \dot{Q}_R / kW | 40.71 | 7.320 |
| \dot{n}_{AC}^3 / (kmol/h) | 0.2638 | 0.4575 |
| \dot{n}_{CF}^3 / (kmol/h) | 0.5000 | 0.4999 |

Table 7.10.: Stream table for a solution of the column depicted in Figure 7.1 that meets the specifications in Table 7.8.

| Stream | 1 | 2 | 3 |
|----------------------|--------|--------|--------|
| \dot{n} / (kmol/h) | 1.0000 | 0.0426 | 0.9574 |
| x_{AC} / (mol/mol) | 0.5000 | 0.9996 | 0.4779 |
| x_{CF} / (mol/mol) | 0.5000 | 0.0004 | 0.5221 |

The presented approach is robust with respect to poor initial values. This is illustrated by choosing a bottom composition on the wrong side of the azeotrope as starting value. A feasible solution is still found within four iterations, cf. Table 7.11 and 7.12 (stream table).

Table 7.11.: Initial values and final values for the optimization variables.

| Optimization variable | Initial value | Final value |
|-----------------------------|---------------|-------------|
| \dot{Q}_R / kW | 86.12 | 45.47 |
| \dot{n}_{AC}^3 / (kmol/h) | 0.1 | 0.3003 |
| \dot{n}_{CF}^3 / (kmol/h) | 0.4 | 0.5000 |

Table 7.12.: Stream table for a solution of the column depicted in Figure 7.1 that meets the specifications in Table 7.8 when starting with poor initial values.

| Stream | 1 | 2 | 3 |
|----------------------|--------|--------|--------|
| \dot{n} / (kmol/h) | 1.0000 | 0.1998 | 0.8002 |
| x_{AC} / (mol/mol) | 0.5000 | 0.9999 | 0.3752 |
| x_{CF} / (mol/mol) | 0.5000 | 0.0001 | 0.6248 |

Process optimization

Additionally, one could include the reboiler duty as objective function aiming for minimal energy costs. If only the specifications listed in Table 7.8 are requested and the reboiler duty is minimized we end up with a solution where the molar flow rate of stream 2 is

0 kmol/h. However, one can easily incorporate an additional lower bound on the yield of acetone in the distillate in the problem formulation, for example $\dot{n}_{AC}^2 \geq 0.23$ kmol/h, cf. Table 7.13. In this example, the maximum yield of acetone in the distillate cannot be significantly larger than 0.23 kmol/h due to the binary azeotrope.

Table 7.13.: Specifications for the distillation column shown in Figure 7.1.

| Stream | Flow rate | Composition |
|--------|-----------------------|----------------------------------|
| 1 | 1 kmol/h | 0.5 mol/mol AC 0.5 mol/mol CF |
| 2 | ≥ 0.23 kmol/h AC | ≥ 0.99 mol/mol AC |

An optimal solution is found in eight iterations. The larger number of iterations illustrates that it is harder to find the optimal solution than to find an arbitrary feasible solution. The initial and final values are summarized in Table 7.14 and 7.15 (stream table).

Table 7.14.: Initial values and final values for the optimization variables.

| Optimization variable | Initial value | Final value |
|-----------------------------|---------------|-------------|
| \dot{Q}_R / kW | 150.00 | 113.64 |
| \dot{n}_{AC}^3 / (kmol/h) | 0.2677 | 0.2700 |
| \dot{n}_{CF}^3 / (kmol/h) | 0.5000 | 0.4977 |

Table 7.15.: Stream table for a solution of the column depicted in Figure 7.1 that meets the specifications in Table 7.8 at minimal energy demand.

| Stream | 1 | 2 | 3 |
|----------------------|--------|--------|--------|
| \dot{n} / (kmol/h) | 1.0000 | 0.2323 | 0.7677 |
| x_{AC} / (mol/mol) | 0.5000 | 0.9900 | 0.3517 |
| x_{CF} / (mol/mol) | 0.5000 | 0.0100 | 0.6483 |

Mixed-integer optimization

For the previous process simulation and optimization example, the feed stage $N_F = 10$ was fixed. In the subsequent example, a mixed-integer optimization algorithm (Exler & Schittkowski, 2007) is applied in order to determine the optimal feed stage which is incorporated now as an integer optimization variable. Again, the specifications in Table 7.13 should be met. An optimal solution is found within 57 iterations and the result

is depicted in Table 7.16 and Table 7.17 (stream table). The result of the mixed-integer optimization problem requires only 94.76 kW compared to 113.64 kW for the result in Table 7.14 where the feed stage is fixed.

Table 7.16.: Initial values and final values for the optimization variables.

| Optimization variable | Initial value | Final value |
|-----------------------------|---------------|-------------|
| \dot{Q}_R / kW | 150.00 | 94.76 |
| \dot{n}_{AC}^3 / (kmol/h) | 0.2677 | 0.2700 |
| \dot{n}_{CF}^3 / (kmol/h) | 0.5000 | 0.4977 |
| N_F | 10 | 13 |

Table 7.17.: Stream table for a solution of the column depicted in Figure 7.1 with optimized feed stage that meets the specifications in Table 7.8 at minimal energy demand.

| Stream | 1 | 2 | 3 |
|----------------------|--------|--------|--------|
| \dot{n} / (kmol/h) | 1.0000 | 0.2323 | 0.7677 |
| x_{AC} / (mol/mol) | 0.5000 | 0.9900 | 0.3538 |
| x_{CF} / (mol/mol) | 0.5000 | 0.0100 | 0.6462 |

It is also possible to vary the total number of stages N_S and to minimize the reboiler duty for every new choice of N_S with optimized feed stage. The number of stages can be plotted against the required minimal reboiler duty as displayed in an N - Q -curve (Zeck, 1990) in Figure 7.2. From this figure one can estimate the minimum number of stages needed for this separation task as well as the minimum reboiler duty needed for a column with infinitely many stages. The optimal feed stage N_F is encoded in Figure 7.2 in the color of the marker and also increases with increasing total number of stages.

Figure 7.2 illustrates the multi-criteria character of this question and facilitates an easy identification of relevant intervals for the two different criteria. However, one could also think of combining the number of stages and the reboiler duty in a cost function which then serves as objective function.

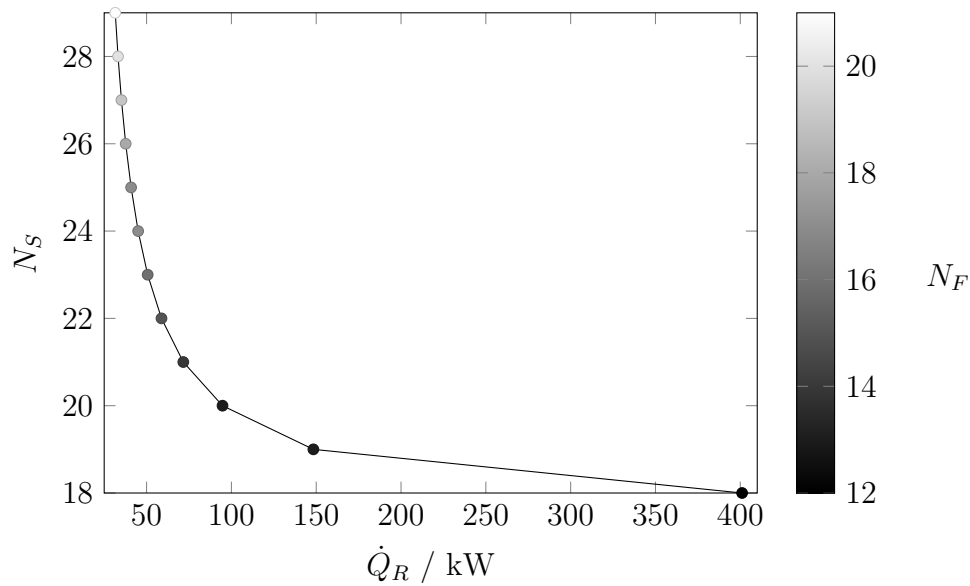


Figure 7.2.: N - Q -curve for the distillation column in Figure 7.1 where the specifications in Table 7.13 are met. The optimal feed stage N_F can be obtained from the greyscale of the marker in combination with the colorbar on the right.

A separation of acetone and chloroform into pure components using simple distillation is not possible due to the fact that the two components form an azeotrope. However, this separation task can be solved using either pressure-swing distillation or an entrainer. These two methods are discussed in the following.

7.3.2. Pressure-swing distillation

This method of separating acetone and chloroform takes advantage of the pressure dependency of the binary azeotrope. For increasing pressure the binary azeotrope contains more chloroform. A flowsheet that takes advantage of this shift is depicted in Figure 7.3. The distillation columns C1 and C2 are assumed to have 35 stages each with feed on stage 18, where C1 operates at 5 bar and C2 at 1 bar.

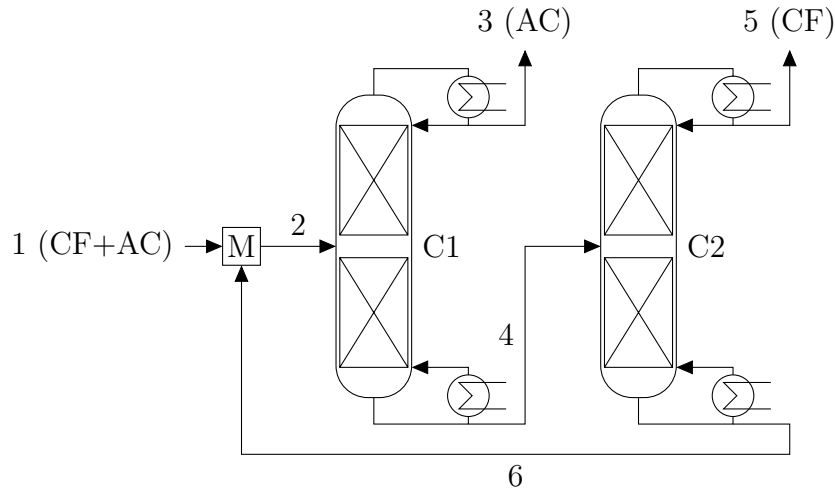


Figure 7.3.: Flowsheet of the pressure-swing distillation process for separating acetone (AC) and chloroform (CF).

Acetone is obtained as distillate of the first distillation column C1. At the top of column C2 the product chloroform is withdrawn. The bottom product of C2 is recycled and mixed in mixer M with the external feed stream 1 giving the feed stream for column C1. So far, a mixer has not been discussed in detail. However, this unit is easy to compute due to the fact that it has no degrees of freedom and the output stream is calculated based on given input streams. The specifications for this flowsheet are stated in Table 7.18.

Table 7.18.: Specifications for the flowsheet shown in Figure 7.3.

| Stream | Flow rate | Composition |
|--------|-----------|----------------------------------|
| 1 | 3 kmol/h | 0.5 mol/mol AC 0.5 mol/mol CF |
| 3 | | ≥ 0.99 mol/mol AC |
| 5 | | ≥ 0.99 mol/mol CF |

Process simulation

First, a feasibility study is conducted, which means that an arbitrary solution that meets the specifications in Table 7.18 is supposed to be found.

Embedding this process simulation task in an optimization framework leads to an optimization problem with six optimization variables. These optimization variables are the reboiler duty of the columns C1 and C2, respectively, as well as the four molar flow rates of the components in streams 4 and 6. Both columns are calculated upward and for

this flowsheet the order of calculation within on iteration for the distillation columns can be chosen arbitrarily. This is due to the fact that the feed stream of C1 is given as the external feed stream 1 and stream 6 serves as optimization variable and is therefore also given in each iteration. The same holds for column C2 with feed stream 4. However, the mixing unit M has to be calculated before calculating C1.

Note that the degrees of freedom do not have to be fixed in order to be able to conduct process simulation by optimization and we can formulate the desired specifications for this flowsheet in a flexible way. Indeed, even if the purities in Table 7.18 would be specified by equalities, there would still be degrees of freedom left for the simulation.

Initial values for the optimization variables can be obtained by ∞/∞ -analysis. These values are depicted in Table 7.19. A feasible flowsheet that meets the desired specifications in Table 7.18 is calculated in 40 iterations. The final values for the optimization variables are shown in Table 7.19 and 7.20 (stream table).

Table 7.19.: Initial values and final values for the optimization variables.

| Optimization variable | Initial value | Final value |
|-----------------------------|---------------|-------------|
| $\dot{Q}_{R,C1}$ / kW | 336.1 | 320.9 |
| \dot{n}_{AC}^4 / (kmol/h) | 0.6598 | 1.1705 |
| \dot{n}_{CF}^4 / (kmol/h) | 2.7502 | 3.7095 |
| $\dot{Q}_{R,C2}$ / kW | 381.3 | 431.6 |
| \dot{n}_{AC}^6 / (kmol/h) | 0.6597 | 1.1657 |
| \dot{n}_{CF}^6 / (kmol/h) | 1.2503 | 2.2143 |

Table 7.20.: Stream table for a solution of the flowsheet depicted in Figure 7.3 that meets the specifications in Table 7.18.

| Stream | 1 | 2 | 3 | 4 | 5 | 6 |
|----------------------|--------|--------|--------|--------|--------|--------|
| \dot{n} / (kmol/h) | 3.00 | 6.38 | 1.50 | 4.88 | 1.50 | 3.38 |
| x_{AC} / (mol/mol) | 0.5000 | 0.4178 | 0.9966 | 0.2399 | 0.0033 | 0.3449 |
| x_{CF} / (mol/mol) | 0.5000 | 0.5822 | 0.0034 | 0.7601 | 0.9967 | 0.6551 |

Process optimization

It is also possible to introduce an objective function for the above example of separating acetone and chloroform by pressure-swing distillation. One reasonable choice is to define the objective function as the sum of the reboiler duties of columns C1 and C2. There is no need to specify the yield for the two product streams in this example due to the

fact that there are no waste streams, i.e. no product loss, hence, it suffices to specify the product purities as stated in Table 7.18. The result of such optimization is summarized in Table 7.21 and 7.22 (stream table).

Table 7.21.: Initial values and final values for the optimization variables.

| Optimization variable | Initial value | Final value |
|-----------------------------|---------------|-------------|
| $\dot{Q}_{R,C1}$ / kW | 488.2 | 259.5 |
| \dot{n}_{AC}^4 / (kmol/h) | 1.5 | 1.5901 |
| \dot{n}_{CF}^4 / (kmol/h) | 4.5 | 4.6799 |
| $\dot{Q}_{R,C2}$ / kW | 835.0 | 131.6 |
| \dot{n}_{AC}^6 / (kmol/h) | 1.32 | 1.5752 |
| \dot{n}_{CF}^6 / (kmol/h) | 2.68 | 3.1948 |

Table 7.22.: Stream table for an energy optimal solution of the flowsheet depicted in Figure 7.3 that meets the specifications in Table 7.18.

| Stream | 1 | 2 | 3 | 4 | 5 | 6 |
|----------------------|--------|--------|--------|--------|--------|--------|
| \dot{n} / (kmol/h) | 3.00 | 7.77 | 1.50 | 6.27 | 1.50 | 4.77 |
| x_{AC} / (mol/mol) | 0.5000 | 0.3958 | 0.9900 | 0.2536 | 0.0100 | 0.3302 |
| x_{CF} / (mol/mol) | 0.5000 | 0.6042 | 0.0100 | 0.7464 | 0.9900 | 0.6698 |

Nothing had to be stated about the streams 4 and 6 of the flowsheet. In commercial flowsheet simulators, the designer would be forced to give two more specifications because the problem corresponding to Table 7.18 is under-specified. These specifications could be on the concentrations or flow rates of streams 4 and 6. How to choose these two specifications is far from trivial and subject to several studies in the literature, e.g. Muñoz et al. (2006); Bonet et al. (2007) and Luyben (2012). The approach of this work eliminates the entire discussion.

7.3.3. Benzene as entrainer

The flowsheet for the entrainer distillation is depicted in Figure 7.4. The entrainer benzene (BE) is added to the binary feed mixture. Assume that the distillation columns C1, C2, and C3 have 40 stages each with feed on stage 20.

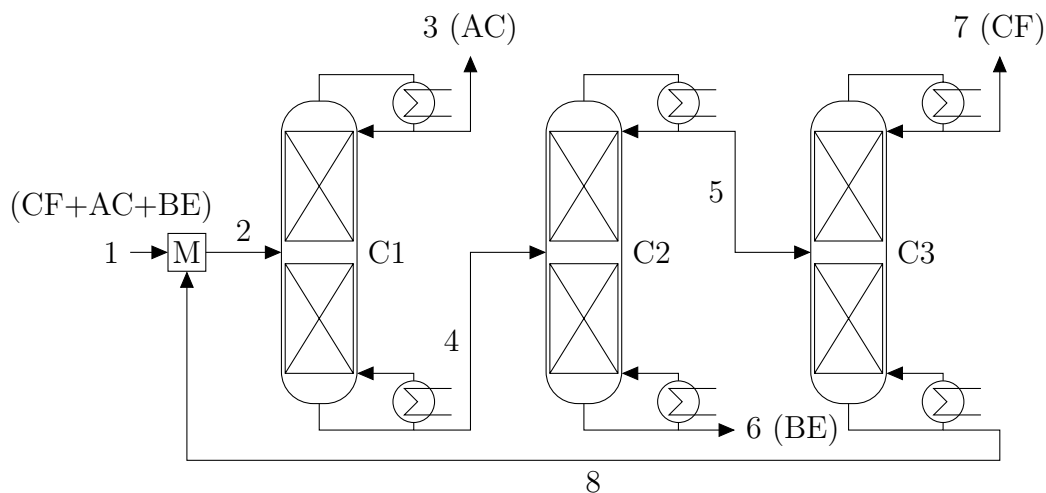


Figure 7.4.: Flowsheet of the entrainer distillation for separating acetone (AC) and chloroform (CF) using benzene (BE) as entrainer.

The distillate of column C1 is acetone and the corresponding bottom product is the feed stream for distillation column C2. From this column benzene is withdrawn as the bottom product. The distillate which contains mainly chloroform and acetone and only a small amount of benzene serves as feed stream for the third column C3. The distillate of C3 is chloroform and the bottom product is recycled to column C1. All columns operate at 1 bar. The specifications for this flowsheet are stated in Table 7.23.

Table 7.23.: Specifications for the flowsheet shown in Figure 7.4.

| Stream | Flow rate | Composition |
|--------|------------|--|
| 1 | 3.6 kmol/h | 0.4 mol/mol AC 0.3 mol/mol CF 0.3 mol/mol BE |
| 3 | | ≥ 0.99 mol/mol AC |
| 6 | | ≥ 0.98 mol/mol BE |
| 7 | | ≥ 0.99 mol/mol CF |

A ternary map of the system, which also shows the distillation boundary, is shown in Figure 7.5. In a first step, only column C1 is considered with a constant feed stream equal to stream 1 as given in Table 7.23. The composition of stream 1 is located in the left distillation region, as is the distillate (stream 3). The initial value for \boldsymbol{x}^4 is deliberately chosen in the other distillation region. Despite this, the optimization algorithm finds a

feasible solution within five iterations. The composition profiles of the liquid phase in column C1 for the different iterations are depicted in Figure 7.5. The initial and final values of the optimization variables are summarized in Table 7.24 and 7.25 (stream table).

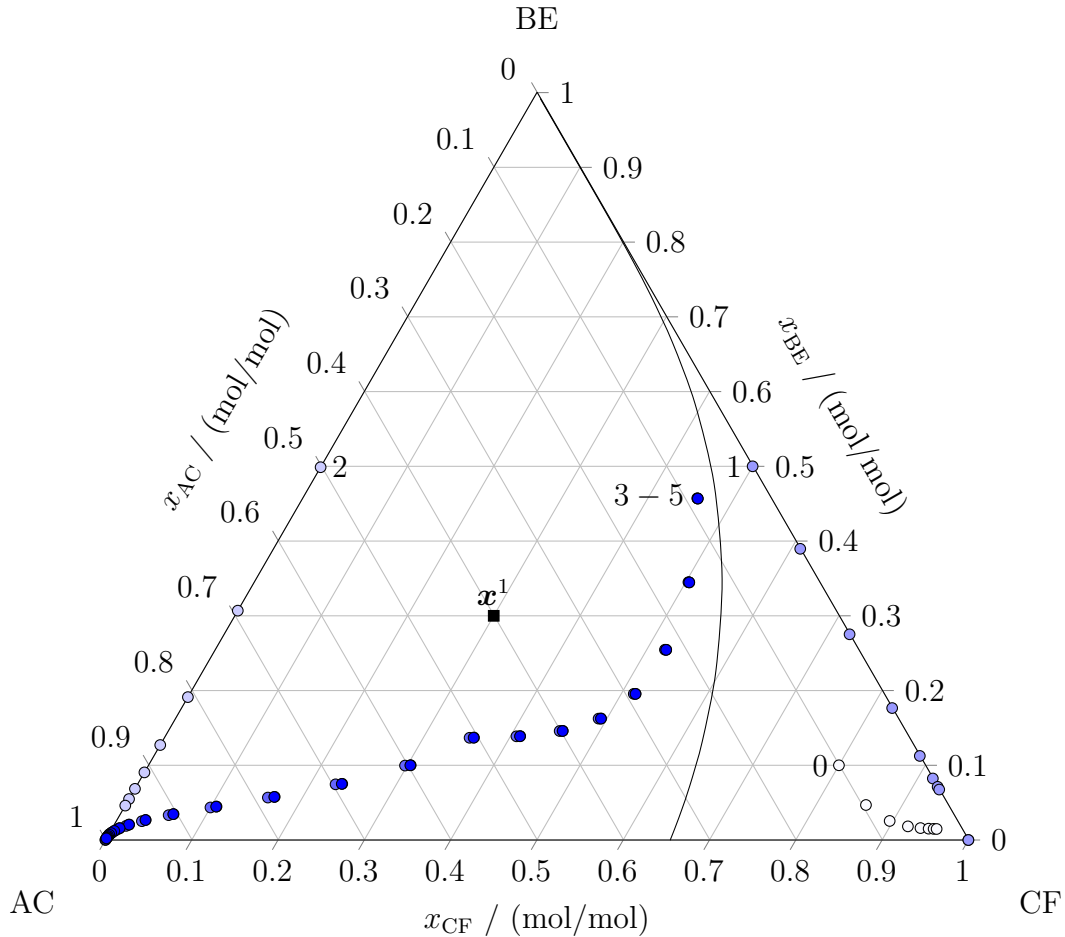


Figure 7.5.: Composition profiles of the liquid phase in the column C1 of the flowsheet in Figure 7.4 when the recycle stream 8 is neglected for iterations 0–5 when using a poor initial value for \boldsymbol{x}^4 . The line indicates the distillation boundary in the system.

Table 7.24.: Initial values and final values for the optimization variables.

| Optimization variable | Initial value | Final value |
|-----------------------------|---------------|-------------|
| $\dot{Q}_{R,C1}$ / kW | 156.9 | 139.4 |
| \dot{n}_{AC}^4 / (kmol/h) | 0.25 | 0.2008 |
| \dot{n}_{CF}^4 / (kmol/h) | 2.00 | 1.0809 |
| \dot{n}_{BE}^4 / (kmol/h) | 0.25 | 1.0782 |

Table 7.25.: Stream table for a solution of column C1 of the flowsheet depicted in Figure 7.4 without recycle stream 8 that meets the specifications in Table 7.23.

| Stream | 1/2 | 3 | 4 |
|----------------------|--------|--------|--------|
| \dot{n} / (kmol/h) | 3.60 | 1.24 | 2.36 |
| x_{AC} / (mol/mol) | 0.4000 | 0.9978 | 0.0851 |
| x_{CF} / (mol/mol) | 0.3000 | 0.0000 | 0.4580 |
| x_{BE} / (mol/mol) | 0.3000 | 0.0022 | 0.4569 |

In a next step, the specifications in Table 7.23 are shown to be feasible for the entire flowsheet by finding a corresponding solution. Distillation columns C1 and C3 are calculated from bottom to the top, whereas column C2 is calculated stage-wise in opposite direction. Once again, the calculation order of the distillation columns can be chosen arbitrarily. If the ideas from Section 3 are now applied to the flowsheet an optimization problem with 12 optimization variables is obtained: The reboiler duties of the columns C1 and C3, the condenser duty of column C2 and the nine molar flow rates of the components in stream 4, 5, and 8. The alternative equation-oriented approach that uses all process variables as optimization variables and the complete system of MESH equations as constraints yields an optimization problem with more than 500 optimization variables and constraints, which clearly requires a large-scale optimization solver. Infeasible path optimization (Biegler & Hughes, 1982) requires the introduction of one tear stream and results in an optimization problem with nine optimization variables (six degrees of freedom and three optimization variables related to one tear stream).

Using starting values that are obtained by ∞/∞ -analysis, a feasible solution is computed within 15 iterations. Hence, the specifications in Table 7.23 are shown to be feasible and the obtained solution could be used as starting point for further investigations of the process. The initial and final values of the optimization variables are stated in Table 7.26 and 7.27 (stream table) and the composition profiles of the liquid phase in each column are depicted in Figure 7.6.

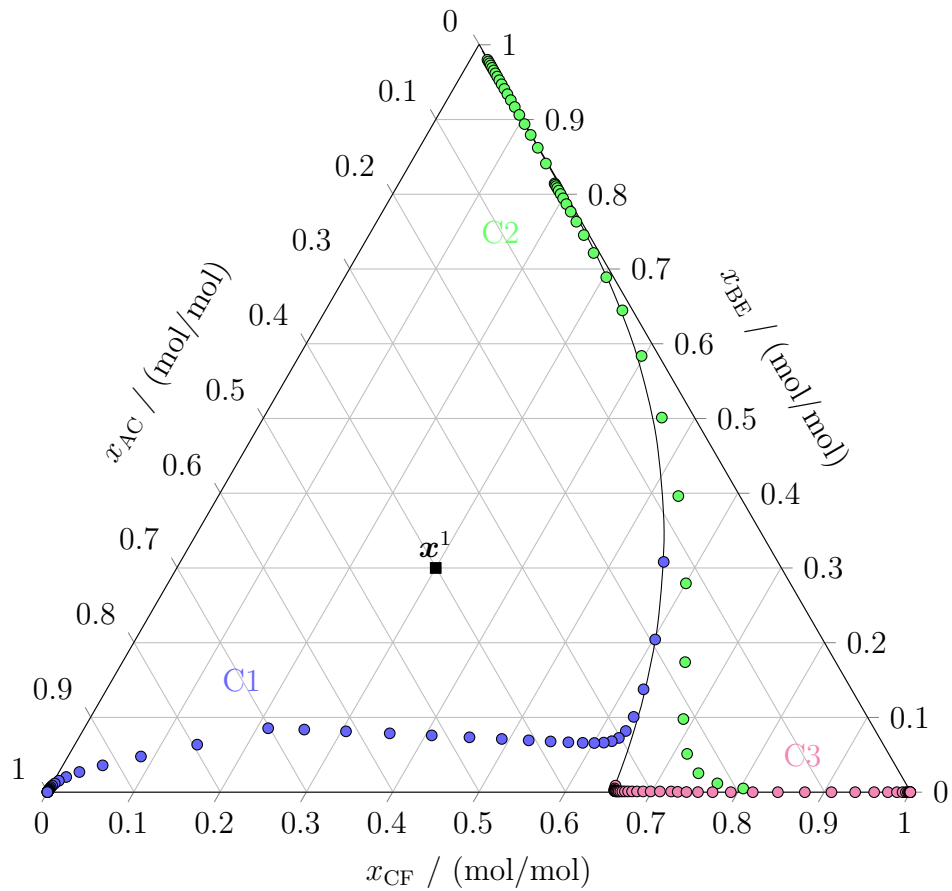


Figure 7.6.: Composition profiles of the liquid phase in the columns C1, C2, and C3 of the process in Figure 7.4. The line indicates the distillation boundary in the system.

Table 7.26.: Initial values and final values for the optimization variables.

| Optimization variable | Initial value | Final value |
|-----------------------------|---------------|-------------|
| $\dot{Q}_{R,C1}$ / kW | 248.5 | 248.5 |
| \dot{n}_{AC}^4 / (kmol/h) | 0.4684 | 0.4664 |
| \dot{n}_{CF}^4 / (kmol/h) | 1.9828 | 1.9829 |
| \dot{n}_{BE}^4 / (kmol/h) | 1.0791 | 1.0907 |
| $Q_{C,C2}$ / kW | -416.6 | -431.3 |
| \dot{n}_{AC}^5 / (kmol/h) | 0.4681 | 0.4665 |
| \dot{n}_{CF}^5 / (kmol/h) | 1.9618 | 1.9614 |
| \dot{n}_{BE}^5 / (kmol/h) | 0.0001 | 0.0121 |
| $\dot{Q}_{R,C3}$ / kW | 182.2 | 181.9 |
| \dot{n}_{AC}^8 / (kmol/h) | 0.4673 | 0.4655 |
| \dot{n}_{CF}^8 / (kmol/h) | 0.9026 | 0.9024 |
| \dot{n}_{BE}^8 / (kmol/h) | 0.0001 | 0.0121 |

Table 7.27.: Stream table for a solution of the flowsheet depicted in Figure 7.4 that meets the specifications in Table 7.23.

| Stream | 1 | 2 | 3 | 4 |
|----------------------|--------|--------|--------|--------|
| \dot{n} / (kmol/h) | 3.60 | 4.98 | 1.44 | 3.54 |
| x_{AC} / (mol/mol) | 0.4000 | 0.3826 | 0.9999 | 0.1317 |
| x_{CF} / (mol/mol) | 0.3000 | 0.3981 | 0.0000 | 0.5601 |
| x_{BE} / (mol/mol) | 0.3000 | 0.2193 | 0.0001 | 0.3081 |
| Stream | 5 | 6 | 7 | 8 |
| \dot{n} / (kmol/h) | 2.44 | 1.1 | 1.06 | 1.38 |
| x_{AC} / (mol/mol) | 0.1912 | 0.0000 | 0.0001 | 0.3373 |
| x_{CF} / (mol/mol) | 0.8038 | 0.0200 | 0.9999 | 0.6539 |
| x_{BE} / (mol/mol) | 0.0050 | 0.9800 | 0.0000 | 0.0088 |

Multi-criteria optimization

The column C1 from the flowsheet in Figure 7.4 is considered with a constant feed stream equal to stream 1 as given in Table 7.23 in order to present an example for multi-criteria optimization. The specifications are stated in Table 7.28. In this example two competing objective functions are considered. One the one hand the reboiler duty $\dot{Q}_{R,C1}$ and on the other hand the molar flow rate of the distillate stream \dot{n}^3 , which immediately influences the acetone yield. Pareto optimal points are determined by applying the ε -constraint method (see textbooks on multi-criteria optimization Steuer (1989); Hillier & Miettinen (1998); Ehrgott (2005) and Section 2.2). We conduct several optimization runs. For each

optimization we impose a lower bound ε kmol/h on the molar flow rate of the distillate stream where $\varepsilon \in [0.15; 1.31]$ and minimize the reboiler duty $\dot{Q}_{R,C1}$. The Pareto optimal solutions, which are obtained in that way, are depicted in Figure 7.7. The set of Pareto optimal solutions is almost linear for $\varepsilon \in [0.15; 1.2]$. In case the lower bound on \dot{n}^3 is chosen to be larger than 1.2 kmol/h the minimum reboiler duty needed rises significantly. Based on the information shown in Figure 7.7 an engineer can choose a good compromise between the two objective functions.

Table 7.28.: Specifications for a multi-criteria example for column C1 shown in Figure 7.4.

| Stream | Flow rate | Composition |
|--------|---------------------------|--|
| 1 | 3.6 kmol/h | 0.4 mol/mol AC 0.3 mol/mol CF 0.3 mol/mol BE |
| 3 | $\geq \varepsilon$ kmol/h | ≥ 0.99 mol/mol AC |

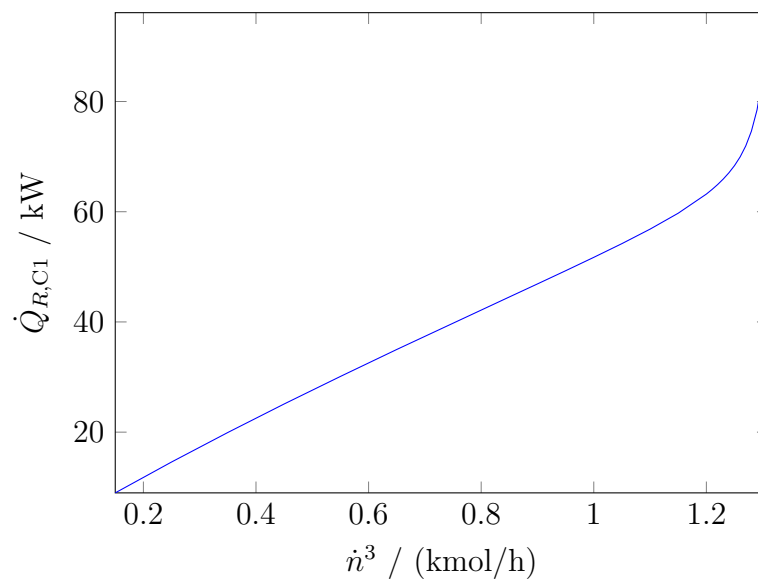


Figure 7.7.: Pareto optimal solutions for column C1 depicted in Figure 7.4 and the objective functions reboiler duty and molar flow rate of the distillate.

7.4. Separation of water and ethanol using tetrahydrofuran as entrainer

The ternary system containing water (W), ethanol (ET), and tetrahydrofuran (THF) is considered. This systems exhibits three binary azeotropes and one ternary azeotrope.

7.4.1. Single distillation column

In a first step, consider a simple distillation column with completely defined ternary feed containing water, ethanol, and tetrahydrofuran as depicted in Figure 7.8.

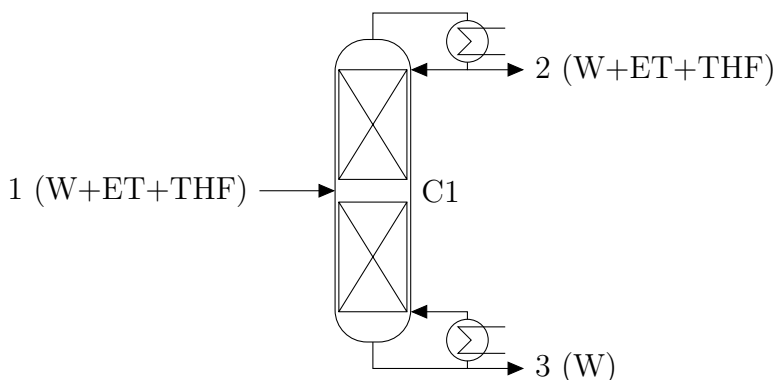


Figure 7.8.: Schematic distillation column with ternary feed containing water (W), ethanol (ET), and tetrahydrofuran (THF).

The distillation column is operated at 1 bar and consists of 30 stages. The feed stage is 15 counted from the bottom. Water is obtained as bottom product. The desired specifications on feed and product streams are summarized in Table 7.29. This example comprises more than 250 process variables. Using the method introduced in Section 3 an optimization problem with four optimization variables, the condenser duty \dot{Q}_C and the three molar flow rates \dot{n}^2 , can be formulated and the desired water purity in the bottom stream is included as an inequality constraint. In order to obtain the remaining process variables the distillation column is computed stage-wise starting from the top. In this example, a feasible distillation column that meets the specifications in Table 7.29 is calculated in three iterations. The initial values as well as the final values are summarized in Table 7.30 and 7.31 (stream table).

Table 7.29.: Specifications for the exemplary simple distillation column.

| Stream | Flow Rate | Composition |
|--------|-----------|--|
| 1 | 4 kmol/h | 0.7 mol/mol W 0.2 mol/mol ET 0.1 mol/mol THF |
| 3 | | ≥ 0.99 mol/mol W |

Table 7.30.: Initial and final values for the optimization variables for the simulation of a distillation column.

| Parameter | Initial Value | Final Value |
|------------------------------|---------------|-------------|
| Q_C / kW | -53.2 | -60.1 |
| \dot{n}_W^2 / (kmol/h) | 0.0984 | 0.4167 |
| \dot{n}_{ET}^2 / (kmol/h) | 0.8008 | 0.7995 |
| \dot{n}_{THF}^2 / (kmol/h) | 0.4004 | 0.3998 |

Table 7.31.: Stream table for a solution of the column depicted in Figure 7.8 which meets the specifications in Table 7.29.

| Stream | 1 | 2 | 3 |
|-----------------------|-----|--------|--------|
| \dot{n} / (kmol/h) | 4 | 1.62 | 2.38 |
| x_W / (mol/mol) | 0.7 | 0.2579 | 0.9997 |
| x_{ET} / (mol/mol) | 0.2 | 0.4948 | 0.0002 |
| x_{THF} / (mol/mol) | 0.1 | 0.2474 | 0.0001 |

Again, the presented approach is shown to be robust with respect to poor initial values. In an exemplary case, the initial value for the composition of the top stream is chosen in a different distillation region than the desired bottom product. However, a feasible solution is found within five iterations. The composition profiles of the liquid phase in the column for iterations 0, 3, and 5 are depicted in Figure 7.9. Iterations 1, 2, and 4 are similar to iteration 0 and 5, respectively, and therefore not shown. The initial and final parameters values are stated in Table 7.32.

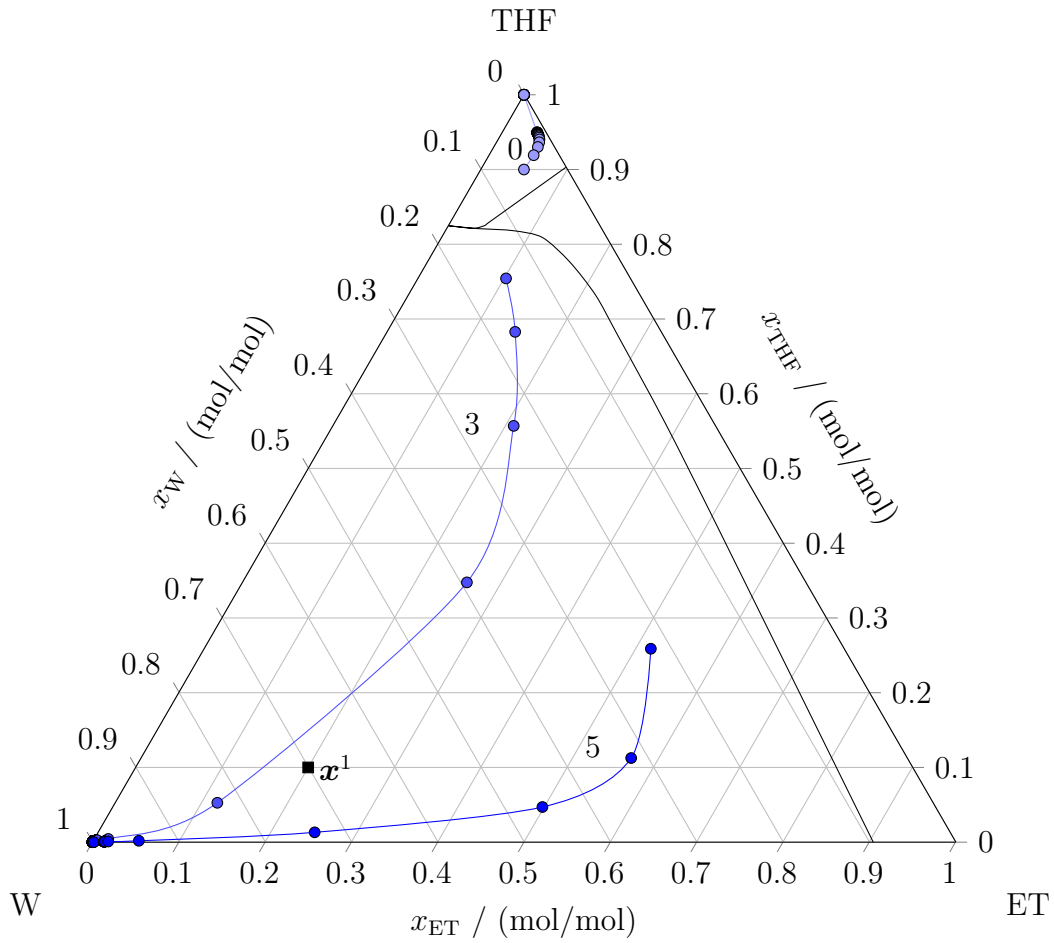


Figure 7.9.: Composition profiles of the liquid phase in the column for iterations 0, 3, and 5 when using a poor initial value for \boldsymbol{x}^2 .

Table 7.32.: Initial values and final values for the optimization variables when using a poor initial value for the composition of \boldsymbol{x}^2 .

| Parameter | Initial Value | Final Value |
|------------------------------|---------------|-------------|
| Q_C / kW | -69.1 | -79.8 |
| \dot{n}_W^2 / (kmol/h) | 0.1 | 0.3455 |
| \dot{n}_{ET}^2 / (kmol/h) | 0.1 | 0.8000 |
| \dot{n}_{THF}^2 / (kmol/h) | 1.8 | 0.4000 |

Table 7.33.: Stream table for a solution of the column depicted in Figure 7.8 that meets the specifications in Table 7.29.

| Stream | 1 | 2 | 3 |
|-----------------------|-----|--------|--------|
| \dot{n} / (kmol/h) | 4 | 1.55 | 2.45 |
| x_W / (mol/mol) | 0.7 | 0.2235 | 1.0000 |
| x_{ET} / (mol/mol) | 0.2 | 0.5176 | 0.0000 |
| x_{THF} / (mol/mol) | 0.1 | 0.2588 | 0.0000 |

7.4.2. A distillation-based flowsheet

Figure 7.10 shows a distillation process to separate water from ethanol with the light-boiling entrainer tetrahydrofuran. Pure THF is added to the process by an additional feed stream, which is mixed with the feed stream containing water and ethanol. The molar flow rate of THF that is added should be less than 0.01 kmol/h. The two bottom streams of column C1 and C2 are supposed to contain water and ethanol with a purity of at least 0.99 mol/mol.

The top stream of column C1 is used as feed stream for column C2 and the top stream of column C2 is used as recycle stream and mixed with stream 1. The specifications used here are summarized in Table 7.34. The distillation columns C1 and C2 have 40 stages each with feed on stage 20. Furthermore, both columns operate at 1 bar.

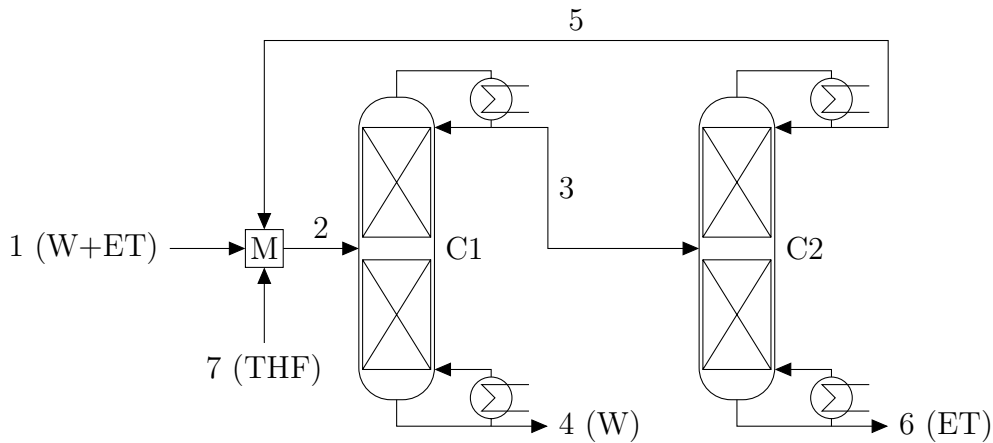


Figure 7.10.: Flowsheet for separating water, ethanol, and tetrahydrofuran.

Table 7.34.: Specifications for the separation of water and ethanol using the light-boiling entrainer tetrahydrofuran.

| Stream | Flow Rate | Composition |
|--------|--------------------|-----------------------------------|
| 1 | 3.6 kmol/h | 0.75 mol/mol W 0.25 mol/mol ET |
| 7 | ≤ 0.01 kmol/h | 1 mol/mol THF |
| 4 | | ≥ 0.99 mol/mol W |
| 6 | | ≥ 0.99 mol/mol ET |

Using the method introduced in Section 3 results in an optimization problem with nine optimization variables. These optimization variables are the reboiler duties of columns C1 and C2, respectively, as well as the six molar flow rates of the components in streams 3 and 6 and the total molar flow rate of stream 7. Column C1 is calculated downward and column C2 upward. The initial values for the product streams are obtained by ∞/∞ -analysis. A feasible flowsheet that meets the specifications in Table 7.34 is obtained in 37 iterations. The initial values as well as the final values are summarized in Table 7.35 and 7.36 (stream table) and the composition profiles of the liquid phase in each column are depicted in Figure 7.11. Using ASPEN PLUS[®] (Evans et al., 1979) the flowsheet can hardly be initialized without prior knowledge about the solution. Hence, the presented approach makes initialization more robust and therefore much easier especially for inexperienced users.

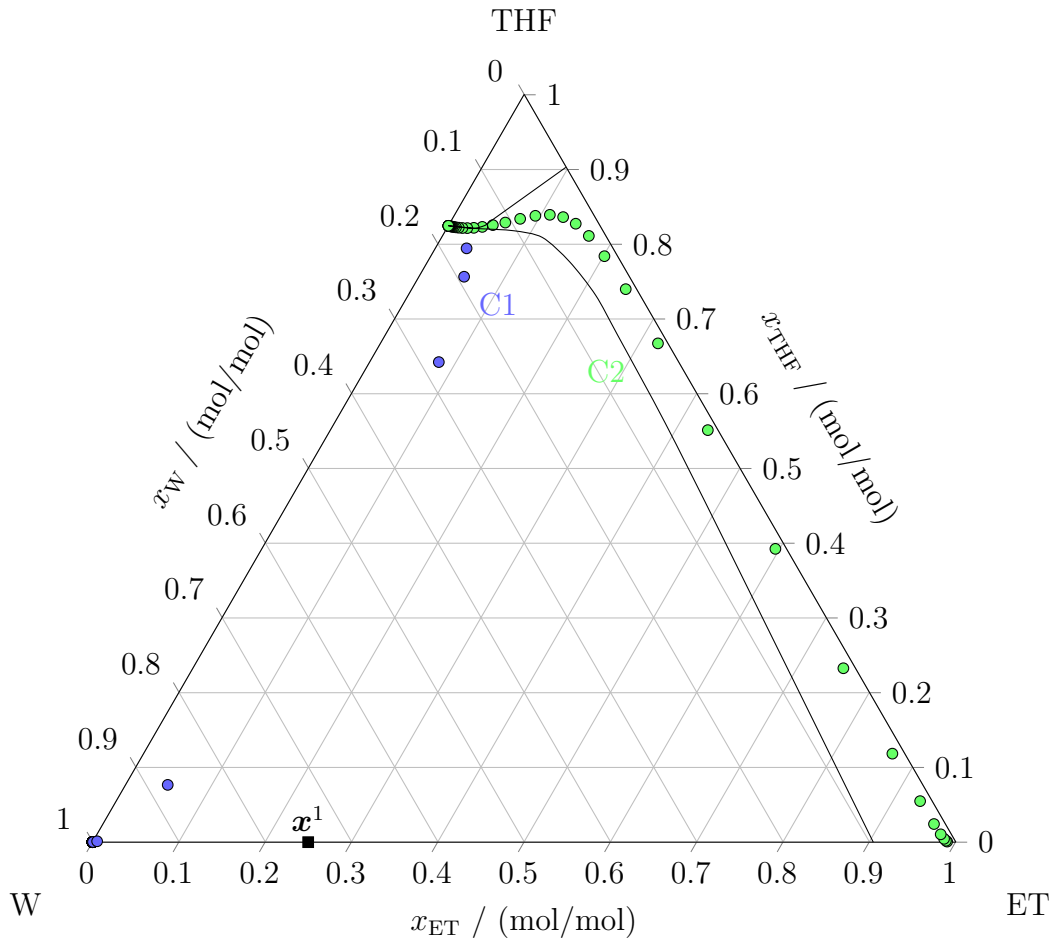


Figure 7.11.: Composition profiles of the liquid phase in the two columns. The black lines indicate the distillation boundaries in the system.

Table 7.35.: Initial and final values for the flowsheet optimization variables.

| Parameter | Initial Value | Final Value |
|-------------------------------------|----------------------|-----------------------|
| $\dot{n}^7 / (\text{kmol/h})$ | 1.0×10^{-4} | 7.46×10^{-4} |
| $\dot{Q}_{C,1} / \text{kW}$ | -523.3 | -10366.7 |
| $\dot{n}_W^3 / (\text{kmol/h})$ | 0.1031 | 4.2024 |
| $\dot{n}_{ET}^3 / (\text{kmol/h})$ | 0.8731 | 0.9012 |
| $\dot{n}_{THF}^3 / (\text{kmol/h})$ | 0.4438 | 19.7364 |
| $\dot{Q}_{C,2} / \text{kW}$ | -173.0 | -79.8 |
| $\dot{n}_W^6 / (\text{kmol/h})$ | 0.0088 | 0.0142 |
| $\dot{n}_{ET}^6 / (\text{kmol/h})$ | 0.8711 | 1.5345 |
| $\dot{n}_{THF}^6 / (\text{kmol/h})$ | 0.0001 | 0.0013 |

7. Numerical results

Table 7.36.: Stream table for a solution of the flowsheet depicted in Figure 7.10 that meets the specifications in Table 7.34.

| Stream | 1 | 2 | 3 | 4 | 5 | 6 | 7 |
|-----------------------|------|--------|--------|-------|--------|--------|-----------------------|
| \dot{n} / (kmol/h) | 3.6 | 26.89 | 24.84 | 2.05 | 23.29 | 1.55 | 7.46×10^{-4} |
| x_W / (mol/mol) | 0.75 | 0.2235 | 0.1692 | 1.000 | 0.1752 | 0.0092 | 0 |
| x_{ET} / (mol/mol) | 0.25 | 0.5176 | 0.0363 | 0.000 | 0.0001 | 0.9900 | 0 |
| x_{THF} / (mol/mol) | 0 | 0.2588 | 0.7945 | 0.000 | 0.8247 | 0.0008 | 1 |

CHAPTER 8

Conclusions and perspectives

In this work, process simulation is formulated as an optimization problem. This optimization problem includes only a small subset of model equations as constraints and only a small number of process variables are chosen as optimization variables. Tailored simulation strategies for the different unit operations, which utilize the remaining model equations, enable numerically robust computation of the entire set of process variables in case values for the optimization variables are given. Composition strategies that determine which model equations serve as constraints and which process variables are incorporated as optimization variables are presented in detail in Chapter 3 for a flash unit and distillation columns.

The simulation routine that determines the remaining process variables for a distillation column involves stage-to-stage calculations based on given values for a particular set of process variables at one end of the column. In order to proceed upward or downward, no additional process variables need to be specified on each stage of the column. For the transition from one stage to the next a fixed-point problem is derived, which is equivalent to the corresponding MESH equations and can be solved by fixed-point iteration. The fixed-point problem is mathematically analyzed by applying the Banach fixed-point theorem. As a consequence, it is possible to choose the values for the input variables for stage-to-stage calculations in such a way that a unique fixed point exists and convergence towards this fixed point is guaranteed. Thus, a mapping from input to output variables is guaranteed

as well. In particular, minimum energy requirements based on the choice of input variables for stage-to-stage calculations can be derived. In the numerical examples shown in this work, the fixed-point iteration convergences within two or three iterations due to a small Lipschitz constant. Chapter 4 and 5 are devoted to the rigorous mathematical analysis of stage-to-stage calculations of simple and general columns with an arbitrary number of feed streams and side-draws and show numerical examples that illustrate the theoretical results.

The new approach can also be extended to flowsheets comprising more than one unit operation, as shown in Chapter 6, and enables robust process simulation and easy initialization of flowsheets even in the presence of recycle streams.

The numerical examples shown in Chapter 7 cover process simulation and optimization of single distillation columns and distillation-based flowsheets comprising several columns and recycle streams. Furthermore, we present numerical examples for feasibility studies, mixed-integer optimization, multi-criteria optimization and compare the performance of different solver implementations.

Once again we want to stress that many ideas applied in this thesis stem from the asymptotic limiting cases of distillation columns with infinite reflux ratio and/or infinite number of stages. As a result, we can combine the Banach fixed-point theorem and the shooting method for BVPs in order to develop and analyze a new approach for simultaneous process simulation and optimization of distillation columns using stage-to-stage calculations.

The presented approach for process simulation and optimization features several significant advantages. For distillation-based flowsheets, we can guarantee a mapping from the input variables to the output variables in a wide range and typically for all physically relevant choices. Thus, the optimization problem that is formulated for distillation-based flowsheets operates not only on the set of feasible values for the optimization variables but also on infeasible ones and optimization and convergence to a feasible solution can be performed simultaneously without a previous simulation run. Large-scale optimization solvers do not have to be applied to the arising optimization problems due to the fact that the number of optimization variables and constraints remains small. Suitable starting values for most of the optimization variables of the arising optimization problems can be generated by employing ∞/∞ -analysis.

Another important advantage of the new method presented here is the tremendous increase in flexibility in process simulation. When applying the classical Newton approach, it is mandatory to specify as many variables as there are degrees of freedom. In this classical approach, neither fewer nor more demands on the process are possible, nor is it possible to set inequality constraints on process variables. The proposed formulation of process simulation as an optimization problem gives the possibility of including an arbitrary number of additional equalities and inequalities. This gain in flexibility allows full exploitation of process limitations and easy process initialization.

As a perspective, the presented ideas could not only be extended to flowsheets with a large number of distillation units or components, which will be a challenging task, but also be transferred to other simple or stage-based unit models including splitters, reactors, heat exchangers, decanters, extraction columns, and absorption columns. Suitable algorithms that facilitate the calculation of all process variables have to be developed as a prerequisite. Especially incorporating reactions and LLE calculations in our models seems to be of special interest and requires sound analysis. Furthermore, the approach could also be applied in the wide field of dynamic process simulation.

APPENDIX A

Chemical modeling

This thesis presents a new approach for steady state process simulation and optimization in chemical engineering with a special focus on distillation-based flowsheets. In this chapter, we define the central terminology used throughout the thesis and give some more details on the modeling principles in chemical engineering and the physical property models of the example systems.

A.1. Terminology

Phase

A *phase* is a domain within a thermodynamical system within the relevant physical properties are uniform. Relevant properties include chemical composition, pressure, temperature, and density. Phases consist of one or multiple substances and we can distinguish between solid, liquid, or vapor phases. In thesis, only liquid and vapor phases are relevant.

Vapor-liquid equilibrium

Vapor-liquid equilibrium is attained between a vapor and a liquid phase if there occurs no net flow of heat, mass, or momentum across the phase boundary (Stichlmair & Fair, 1998, Chap. 2).

Azeotrope

An *azeotrope* is a point in the composition space, where the composition of the vapor phase and the liquid phase in vapor-liquid equilibrium coincide. Hence, the composition cannot be altered by distillation. There exist azeotropes for binary mixtures, but also for mixtures of three components and more azeotropes are known.

Distillation line

If an initial concentration of the liquid phase $\mathbf{x}^0 = (x_1^0, \dots, x_{N_C}^0)$, where N_C is the number of components, is assumed, the equilibrium vapor concentration \mathbf{y}^0 can be determined for given pressure p . The vapor is then assumed to be totally condensed. Thus, a new liquid with composition $\mathbf{x}^1 = \mathbf{y}^0$ is obtained. The vapor state \mathbf{y}^1 in equilibrium with this liquid state \mathbf{x}^1 is, in turn, determined and so on. Via this procedure a series of liquid states is obtained and these points can be joined together to give a *distillation line* (Stichlmair & Fair, 1998, Chap. 2).

Distillation boundary

A ternary system can be divided into areas whose distillation lines have different end points. The distillation line that forms the boundary between these areas is called *distillation boundary*.

Equilibrium stage

An *equilibrium stage* is the region in which two phases, such as the liquid and vapor phase, establish an equilibrium with each other.

MESH equations

The equations that model an equilibrium stage are known as *MESH equations*. The four letters stand for the different types of equations. Here, the MESH equations are stated for an equilibrium stage displayed in Figure A.1. We use the notation as introduced within the scope of this thesis.

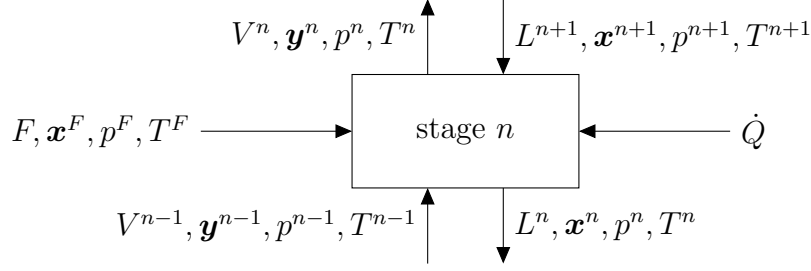


Figure A.1.: Schematic of a single equilibrium stage.

- M: Material balances

$$F x_i^F + L^{n+1} x_i^{n+1} + V^{n-1} y_i^{n-1} - L^n x_i^n - V^n y_i^n = 0, \quad \text{for } i = 1, \dots, N_C \quad (\text{A.1})$$

- E: Equilibrium conditions

$$p_i^S(T^n) x_i^n \gamma_i(\mathbf{x}^n, T^n) = p^n y_i^n, \quad \text{for } i = 1, \dots, N_C, \quad (\text{A.2})$$

- S: Summation equations

$$\sum_{i=1}^{N_C} x_i^n = 1, \quad \text{and} \quad \sum_{i=1}^{N_C} y_i^n = 1 \quad (\text{A.3})$$

- H: Heat or energy balance

$$\begin{aligned} \dot{Q} + F h^l(\mathbf{x}^F, T^F) + L^{n+1} h^l(\mathbf{x}^{n+1}, T^{n+1}) + V^{n-1} h^v(\mathbf{y}^{n-1}, T^{n-1}) \\ - L^n h^l(\mathbf{x}^n, T^n) - V^n h^v(\mathbf{y}^n, T^n) = 0 \end{aligned} \quad (\text{A.4})$$

A.2. Physical property models of the example systems

A.2.1. Pure component properties

The pure component properties required for the simulation are: vapor pressure, enthalpy of vaporization, heat capacity at constant pressure of the ideal gas. The models for these properties are taken from the DIPPR Database (DIPPR Project 801, 2005).

The vapor pressure p_i^S of the pure component i is modeled with the following correlation:

$$\ln \left(\frac{p_i^S}{\text{bar}} \right) = A_i + \frac{B_i}{T/\text{K}} + C_i \cdot \ln \left(\frac{T}{\text{K}} \right) + D_i \left(\frac{T}{\text{K}} \right)^{E_i} \quad (\text{A.5})$$

The parameters A_i – E_i for the different pure components considered in this thesis are given in Table A.1.

Table A.1.: Parameters for the correlation of the vapor pressure (cf. Equation (A.5)).

| Component i | A_i | B_i | C_i | D_i | E_i |
|-----------------|--------|---------|---------|--------------------------|-------|
| Acetone | 57.493 | -5599.6 | -7.0985 | 6.2237×10^{-6} | 2 |
| Benzene | 71.594 | -6486.2 | -9.2194 | 6.9844×10^{-6} | 2 |
| Chloroform | 134.92 | -7792.3 | -20.614 | 0.024578 | 1 |
| Water | 52.853 | -6956.0 | -5.8022 | 3.1149×10^{-9} | 3 |
| Ethanol | 47.627 | -6608.5 | -4.9151 | 0 | 6 |
| Tetrahydrofuran | 42.971 | -5292.4 | -4.6979 | 1.3446×10^{-17} | 6 |

The enthalpy of vaporization $\Delta h_{v,i}$ is modeled with the following equation:

$$\frac{\Delta h_{v,i}}{\text{J/kmol}} = A_i \cdot (1 - T_r)^{(B_i + T_r(C_i + T_r(D_i + E_i \cdot T_r)))}, \quad (\text{A.6})$$

where $T_r = \frac{T}{F_i}$. In general $F_i = T_{c,i}$, where $T_{c,i}$ is the critical temperature of component i . The parameters A_i – F_i for the different pure components considered in this thesis are given in Table A.2.

Table A.2.: Parameters for the correlation of the enthalpy of vaporization (cf. Equation (A.6)).

| Component i | A_i | B_i | C_i | D_i | E_i | F_i |
|-----------------|----------|---------|----------|---------|---------|--------|
| Acetone | 42150000 | 0.33970 | 0 | 0 | 0 | 508.20 |
| Benzene | 45346000 | 0.39053 | 0 | 0 | 0 | 562.05 |
| Chloroform | 41860000 | 0.35840 | 0 | 0 | 0 | 536.40 |
| Water | 52495400 | 0.33799 | -0.22365 | 0.25301 | 0 | 647.13 |
| Ethanol | 68846922 | 1.4008 | -2.1588 | 1.2081 | 0 | 513.92 |
| Tetrahydrofuran | 48843265 | 1.3655 | -3.1467 | 3.9167 | -1.7640 | 540.15 |

Finally, the heat capacity at constant pressure of the ideal gas $c_{p,i}^v$ of component i is modeled as follows:

$$\frac{c_{p,i}^v}{\text{J}/(\text{kmol} \cdot \text{K})} = A_i + B_i \cdot \left(\frac{C_i/(T/\text{K})}{\sinh(C_i/(T/\text{K}))} \right)^2 + D_i \cdot \left(\frac{E_i/(T/\text{K})}{\cosh(E_i/(T/\text{K}))} \right)^2 \quad (\text{A.7})$$

The parameters A_i – E_i for the different pure components considered in this thesis are given in Table A.3.

Table A.3.: Parameters for the correlation of the heat capacity at constant pressure of the ideal gas (cf. Equation (A.7)).

| Component i | A_i | B_i | C_i | D_i | E_i |
|-----------------|-------|--------|--------|---------|--------|
| Acetone | 57040 | 163200 | 1607 | 96800 | 731.5 |
| Benzene | 44767 | 230850 | 1479.2 | 168360 | 677.66 |
| Chloroform | 39420 | 65730 | 928 | 49300 | 399.6 |
| Water | 33416 | 29833 | 1457.8 | -19410 | 1602.9 |
| Ethanol | 39437 | 149597 | 511.43 | -121432 | 598.60 |
| Tetrahydrofuran | 38953 | 244350 | 542.69 | -169255 | 571.39 |

A.2.2. Vapor-liquid equilibrium

The extended Raoult's law is used for describing the VLE

$$p_i^S(T) x_i \gamma_i(\mathbf{x}, T) = p y_i, \quad i = 1, \dots, N_C \quad (\text{A.8})$$

where p is the pressure, p_i^S is the vapor pressure of pure component i , x_i and y_i are the mole fractions of component i in the liquid and vapor phase, respectively, and γ_i is the activity coefficient of component i . We assume throughout this thesis that Equation (A.8) has a unique solution.

The vapor phase is treated as ideal. For the non-ideality of the liquid phase the NRTL model is used (Renon & Prausnitz, 1968). The temperature-dependent parameters for the example systems in this work are given in Table A.4 and A.5.

Table A.4.: NRTL model parameters for the description of the vapor-liquid equilibrium in the ternary system acetone, benzene, chloroform with $\tau_{ij} = a_{ij} + b_{ij}/(T/K)$.

| Component i | Acetone | Acetone | Benzene |
|---------------|------------|-----------|------------|
| Component j | Chloroform | Benzene | Chloroform |
| a_{ij} | 0.9646 | -0.1015 | 0 |
| a_{ji} | 0.5382 | 0.4224 | 0 |
| b_{ij} | -590.026 | 306.0663 | 313.0115 |
| b_{ji} | -106.4216 | -239.9009 | -375.4311 |
| α_{ij} | 0.3 | 0.3 | 0.47 |

Table A.5.: NRTL model parameters for the description of the vapor-liquid equilibrium in the ternary system water, ethanol, tetrahydrofuran with $\tau_{ij} = a_{ij} + b_{ij}/(T/K)$.

| Component i | Water | Water | Tetrahydrofuran |
|---------------|-----------|-----------------|-----------------|
| Component j | Ethanol | Tetrahydrofuran | Ethanol |
| a_{ij} | 5.237912 | 6.32978879 | 0 |
| a_{ji} | -2.370148 | -0.4677208 | 0 |
| b_{ij} | -1063.74 | -1278.382 | 331.607875 |
| b_{ji} | 658.4101 | 642.179685 | -86.741683 |
| α_{ij} | 0.2 | 0.44 | 0.3 |

A.2.3. Caloric data for the example systems

The caloric data for the binary system acetone, chloroform at 1 bar which is needed to derive energy bounds from Section 4.4.2 is given in Table A.6 and A.7. For the ternary system acetone, benzene, and chloroform at 1 bar the caloric data is depicted in Table A.8 and A.9.

Table A.6.: Minimum and maximum values of molar liquid and vapor enthalpy for a system containing acetone and chloroform at 1 bar. The enthalpy of the vapor phase at 298 K of each component i is set to 0 kJ/mol.

| Type | Value / (kJ/mol) |
|--|------------------|
| $\max_{\mathbf{x} \in \mathcal{F}_{NC}} l(\mathbf{x})$ | -26.513 |
| $\min_{\mathbf{x} \in \mathcal{F}_{NC}} l(\mathbf{x})$ | -27.212 |
| $\max_{\mathbf{x} \in \mathcal{F}_{NC}} v(\mathbf{x})$ | 2.7970 |
| $\min_{\mathbf{x} \in \mathcal{F}_{NC}} v(\mathbf{x})$ | 2.3823 |

Table A.7.: Caloric data needed for the derivation of energy bounds. The values are computed for the system consisting of acetone and chloroform at 1 bar.

| Type | Value / (kJ/mol) |
|---|------------------|
| $\max_{\mathbf{x} \in \mathcal{F}_{NC}} \frac{\partial l}{\partial x_1}(\mathbf{x})$ | -29.379 |
| $\min_{\mathbf{x} \in \mathcal{F}_{NC}} \frac{\partial l}{\partial x_1}(\mathbf{x})$ | -30.825 |
| $\max_{\mathbf{x} \in \mathcal{F}_{NC}} \frac{\partial l}{\partial x_2}(\mathbf{x})$ | -28.514 |
| $\min_{\mathbf{x} \in \mathcal{F}_{NC}} \frac{\partial l}{\partial x_2}(\mathbf{x})$ | -31.055 |
| $\max_{\mathbf{x} \in \mathcal{F}_{NC}} \left \frac{\partial l}{\partial x_1}(\mathbf{x}) - \frac{\partial l}{\partial x_2}(\mathbf{x}) \right $ | 2.3013 |

Table A.8.: Minimum and maximum values of molar liquid and vapor enthalpy for a system containing acetone, benzene, and chloroform at 1 bar. The enthalpy of the vapor phase at 298 K of each component i is set to 0 kJ/mol.

| Type | Value / (kJ/mol) |
|--|------------------|
| $\max_{\mathbf{x} \in \mathcal{F}_{NC}} l(\mathbf{x})$ | -25.718 |
| $\min_{\mathbf{x} \in \mathcal{F}_{NC}} l(\mathbf{x})$ | -27.468 |
| $\max_{\mathbf{x} \in \mathcal{F}_{NC}} v(\mathbf{x})$ | 5.0052 |
| $\min_{\mathbf{x} \in \mathcal{F}_{NC}} v(\mathbf{x})$ | 2.3823 |

Table A.9.: Caloric data needed for the derivation of energy bounds. The values are computed for the exemplary multi-component system consisting of acetone, benzene, and chloroform at 1 bar.

| Type | Value / (kJ/mol) |
|---|------------------|
| $\max_{\mathbf{x} \in \mathcal{F}_{NC}} \frac{\partial l}{\partial x_1}(\mathbf{x})$ | -29.290 |
| $\min_{\mathbf{x} \in \mathcal{F}_{NC}} \frac{\partial l}{\partial x_1}(\mathbf{x})$ | -31.383 |
| $\max_{\mathbf{x} \in \mathcal{F}_{NC}} \frac{\partial l}{\partial x_2}(\mathbf{x})$ | -28.439 |
| $\min_{\mathbf{x} \in \mathcal{F}_{NC}} \frac{\partial l}{\partial x_2}(\mathbf{x})$ | -39.593 |
| $\max_{\mathbf{x} \in \mathcal{F}_{NC}} \frac{\partial l}{\partial x_3}(\mathbf{x})$ | -28.679 |
| $\min_{\mathbf{x} \in \mathcal{F}_{NC}} \frac{\partial l}{\partial x_3}(\mathbf{x})$ | -32.261 |
| $\max_{\mathbf{x} \in \mathcal{F}_{NC}} \left \frac{\partial l}{\partial x_1}(\mathbf{x}) - \frac{\partial l}{\partial x_2}(\mathbf{x}) \right $ | 9.0983 |
| $\max_{\mathbf{x} \in \mathcal{F}_{NC}} \left \frac{\partial l}{\partial x_1}(\mathbf{x}) - \frac{\partial l}{\partial x_3}(\mathbf{x}) \right $ | 2.8133 |
| $\max_{\mathbf{x} \in \mathcal{F}_{NC}} \left \frac{\partial l}{\partial x_2}(\mathbf{x}) - \frac{\partial l}{\partial x_3}(\mathbf{x}) \right $ | 8.6858 |

APPENDIX B

Comments on Assumption 4.3

Let all components be sub-critical at the studied temperature and the pressure p be given. The interval

$$T^{\text{lower}} < T < T^{\text{upper}} \quad (\text{B.1})$$

gives the temperature range in which the mixture exhibits a VLE. In zeotropic systems T^{lower} is the boiling point of the lightest-boiling substance or azeotrope, T^{upper} the one of the highest-boiling substance or azeotrope.

Let the vapor phase enthalpy $h_i^v(T)$ of all components i be normalized to 0 at a common temperature T^{lower} .

If for every component i it holds that

$$\Delta h_{v,i}(T^{\text{lower}}) > \int_{T^{\text{lower}}}^{T^{\text{upper}}} c_{p,i}^l dT, \quad (\text{B.2})$$

then Assumption 4.3 is fulfilled as $h_i^l < 0$. Thereby, $\Delta h_{v,i}$ denotes the enthalpy of vaporization of component i , and $c_{p,i}^l$ the heat capacity at constant pressure of the liquid phase. Typically the enthalpy change induced by the heat capacity (right hand side of Equation (B.2)) is small compared to the enthalpy change induced by phase transition (left hand side of Equation (B.2)). Thus, Assumption 4.3 is plausible.

List of publications

Parts of this thesis have been submitted or published in the following articles.

Hoffmann, A., Bortz, M., Burger, J., Küfer, K.-H., & Hasse, H. (2015). Robuste Simulation und gleichzeitige Optimierung von Fließbildern mittels Schießverfahren. *Chemie Ingenieur Technik*, *87*, 1059.

Hoffmann, A., Bortz, M., Burger, J., Hasse, H., & Küfer, K.-H. (2016). A new scheme for process simulation by optimization: distillation as an example. In *26th European Symposium on Computer Aided Process Engineering* (pp. 205–210). Elsevier volume 38 of *Computer Aided Chemical Engineering*.

Hoffmann, A., Bortz, M., Welke, R., Burger, J., Küfer, K.-H., & Hasse, H. (2017). Stage-to-stage calculations of distillation columns by fixed-point iteration and application of the Banach fixed-point theorem. *Chemical Engineering Science*, *164*, 188–201.

Bibliography

- ALGLIB (2016). A cross-platform numerical analysis and data processing library. URL: <http://www.alglib.net/>.
- Amundson, N. R., & Pontinen, A. J. (1958). Multicomponent distillation calculations on a large digital computer. *Industrial & Engineering Chemistry*, 50, 730–736.
- ASPEN HYSYS[®] (2016). A process simulation environment. URL: <http://www.aspentech.com/>.
- ASPEN PLUS[®] (2016). A process simulation environment. URL: <http://www.aspentech.com/>.
- Bausa, J., Watzdorf, R. v., & Marquardt, W. (1998). Shortcut methods for nonideal multicomponent distillation: I. Simple columns. *AIChE Journal*, 44, 2181–2198.
- Bazaraa, M. S., Sherali, H. D., & Shetty, C. M. (1993). *Nonlinear programming: Theory and algorithms*. (2nd ed.). New York and Chichester: Wiley.
- Bekiaris, N., Meski, G. A., & Morari, M. (1996). Multiple steady states in heterogeneous azeotropic distillation. *Industrial & Engineering Chemistry Research*, 35, 207–227.
- Bekiaris, N., Meski, G. A., Radu, C. M., & Morari, M. (1993). Multiple steady states in homogeneous azeotropic distillation. *Industrial & Engineering Chemistry Research*, 32, 2023–2038.

- Bekiaris, N., & Morari, M. (1996). Multiple steady states in distillation: ∞/∞ predictions, extensions, and implications for design, synthesis, and simulation. *Industrial & Engineering Chemistry Research*, *35*, 4264–4280.
- Bertsekas, D. P. (1999). *Nonlinear programming*. (2nd ed.). Belmont, Mass.: Athena Scientific.
- Biegler, L. T. (1985). Improved infeasible path optimization for sequential modular simulators—i: The interface. *Computers & Chemical Engineering*, *9*, 245–256.
- Biegler, L. T. (2014). Recent advances in chemical process optimization. *Chemie Ingenieur Technik*, *86*, 943–952.
- Biegler, L. T., & Cuthrell, J. E. (1985). Improved infeasible path optimization for sequential modular simulators—ii: The optimization algorithm. *Computers & Chemical Engineering*, *9*, 257–267.
- Biegler, L. T., Grossmann, I. E., & Westerberg, A. W. (1997). *Systematic methods of chemical process design*. Prentice Hall international series in the physical and chemical engineering sciences. Prentice Hall PTR.
- Biegler, L. T., & Hughes, R. R. (1982). Infeasible path optimization with sequential modular simulators. *AIChE Journal*, *28*, 994–1002.
- Biegler, L. T., Nocedal, J., & Schmid, C. (1995). A reduced Hessian method for large-scale constrained optimization. *SIAM Journal on Optimization*, *5*, 314–347.
- Billingsley, D. S. (1970). On the numerical solution of problems in multicomponent distillation at the steady state II. *AIChE Journal*, *16*, 441–445.
- Bonet, J., They, R., Meyer, X.-M., Meyer, M., Reneaume, J.-M., Galan, M.-I., & Costa, J. (2007). Infinite/infinite analysis as a tool for an early oriented synthesis of a reactive pressure swing distillation. *Computers & Chemical Engineering*, *31*, 487–495.
- Bortz, M., Burger, J., Asprion, N., Blagov, S., Böttcher, R., Nowak, U., Scheithauer, A., Welke, R., Küfer, K. H., & Hasse, H. (2014). Multi-criteria optimization in chemical process design and decision support by navigation on Pareto sets. *Computers & Chemical Engineering*, *60*, 354–363.

- Boston, J. F., & Sullivan, S. L. (1974). A new class of solution methods for multicomponent, multistage separation processes. *The Canadian Journal of Chemical Engineering*, 52, 52–63.
- Burningham, D. W., & Otto, F. D. (1967). Which computer design for absorbers? *Hydrocarbon Processing & Petroleum Refiner*, 46, 163–170.
- Censor, Y. (1977). Pareto optimality in multiobjective problems. *Applied Mathematics & Optimization*, 4, 41–59.
- Cho, Y. S., & Joseph, B. (1983a). Reduced-order steady-state and dynamic models for separation processes. Part I. Development of the model reduction procedure. *AIChE Journal*, 29, 261–269.
- Cho, Y. S., & Joseph, B. (1983b). Reduced-order steady-state and dynamic models for separation processes. Part II. Application to nonlinear multicomponent systems. *AIChE Journal*, 29, 270–276.
- Cho, Y. S., & Joseph, B. (1984). Reduced-order models for separation columns—III. Application to columns with multiple feeds and sidestreams. *Computers & Chemical Engineering*, 8, 81–90.
- Dennis, J. E., & Schnabel, R. B. (1996). *Numerical methods for unconstrained optimization and nonlinear equations* volume 16 of *Classics in applied mathematics*. Philadelphia: Society for Industrial and Applied Mathematics.
- Deuffhard, P., & Bornemann, F. (2008). *Gewöhnliche Differentialgleichungen: Ordinary differential equations* volume 2 of *De Gruyter Lehrbuch*. (3rd ed.). Berlin [u.a.]: de Gruyter.
- DIPPR Project 801 (2005). Full version: Evaluated standard thermophysical property values.
- Dowling, A. W., & Biegler, L. T. (2015). A framework for efficient large scale equation-oriented flowsheet optimization. *Computers & Chemical Engineering*, 72, 3–20.
- Ehrgott, M. (2005). *Multicriteria optimization*. (2nd ed.). Berlin and New York: Springer.

- Evans, L. B., Boston, J. F., Britt, H. I., Gallier, P. W., Gupta, P. K., Joseph, B., Mahalec, V., Ng, E., Seider, W. D., & Yagi, H. (1979). Aspen: An advanced system for process engineering. *Computers & Chemical Engineering*, *3*, 319–327.
- Exler, O., & Schittkowski, K. (2007). A trust region SQP algorithm for mixed-integer nonlinear programming. *Optimization Letters*, *1*, 269–280.
- Forster, O. (2013). *Analysis 1: Differential- und Integralrechnung einer Veränderlichen*. Grundkurs Mathematik (11th ed.). Wiesbaden: Springer Fachmedien.
- Friday, J. R., & Smith, B. D. (1964). An analysis of the equilibrium stage separations problem—formulation and convergence. *AIChE Journal*, *10*, 698–707.
- Gass, S., & Saaty, T. (1955). The computational algorithm for the parametric objective function. *Naval Research Logistics Quarterly*, *2*, 39–45.
- Geiger, C., & Kanzow, C. (1999). *Numerische Verfahren zur Lösung unrestringierter Optimierungsaufgaben*. Springer-Lehrbuch. Berlin: Springer.
- Geiger, C., & Kanzow, C. (2002). *Theorie und Numerik restringierter Optimierungsaufgaben: [mit 140 Übungsaufgaben]*. Berlin [u.a.]: Springer.
- Grüne, L., & Junge, O. (2009). *Gewöhnliche Differentialgleichungen: Eine Einführung aus der Perspektive der dynamischen Systeme*. Studium : Bachelorkurs Mathematik (1st ed.). Wiesbaden: Vieweg + Teubner.
- Güttinger, T. E., & Morari, M. (1997). Predicting multiple steady states in distillation: Singularity analysis and reactive systems. *Computers & Chemical Engineering*, *21*, *Supplement*, 995 – 1000.
- Haas, J. R., Alejandro, G. M., & Holland, C. D. (2007). Generalization of the Theta methods of convergence for solving distillation and absorber-type problems. *Separation Science and Technology*, *16*, 1–24.
- Haimes, Y. V., Lasdon, L. S., & Wismer, D. A. (1971). On a bicriterion formation of the problems of integrated system identification and system optimization. *IEEE Transactions on Systems, Man and Cybernetics*, *SMC-1*, 296–297.

- Hairer, E., Nørsett, S. P., & Wanner, G. (1993). *Solving ordinary differential equations* volume 8 of *Springer series in computational mathematics*. (Second revised edition ed.). Berlin: Springer-Verlag.
- Halvorsen, I. J., & Skogestad, S. (2003). Minimum energy consumption in multicomponent distillation. 1. V_{\min} diagram for a two-product column. *Industrial & Engineering Chemistry Research*, *42*, 596–604.
- Han, S. P. (1977). A globally convergent method for nonlinear programming. *Journal of Optimization Theory and Applications*, *22*, 297–309.
- Hasse, H., Bessling, B., & Böttcher, R. (2006). OPEN CHEMASIMTM: Breaking paradigms in process simulation. In W. Marquardt, & C. Pantelides (Eds.), *16th European Symposium on Computer Aided Process Engineering and 9th International Symposium on Process Systems Engineering* (pp. 255–260). Amsterdam and Boston: Elsevier volume 21 of *Computer-aided chemical engineering*.
- Heuser, H. (2008). *Lehrbuch der Analysis, Teil 2*. Studium (14th ed.). Stuttgart: Teubner.
- Hillier, F. S., & Miettinen, K. (1998). *Nonlinear Multiobjective Optimization* volume 12. Boston, MA: Springer US.
- Holland, C. D. (1963). *Multicomponent Distillation*. Englewood Cliffs, NJ: Prentice-Hall Inc.
- Holland, C. D. (1981). *Fundamentals of multicomponent distillation*. McGraw-Hill chemical engineering series. New York: McGraw-Hill.
- Holland, S. T., Tapp, M., Hildebrandt, D., & Glasser, D. (2004). Column profile maps. 2. Singular points and phase diagram behaviour in ideal and nonideal systems. *Industrial & Engineering Chemistry Research*, *43*, 3590–3603.
- Huss, R. S., & Westerberg, A. W. (1996a). Collocation methods for distillation design. 1. Model description and testing. *Industrial & Engineering Chemistry Research*, *35*, 1603–1610.
- Huss, R. S., & Westerberg, A. W. (1996b). Collocation methods for distillation design. 2. Applications for distillation. *Industrial & Engineering Chemistry Research*, *35*, 1611–1623.

- Ishii, Y., & Otto, F. D. (1973). A general algorithm for multistage multicomponent separation calculations. *The Canadian Journal of Chemical Engineering*, *51*, 601–606.
- Julka, V., & Doherty, M. F. (1990). Geometric behavior and minimum flows for nonideal multicomponent distillation. *Chemical Engineering Science*, *45*, 1801–1822.
- Kelley, C. T. (1995). *Iterative methods for linear and nonlinear equations* volume 16 of *Frontiers in applied mathematics*. Philadelphia: Society for Industrial and Applied Mathematics.
- Ketchum, R. G. (1979). A combined relaxation-newton method as a new global approach to the computation of thermal separation processes. *Chemical Engineering Science*, *34*, 387–395.
- Kim, S. B., & Linninger, A. A. (2010). Rigorous separation design. 2. Network design solutions for mixtures with various volatility differences and feed compositions. *Industrial & Engineering Chemistry Research*, *49*, 8670–8684.
- Kim, S. B., Ruiz, G. J., & Linninger, A. A. (2010). Rigorous separation design. 1. Multicomponent mixtures, nonideal mixtures, and prefractionating column networks. *Industrial & Engineering Chemistry Research*, *49*, 6499–6513.
- Köhler, J., Aguirre, P., & Blass, E. (1991). Minimum reflux calculations for nonideal mixtures using the reversible distillation model. *Chemical Engineering Science*, *46*, 3007–3021.
- Köhler, J., Pöllmann, P., & Blass, E. (1995). A review on minimum energy calculations for ideal and nonideal distillations. *Industrial & Engineering Chemistry Research*, *34*, 1003–1020.
- Krumke, S. O., & Noltemeier, H. (2012). *Graphentheoretische Konzepte und Algorithmen*. Leitfäden der Informatik (3rd ed.). Wiesbaden: Vieweg+Teubner Verlag.
- Levy, S. G., & Doherty, M. F. (1986). A simple exact method for calculating tangent pinch points in multicomponent nonideal mixtures by bifurcation theory. *Chemical Engineering Science*, *41*, 3155–3160.
- Levy, S. G., Van Dongen, D. B., & Doherty, M. F. (1985). Design and synthesis of homogeneous azeotropic distillations. 2. Minimum reflux calculations for nonideal and azeotropic columns. *Industrial & Engineering Chemistry Fundamentals*, *24*, 463–474.

- Lewis, W. K., & Matheson, G. L. (1932). Studies in distillation. *Industrial & Engineering Chemistry*, *24*, 494–498.
- Lucia, A., Amale, A., & Taylor, R. (2006). Energy efficient hybrid separation processes. *Industrial & Engineering Chemistry Research*, *45*, 8319–8328.
- Lucia, A., Amale, A., & Taylor, R. (2008). Distillation pinch points and more. *Computers & Chemical Engineering*, *32*, 1342–1364.
- Lucia, A., & Li, H. (1992). Constrained separations and the analysis of binary homogeneous separators. *Industrial & Engineering Chemistry Research*, *31*, 2579–2587.
- Luyben, W. L. (2012). Pressure-swing distillation for minimum- and maximum-boiling homogeneous azeotropes. *Industrial & Engineering Chemistry Research*, *51*, 10881–10886.
- Mah, R. S., Stanley, G. M., & Downing, D. M. (1976). Reconciliation and rectification of process flow and inventory data. *Industrial & Engineering Chemistry Process Design and Development*, *15*, 175–183.
- McCabe, W. L., & Thiele, E. W. (1925). Graphical design of fractionating columns. *Industrial & Engineering Chemistry*, *17*, 605–611.
- Mori, H., Yamada, I., Aragaki, T., Kondo, Y., Liu, F.-Z., & Tsuiki, T. (1990). Distillation calculation by multistage relaxation methods. *Journal of chemical engineering of Japan*, *23*, 269–274.
- Mori, H., Yamada, I., Hiraoka, S., & Tsuiki, T. (1987a). Distillation calculation by a successive relaxation method with simultaneous correction of liquid composition and temperature. *Journal of chemical engineering of Japan*, *20*, 220–226.
- Mori, H., Yamada, I., Tsuiki, T., & Hiraoka, S. (1987b). Multicomponent distillation calculation by a successive relaxation method using a finite difference approximation. *Journal of chemical engineering of Japan*, *20*, 460–467.
- Muñoz, R., Montón, J. B., Burguet, M. C., & de La Torre, J. (2006). Separation of isobutyl alcohol and isobutyl acetate by extractive distillation and pressure-swing distillation: Simulation and optimization. *Separation and Purification Technology*, *50*, 175–183.

- Murray, W., & Wright, M. H. (1978). *Projected Lagrangian Methods Based on the Trajectories of Penalty and Barrier Functions* volume 78-23 of *SOL*. Stanford, Calif.: Department of Operations Research (SOL), Stanford University.
- Naphtali, L. M., & Sandholm, D. P. (1971). Multicomponent separation calculations by linearization. *AIChE Journal*, *17*, 148–153.
- Narasimhan, S., & Jordache, C. (2000). *Data reconciliation & gross error detection: An intelligent use of process data*. Houston: Gulf Pub. Co.
- Nocedal, J., & Overton, M. L. (1985). Projected Hessian updating algorithms for nonlinearly constrained optimization. *SIAM Journal on Numerical Analysis*, *22*, 821–850.
- Nocedal, J., & Wright, S. J. (2006). *Numerical optimization*. Springer series in operations research and financial engineering (2nd ed.). New York: Springer.
- Petlyuk, F., Danilov, R., & Burger, J. (2015). A novel method for the search and identification of feasible splits of extractive distillations in ternary mixtures. *Chemical Engineering Research and Design*, *99*, 132–148.
- Petlyuk, F. B., & Avet'yan, V. S. (1971). Investigation of the rectification of three-component mixtures with infinite reflux. *Theoretical Foundations of Chemical Engineering*, *5*, 499–507.
- Pöllmann, P., Glanz, S., & Blass, E. (1994). Calculating minimum reflux of nonideal multicomponent distillation using eigenvalue theory. *Computers & Chemical Engineering*, *18*, S49–S53.
- Powell, M. J. D. (1978). A fast algorithm for nonlinearly constrained optimization calculations. In G. A. Watson (Ed.), *Numerical analysis* (pp. 144–157). Berlin and New York: Springer-Verlag volume 630 of *Lecture notes in mathematics*.
- PRO/II[®] (2016). A process simulation environment. URL: <http://software.schneider-electric.com/products/simsci/design/pro-ii/>.
- Rangaiah, G. P. (2009). *Multi-objective optimization: Techniques and applications in chemical engineering* volume 1 of *Advances in process systems engineering*. Singapore: Hackensack, N.J. and World Scientific.

- Renon, H., & Prausnitz, J. M. (1968). Local compositions in thermodynamic excess functions for liquid mixtures. *AIChE Journal*, *14*, 135–144.
- Rose, A., Sweeny, R. F., & Schrodt, V. N. (1958). Continuous distillation calculations by relaxation method. *Industrial & Engineering Chemistry*, *50*, 737–740.
- Ruiz, G. J., Kim, S. B., Moes, L., & Linninger, A. A. (2011). Rigorous synthesis and simulation of complex distillation networks. *AIChE Journal*, *57*, 136–148.
- Ryll, O., Blagov, S., & Hasse, H. (2012). ∞/∞ -analysis of homogeneous distillation processes. *Chemical Engineering Science*, *84*, 315–332.
- Ryll, O., Blagov, S., & Hasse, H. (2013). ∞/∞ -analysis of heterogeneous distillation processes. *Chemical Engineering Science*, *104*, 374–388.
- Schittkowski, K. (2009). NLPQLP: A Fortran implementation of a sequential quadratic programming algorithm with distributed and non-monotone line search - users guide, version 4.2 -. Report. Department of Computer Science, University of Bayreuth.
- Schittkowski, K. (2011). A robust implementation of a sequential quadratic programming algorithm with successive error restoration. *Optimization Letters*, *5*, 283–296.
- Schmid, C., & Biegler, L. T. (1994). Quadratic programming methods for reduced Hessian SQP. *Computers & Chemical Engineering*, *18*, 817–832.
- Serafimov, L. A., Zharov, V. T., & Timofeev, V. S. (1973). Rectification of multicomponent mixtures. II. Local and general characteristics of the trajectories of rectification processes at infinite reflux ratio. *Acta Chimica Academiae Scientiarum Hungaricae*, *75*, 193–211.
- Sridhar, L. N., & Lucia, A. (1990a). Analysis of multicomponent, multistage separation processes: Fixed temperature and fixed pressure profiles. *Industrial & Engineering Chemistry Research*, *29*, 1668–1675.
- Sridhar, L. N., & Lucia, A. (1990b). Tearing algorithms for separation process simulation. *Computers & Chemical Engineering*, *14*, 901–905.
- Srivastava, R. K., & Joseph, B. (1985). Reduced-order models for separation columns—V. Selection of collocation points. *Computers & Chemical Engineering*, *9*, 601–613.

- Srivastava, R. K., & Joseph, B. (1987a). Reduced-order models for separation columns—IV. Treatment of columns with multiple feeds and sidestreams via spline fitting. *Computers & Chemical Engineering*, *11*, 159–164.
- Srivastava, R. K., & Joseph, B. (1987b). Reduced-order models for staged separation columns—VI. Columns with steep and flat composition profiles. *Computers & Chemical Engineering*, *11*, 165–176.
- Steuer, R. E. (1989). *Multiple criteria optimization: Theory, computation, and application*. Malabar, Fla.: Krieger.
- Stewart, W. E., Levien, K. L., & Morari, M. (1985). Simulation of fractionation by orthogonal collocation. *Chemical Engineering Science*, *40*, 409–421.
- Stichlmair, J., & Fair, J. R. (1998). *Distillation: Principles and practice*. New York and Chichester: Wiley-VCH.
- Stoer, J., & Bulirsch, R. (2005). *Numerische Mathematik 2: Eine Einführung – unter Berücksichtigung von Vorlesungen von F.L. Bauer*. Springer-Lehrbuch (5th ed.). Berlin, Heidelberg: Springer-Verlag Berlin Heidelberg.
- Sujata, A. D. (1961). Absorber stripper calculation made easier. *Hydrocarbon Processing*, *40*, 137–144.
- Tapp, M., Holland, S. T., Hildebrandt, D., & Glasser, D. (2004). Column profile maps. 1. Derivation and interpretation. *Industrial & Engineering Chemistry Research*, *43*, 364–374.
- Teschl, G. (2012). *Ordinary differential equations and dynamical systems* volume v. 140 of *Graduate studies in mathematics*. Providence, R.I.: American Mathematical Society.
- Thiele, E. W., & Geddes, R. L. (1933). Computation of distillation apparatus for hydrocarbon mixtures. *Industrial & Engineering Chemistry*, *25*, 289–295.
- Underwood, A. J. V. (1948). Fractional distillation of multicomponent mixtures. *Chemical Engineering Progress*, *44*, 603–614.

- Urdaneta, R. Y., Bausa, J., & Marquardt, W. (2004). Minimum energy demand and split feasibility for a class of reactive distillation columns. In *European Symposium on Computer-Aided Process Engineering-14, 37th European Symposium of the Working Party on Computer-Aided Process Engineering* (pp. 517–522). Elsevier volume 18 of *Computer Aided Chemical Engineering*.
- Václavek, V. (1969). Studies on system engineering — III Optimal choice of the balance measurements in complicated chemical engineering systems. *Chemical Engineering Science, 24*, 947–955.
- Václavek, V., & Loučka, M. (1976). Selection of measurements necessary to achieve multicomponent mass balances in chemical plant. *Chemical Engineering Science, 31*, 1199–1205.
- Van Dongen, D. B., & Doherty, M. F. (1985). Design and synthesis of homogeneous azeotropic distillations. 1. Problem formulation for a single column. *Industrial & Engineering Chemistry Fundamentals, 24*, 454–463.
- Vickery, D. J., & Taylor, R. (1986). Path-following approaches to the solution of multi-component, multistage separation process problems. *AIChE Journal, 32*, 547–556.
- Wächter, A., & Biegler, L. T. (2006). On the implementation of an interior-point filter line-search algorithm for large-scale nonlinear programming. *Mathematical Programming, 106*, 25–57.
- Wang, J. C., & Henke, G. E. (1966). Tridiagonal matrix for distillation. *Hydrocarbon Processing, 45*, 155–163.
- Welke, R. (2013). *Multicriteria Optimization in Chemical Engineering*. Dissertation Technische Universität Kaiserslautern.
- Wolff, E. A., & Skogestad, S. (1995). Operation of integrated three-product (Petlyuk) distillation columns. *Industrial & Engineering Chemistry Research, 34*, 2094–2103.
- Zadeh, L. (1963). Optimality and non-scalar-valued performance criteria. *IEEE Transactions on Automatic Control, 8*, 59–60.
- Zeck, S. (1990). Einfluß von thermophysikalischen Stoffdaten auf die Auslegung und den Betrieb von Destillationskolonnen. *Chemie Ingenieur Technik, 62*, 707–717.

- Zhang, L., & Linninger, A. A. (2004). Temperature collocation algorithm for fast and robust distillation design. *Industrial & Engineering Chemistry Research*, *43*, 3163–3182.

Index

- ∞/∞ -analysis, 5, 11, 39
- ε -constraint method, 20, 138
- absorption column, 40
- asymptotic limiting case, 5
- azeotrope, 73, 152
- Banach fixed-point theorem, 6, 51
- boundary condition, 22
- boundary value method, 10
- boundary value problem, 6, 14, 22, 35
- bubble-point method, 13
- collocation method, 10
- column profile maps, 11
- commercial simulation environment, 4, 8
- conceptual process design, 10, 38
- condenser duty, 32
- constant molar overflow, 10
- constant relative volatility, 10
- constrained optimization problem, 18
- control volume, 32, 46
- decanter, 41
- decision variables, 20
- distillation boundary, 134, 152
- distillation column, 4, 32, 45
- distillation line, 54, 152
- efficient set, 20
- efficient solution, 20
- eigenvalue method, 11
- equality constraint, 18
- equation-oriented mode, 8, 109
- equilibrium stage, 4, 152
- equilibrium stage model, 7, 45
- extended Raoult's law, 29, 47, 155
- extractive column, 41
- feasible region, 20
- feasible solution, 18
- fixed point, 51
- fixed-point problem, 6, 48, 92
- flash unit, 29
- flowsheet, 3, 109

- heat duty, 29
- inequality constraint, 18
- infeasible path optimization, 9
- initial value, 22
- initial value problem, 22
- inside-out method, 8

- Lagrange multiplier, 19
- Lagrangian function, 19
- linear optimization problem, 18
- Lipschitz constant, 51
- liquid-liquid equilibrium, 41

- McCabe-Thiele method, 87
- MESH equations, 7, 29, 153
- minimum energy demand, 10
- mixed-integer optimization, 128
- mixed-integer optimization problem, 18
- modular mode, 8, 109
- multi-criteria optimization, 41
- multi-criteria optimization problem, 20

- Newton-type methods, 4, 8
- nondominated point, 20
- nonlinear optimization problem, 18

- objective function, 18, 20
- optimal solution, 18
- optimization problem, 17
- ordinary differential equation, 6, 14, 21, 35

- Pareto optimal solution, 20, 139
- Pareto set, 20, 139
- Petlyuk distillation column, 40
- phase, 30, 47, 151

- process, 3
- process design, 3
- process optimization, 3, 25
- process simulation, 3, 25
- process variables, 3

- rate of convergence, 72
- reactor, 40
- reboiler duty, 32
- rectification body method, 11
- rectifying section, 11
- recycle stream, 9, 109
- reflux ratio, 5, 32
- relaxation method, 13

- sequential quadratic programming, 18
- shooting method, 7, 14, 22, 35
- shortcut techniques, 10
- shortest stripping line approach, 11
- side-draw, 40, 45, 91
- splitter, 41
- stage-to-stage calculations, 6, 10, 45, 91
- steady state, 3, 38, 151
- stripping section, 11
- sum-rates method, 13

- tear stream, 9, 109

- unconstrained optimization problem, 18
- unit operation, 3, 40

- vapor-liquid equilibrium, 152

- weighting method, 20

- zero-volume criterion, 10

Scientific Career

- 03/1989 Born in Saarlouis, Germany
- 10/2008 - 09/2011 Bachelor of Science in Mathematics
at the University of Kaiserslautern
- Bachelor Thesis: Physical and Mathematical Modeling
in Focused Ultrasound Therapy
- 08/2011 - 12/2011 Semester abroad
Chalmers, Göteborg, Sweden
- 10/2011 - 09/2013 Master of Science in Mathematics
at the University of Kaiserslautern
- Master Thesis: Chemotherapy Planning: Mathematical Modeling,
Plan Optimization and Quality Robustness
- 10/2013 - 10/2016 PhD candidate in Mathematics
at the University of Kaiserslautern
(funded by a scholarship of the Fraunhofer ITWM
and the University of Kaiserslautern)
- 11/2016 - 01/2017 Member of the research staff in the Department
of Optimization at the Fraunhofer ITWM

Wissenschaftlicher Werdegang

- 03/1989 Geboren in Saarlouis
- 10/2008 - 09/2011 Bachelor of Science in Mathematik
an der Technischen Universität Kaiserslautern
- Bachelor Thesis: Physikalische und mathematische
Modellbildung in der fokussierten Ultraschalltherapie
- 08/2011 - 12/2011 Auslandssemester
Chalmers, Göteborg, Schweden
- 10/2011 - 09/2013 Master of Science in Mathematik
an der Technischen Universität Kaiserslautern
- Master Thesis: Chemotherapy Planning: Mathematical Modeling,
Plan Optimization and Quality Robustness
- 10/2013 - 10/2016 Promotionsstudium in Mathematik
an der Technischen Universität Kaiserslautern
(finanziert von einem Stipendium des Fraunhofer ITWM
und der Technischen Universität Kaiserslautern)
- 11/2016 - 01/2017 Wissenschaftliche Mitarbeiterin in der Abteilung
Optimierung am Fraunhofer ITWM

Die vorliegende Arbeit ist durch die chemische Verfahrenstechnik motiviert: Prozesssimulation und -optimierung mit Schwerpunkt auf destillationsbasierten Fließbildern. In diesem Kontext besteht ein Prozess aus einer gewissen Anzahl von Apparaten, die durch Ströme verbunden sind. Eine solche Struktur kann durch ein sogenanntes Fließbild repräsentiert werden. Im Allgemeinen sollte ein Prozess so konzipiert werden, dass gewisse technische Anforderungen erfüllt werden, z. B. Produktreinheiten, Produktausbeute oder maximale Kosten. Die Auslegung eines Prozesses im stationären Zustand beinhaltet die Wahl der Apparate in Kombination mit ihren jeweiligen Verschaltungen und auch die Wahl der Werte für die spezifischen Designvariablen für jeden Apparat. Im Rahmen dieser Arbeit gehen wir davon aus, dass die Topologie des Fließbilds gegeben ist und wir konzentrieren uns darauf, die Designvariablen für jeden Apparat zu wählen. In dieser Arbeit wird ein Ansatz vorgestellt, der eine robuste, flexible und simultane Prozesssimulation und -optimierung von destillationsbasierten Fließbildern im stationären Zustand möglich macht.

ISBN 978-3-8396-1179-1



FRAUNHOFER VERLAG